i.a

EADAP

Enhanced Arch Dam Analysis Program

User's Manual

by

Yusof Ghanaat

Ray W. Clough

Report No. UCB/EERC-89/07
Earthquake Engineering Research Center
University of California
Berkeley, California

November 1989

50272-101

REPORT DOCUMENTATION PAGE	1. REPORT NO. NSF/ENG-89028	2.	PB91-212522

4. Title and Subtitle EADAP
Enhanced Arch Dam Analysis Program
User's Manual

5. Report Date November 1989

6.

7. Author(s) Y. Ghanaat, R.W. Clough

8. Performing Organization Rept. No. UCB/EERC-89/07

9. Performing Organization Name and Address
Earthquake Engineering Research Center
University of California, Berkeley
1301 S 46th St.
Richmond, CA 94804

10. Project/Task/Work Unit No.

11. Contract(C) or Grant(G) No.
(C)
(G) CEE-8214198

12. Sponsoring Organization Name and Address
National Science Foundation
1800 G. St. NW
Washington, DC 20550

13. Type of Report & Period Covered

14.

15. Supplementary Notes

16. Abstract (Limit: 200 words)

The original ADAP program, as developed for the CDC machines did not include hydrodynamic effects of the reservoir water. In 1979, a separate subroutine (RSVOIR) was developed using an incompressible finite-element formulation to approximate hydrodynamic effects of the water by an equivalent added-mass matrix that would be added to the mass of the concrete in dynamic analysis. The present version of the program is called EADAP for Enhanced Arch Dam Analysis Program. INCRES, for INCompressible REServoir, is the name given to the new version of the previous RSVOIR subroutine. These programs can also be installed on a UNIX environment with minimal modifications. This report is intended as a user's manual for the EADAP and INCRES programs. The most important features of the program including the system idealization, element types, and the analysis procedures are described. The input data and the output results are discussed, and a sample problem is presented.

17. Document Analysis a. Descriptors

b. Identifiers/Open-Ended Terms

c. COSATI Field/Group

18. Availability Statement	19. Security Class (This Report)	21. No. of Pages
Release Unlimited	unclassified	106
	20. Security Class (This Page) unclassified	22. Price

ACKNOWLEDGEMENTS

The authors wish to thank the US Bureau of Reclamation for its financial support which led to the original development of the program ADAP. Thanks are also due to Dr. J. S-H. Kuo who, with NSF funding, developed the original RSVOIR, a pre-processor for calculating the added-mass of incompressible reservoirs.

The program EADAP, an enhanced version of the previous ADAP program is an outgrowth of a 4-year US-China cooperative research project on "*Interaction Effects in the Seismic Response of Arch Dams.*" The financial support of the National Science Foundation for the US-China Cooperative project is gratefully acknowledged. The computer facilities at the Lawrence Berkeley Laboratory were used to perform the analytical calculations related to the cooperative project and to carry out the initial debugging and improvements of the program.

In 1985 another research project similar to the US-China cooperative project was initiated to study dynamic reservoir interaction with the Monticello Dam in California. During this project which lasted over two years, QUEST Structures provided significant and long standing contributions to the project which included further modifications of the code, conversion and installation of the program on VAX computers, and free computer facilities to carry out the computer analyses. Furthermore, Quest Structures contributed significantly to the preparation of this report with partial financial support from a group of private and government organizations (EPRI, PG&E, LA County Flood Control District, and HARZA Engineering Company).

TABLE OF CONTENTS

1. INTRODUCTION

In 1981 a four-year NSF funded cooperative research program on "*Interaction Effects in the Seismic Response of Arch Dams*" was initiated under the US-China Protocol for Scientific and Technical Cooperation in Earthquake Studies. Under this research program, two arch dams in China, Xiang Hong Dian [1] and Quan Shui [2], were excited by rotating mass shakers to measure vibration properties of the selected dams and the resulting hydrodynamic pressures induced in the reservoir. The measured data were then compared with predicted values calculated by an enhanced version of the previous ADAP [3] program. The research program, thus, provided a unique opportunity to verify, enhance and modify the Arch Dam Analysis Program (ADAP) that had been developed for the US Bureau of Reclamation in 1973.

The original ADAP program, as developed for the CDC machines did not include hydrodynamic effects of the reservoir water. In 1979, a separate subroutine (RSVOIR) [4] was developed using an incompressible finite-element formulation to approximate hydrodynamic effects of the water by an equivalent added-mass matrix that would be added to the mass of the concrete in dynamic analysis. However, no documentation was provided for the RSVOIR program. In addition, difficulties were encountered in installing the ADAP program on computers other than CDC, partly associated with minor coding bugs that had existed in the original distribution copy of ADAP. The results of these circumstances was that the ADAP program did not gain wide use in practice.

Under the US-China cooperative research project, working versions of the ADAP and RSVOIR programs were assembled on the CDC-7600 of the Lawrence Berkeley Laboratory, to predict the test results for the Xiang Hong Dian and Quan Shui dams analytically. Later, QUEST Structures converted the programs for DEC-VAX/VMS mini-computers and provided several enhancement and modifications to the code. Subsequently, this latest version was used in the Monticello Dam Research Project [5]. The present version of the program is called EADAP for Enhanced Arch Dam Analysis Program. INCRES, for INCompressible REServoir, is the name given to the new version of the

previous RSVOIR subroutine. These programs can also be installed on a UNIX environment with minimal modifications. The following is a list of the major modifications and enhancements:

- *Hydrodynamic effects are accounted for by calculating an equivalent added-mass matrix using the INCRES program.*
- *EADAP accepts the added-mass matrix as an input to account for the inertial forces of the reservoir water.*
- *The mesh generator has been extended to automatically generate finite-element mesh for the arch dams built in U-shaped valleys in addition to the V-shaped cases.*
- *Temperature loads due to both uniform and linearly varying temperature changes through the dam thickness are now supported.*
- *The foundation rock model is now generated more realisticly near the crest of the dam.*
- *New trial load vectors have been developed for the eigen solution.*

This report is intended as a user's manual for the EADAP and INCRES programs. The most important features of the program including the system idealization, element types, and the analysis procedures are described. The input data and the output results are discussed, and a sample problem is presented.

2. SYSTEM IDEALIZATION

2.1 General

Arch dams are treated as three-dimensional systems consisting of a concrete arch supported by flexible foundation rock and impounding a reservoir of water. Idealization of the system should represent not only the concrete arch, but also a significant portion of the foundation rock and the impounded reservoir of water (Figure 2.1). The reason for this is that the flexibility of the foundation and the inertial forces of water significantly influence the stresses developed in the dam.

Using finite-element procedures, each component of the dam-foundation-reservoir system is idealized as an assemblage of finite elements of appropriate shapes and types. Different types of elements are used to represent the conrete arch and the foundation rock, because the arch component is essentially a thick shell, whereas the foundation rock is an arbitrary three-dimensional solid medium. Similarly, the reservoir water is idealized using an appropriate type of element such as quadratic liquid elements.

The definition of the finite-element mesh in the analysis of arch dams is a laborious task because it involves dealing with arbitrary three-dimensional geometry. It requires the specification of the Cartesian coordinates of all element nodes, the numbering of the nodes and of the elements in a logical sequence, and the prescription of material properties and the surface loads for each element. For this reason, the EADAP program which has been developed specifically for arch dams, includes automatic mesh generator capabilities for the concrete arch and the foundation rock; the reservoir mesh is then derived from the concrete nodes located on the upstream face of the dam.

The automatic mesh generator of the present program can handle a general three-centered arch dam of regular geometry. One and two-centered geometry and other types of dams with less complex geometry are treated as special cases. In particular, the mesh generator can produce a finite-element mesh for a symmetrical half-system with the crown section being assumed as the plane of symmetry.

In that case, symmetric and anti-symmetric boundary conditions are introduced along the crown section. Arch dams of irregular geometry can be handled by the program, but the resulting mesh is non-uniform and may include extremely small or large elements with very large aspect ratios. The general concepts of the mesh generation for the dam and foundation rock are described below and a procedure for handling the irregular geometries is presented. A complete description of the generation procedures are given in Reference [3].

2.2 Concrete Arch Dam

The dam body is idealized as an assemblage of finite elements with the concrete nodes being arranged along horizontal and vertical sections. These sections are identified first on the reference surface of the dam which is a vertical cylindrical surface passing through the upstream edge of the crest. The coordinates of the concrete nodes are then obtained by radial projection from the reference surface. The horizontal sections, which are called mesh elevations, are defined by the user, and the vertical sections are projected from the intersection of mesh elevations with the abutment on the reference surface. The finite element mesh is automatically generated from a minimum amount of geometric data which are specified at design elevations (Figure 2.2).

In general, mesh elevations are different from the design elevations; thus all geometric data at the mesh elevations are computed by cubic interpolation from the corresponding data specified at the design elevations. Figure 2.2 shows a typical horizontal section for a three-centered arch dam. The coordinate system is a right-handed set with z vertical (up), y horizontal and pointing downstream, and x cross-stream; the origin is the intersection point of the reference surface with the crown cantilever at the dam base.

The mesh generator provides for two types of finite element meshes differing with respect to the element types used to idealize the dam body. In type one, the curved surfaces of the dam are modeled by a combination of thick-shell and 16-node shell (3D-SHELL) elements; all element nodes are

located on the faces of the dam. The thick-shell elements whose sixteen nodes are reduced to eight mid-surface nodes are utilized in the interior region of the arch; the 16-node shell elements are used in the regions near the abutments, where they also provide a convenient connection with the foundation elements. Figure 2.3 is a developed view of the mesh layout for the two types of shell elements on the reference surface. In the second type of mesh, the concrete arch is idealized by eight-node three-dimensional solid elements where three elements are used through the dam thickness. The mesh layout for 8-node elements is similar to the previous case, but without the mid-side nodes; additional interior nodes within the dam are specified at one-third points along the straight line connecting the two surface nodes.

The procedure described above applies only to arch dams built in V-shaped canyons. However, The mesh generator of EADAP has been extended to include the location of arch dams in U-shaped canyons where a significant portion of the bottom surface of the dam might be flat (Figure 2.4). In this case, the mesh layout is extended below the base of the dam to form a V-shaped profile, so that the same generation concept described earlier can be employed; concrete elements in this region (shown with dashed lines) are fictitious and are not generated.

The present mesh generator is not appropriate for a dam that has irregular geometry or is located in a very wide or narrow canyon, because it generates a non-uniform mesh with large aspect ratios for some elements (Figure 2.5a). In these situations the finite element mesh may be improved by adding or removing certain horizontal and/or vertical mesh lines from the mesh layout (Figure 2.5b). For this purpose, if needed, additional horizontal or vertical mesh lines are provided as input data by introducing a corresponding mesh elevation; then a finite element mesh based on the new data is generated; and finally the generated output file which contains nodal coordinates, boundary conditions, and the element connectivities is modified to manually remove the undesired data associated with the extra mesh lines. The modified data is assembled according to the description given in Chapter 7 (with no mesh generation option) for the subsequent analysis.

2.3 Foundation Rock

The effects of foundation-dam interaction are accounted for by including an appropriate portion of the foundation rock as part of the finite-element idealization. The inertial and damping effects of the foundation rock are ignored and only its flexibility is considered in the analysis using the EADAP. Thus the only controlling parameters in specifying the finite-element mesh for the foundation are the mesh geometry, volume of rock, and the number of elements to be included in the mesh. In general, the geometry of the rock supporting the concrete arch will be completely different for different dams and cannot be represented by a single mesh generation algorithm. Therefore, the EADAP program assumes a prismatic shape for the valley and uses special schemes to generate a simplified foundation mesh (Figure 2.1c). The program also provides an option to modify the generated coordinates of any points in the system by means of additional input data. With this combined approach, the program can be used to analyze a great variety of arch dam systems.

The volume of rock and the number of elements to be considered in the foundation mesh depend on the site conditions, material properties of the rock and the mass concrete, and on the geometry of the dam. For these reasons, the EADAP program permits development of finite-element rock models with three degrees of refinement that can be adapted to different conditions.

The foundation mesh is constructed on semi-circular planes cut into the canyon walls in the direction normal to the dam-foundation contact surface (Figures 2.1c and 2.6). Figure 2.6 shows the traces of these normal planes as they intersect the dam profile. However, in the new EADAP program, the locations of the two upper planes are rotated up so that the ground surface at the crest level is represented more realistically; the top plane is rotated to a horizontal position and the slope of the lower plane is divided by two. A brief description of each foundation rock mesh for the case where thick shell elements are used in the dam is given first. The minor differences in the foundation mesh when eight-node solid elements are employed in the dam are discussed at the end.

Mesh 1: This is the coarsest foundation mesh; the nodal point arrangement on the inclined plane for this mesh is shown in Figure 2.7. Nodes 1 and 2 correspond to the concrete nodes on the upstream and downstream faces where the foundation and dam are connected. The radius of the semi-circle is equal to one height of dam and its center is located at the mid-point of the segment connecting the pair of interface nodes. Line 5-3-18-20 is oriented along the channel and represents the intersection between the inclined plane and the surface of the prismatic valley. The nodes along the perimeter of inclined planes are located at equal intervals and are fixed in space because the region beyond this foundation mesh is assumed to be rigid. Eight-node solid elements are used to descretize the foundation rock; eight of these elements are used in each portion of rock between the two adjacent inclined planes.

Mesh 2: This mesh includes the same volume of rock as in Mesh 1, but the number of elements on each inclined plane is increased by five. Thus the descretization is more refined and includes 13 eight-node solid elements in the segment between each of the two adjacent inclined planes. The additional elements are accommodated by introducing six more nodes (4,7,..,19) at equal intervals along the perimeter of a smaller semi-circle. The center of this semi-circle is at Point O and its radius is selected such that the distance 3-4 is one-third of 3-5 (Figure 2.8).

Mesh 3: In this mesh the foundation rock idealization is extended to a distance of about two dam heights and includes 18 solid elements in each segment between two adjacent inclined planes. Figure 2.9 is a typical layout of the mesh on the inclined plane. Nodal points 1 to 20 are specified exactly as in Mesh 2; the additional boundary nodes (21 to 26) are located on a semi-circle with a radius of approximately two dam heights which satisfies the following relationship:

$$\frac{3\text{-}4}{4\text{-}5} = \frac{4\text{-}5}{5\text{-}21}$$

The above procedure of foundation mesh generation can also be applied with minor adjustments to dams descretized by three layers of eight-node solid elements. In that case, two additional nodes corresponding to the interior concrete nodes are located along the segment 1-2 for each foundation mesh type. These two added nodes generate two more foundation elements as indicated by dashed lines in Figures 2.7 to 2.9. Thus each segment of the foundation for the dams with three layers of solid elements includes 10, 15, and 20 elements for Meshes 1, 2, and 3, respectively.

2.4 Reservoir Water

The inertial effects of the water in the reservoir due to seismic loading are represented by equivalent added-mass which is added to the mass of the concrete for the dynamic analysis. To calculate the added-mass, the reservoir water is idealized by a finite-element mesh of incompressible liquid elements extending to a finite distance from the upstream face of the dam (Figure 2.1a). Based on previous studies of incompressible reservoirs [1,2], a reservoir length about three times the height of the dam is recommended for most practical work, because the reservoir reach beyond this length has practically no effect on the incompressible added-mass.

Any complicated geometry of the impounded water can be represented in the finite-element idealization. However, specification of the nodal coordinates from the topographic map of the reservoir bottom is a laborious and time- consuming task. An effective approach that is adequate for most cases, is to assume that the reservoir is bounded by a cylindrical surface obtained by translating the dam-canyon wall interface upstream. The reservoir elements are then arranged in successive layers with the nodes on successive sections located to correspond with the dam-reservoir interface nodes. The number of liquid layers in any case may be specified arbitrarily, but thinner layers should be provided near the face of the dam where the hydrodynamic pressure gradient is the largest. The coordinates of nodes on each vertical section are obtained from the concrete interface nodes by projection in the upstream direction. Figure 2.10a shows an isometric view of a prismatic reservoir

consisting of three liquid layers, and Figure 2.10b demonstrates the node numbering scheme of the finite-element mesh. Boundary nodes at the reservoir-rock interface and at the upstream end of the finite-element model are assumed to be fixed; hydrodynamic pressures at the free top surface of the reservoir are set to zero (i.e. surface wave action is neglected). Each liquid layer is descretized by three-dimensional liquid elements, whereas the actual interface between water and dam is represented by curvilinear two-dimensional liquid elements that will be discussed in the next chapter.

When the reservoir is not filled to the crest of the dam, the nodes of the top layer of liquid elements may not coincide with the corresponding concrete dam nodes. In that case, the accelerations that control the hydrodynamic pressures at these liquid nodes must be established by special procedures. In the INCRES program, the accelerations are calculated at integration points of the liquid elements using the displacement interpolation functions defined for the concrete elements.

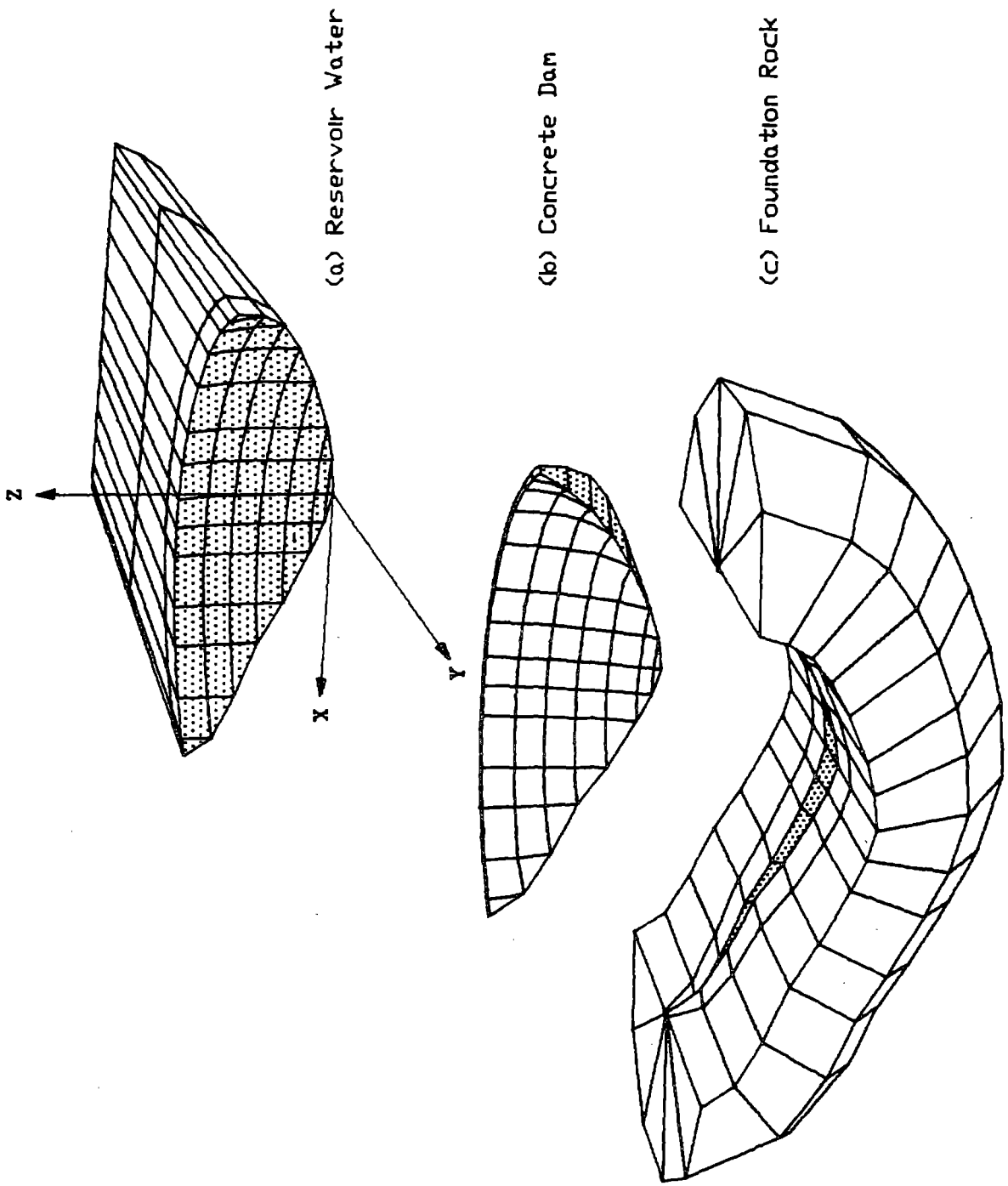

Figure 2.1 Finite Element Models of Dam, Foundation, and Reservoir

$\phi 1$ = Compounding Angle of Right Intrados

$\phi 2$ = Compounding Angle of Left Intrados

$\phi 3$ = Compounding Angle of Right Extrados

$\phi 4$ = Compounding Angle of Left Extrados

$\phi 5$ = Angle to Right Abutment

$\phi 6$ = Angle to Left Abutment

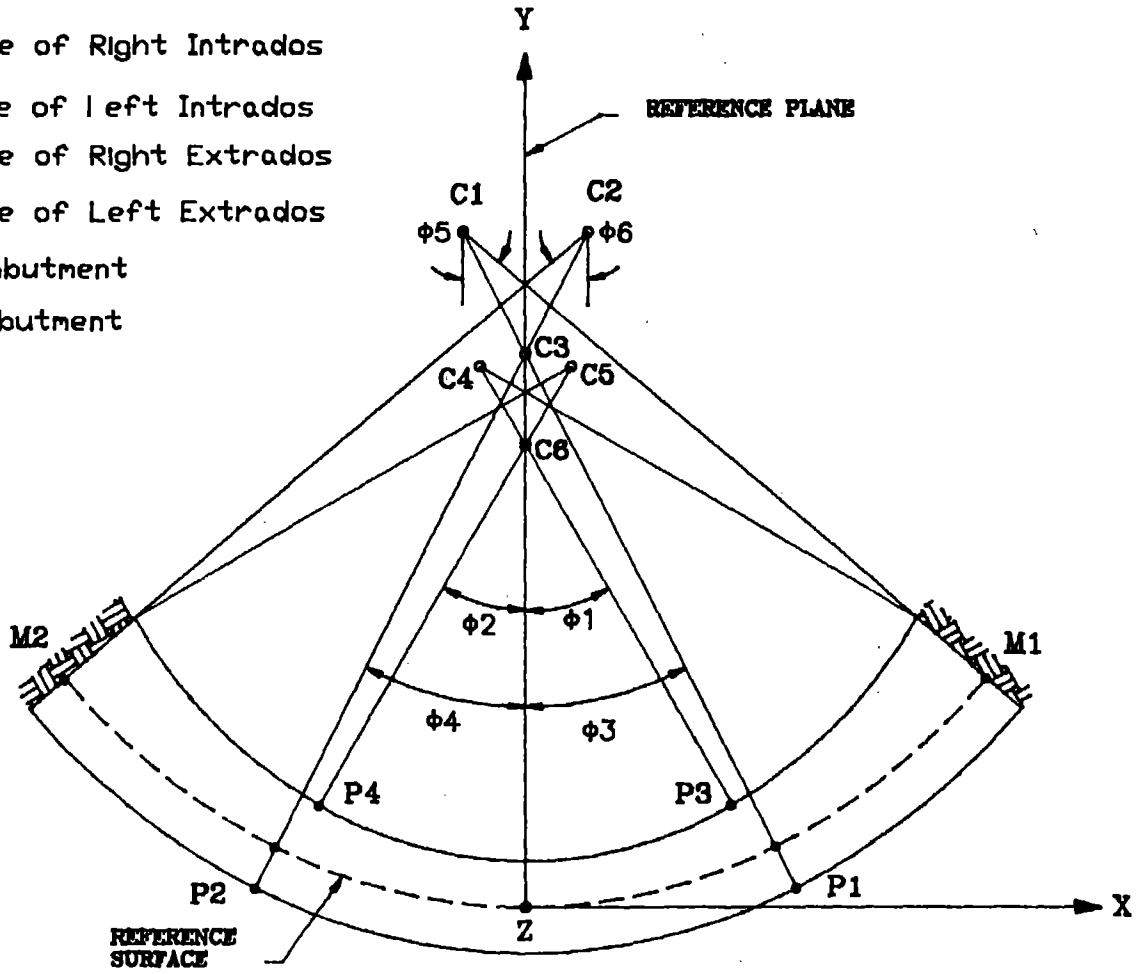

Figure 2.2 Typical Horizontal Section of a Three-Centered Arch Dam

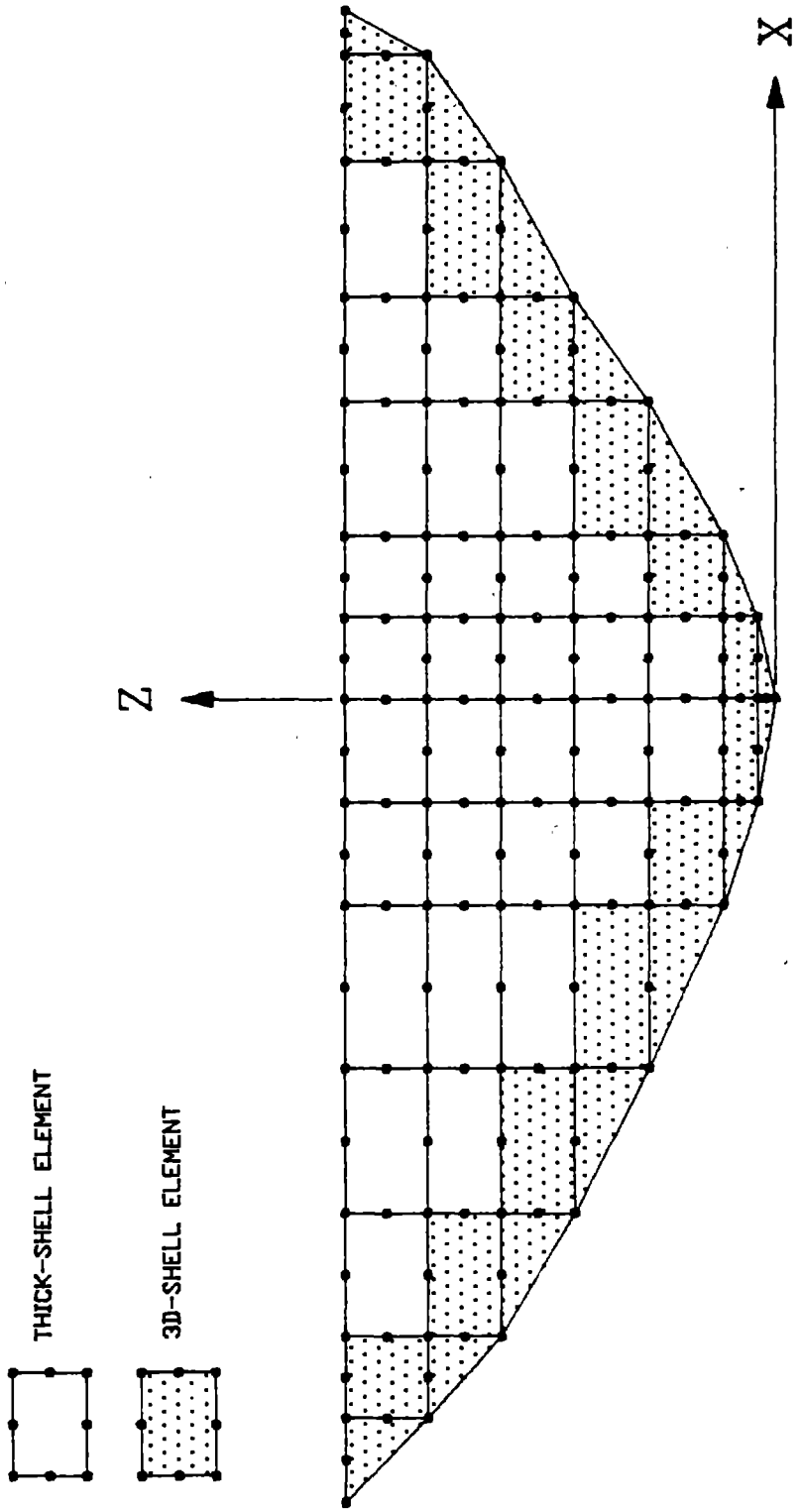

Figure 2.3 Mesh Layout of Shell Elements on Developed Reference Surface (V-Shaped Valley)

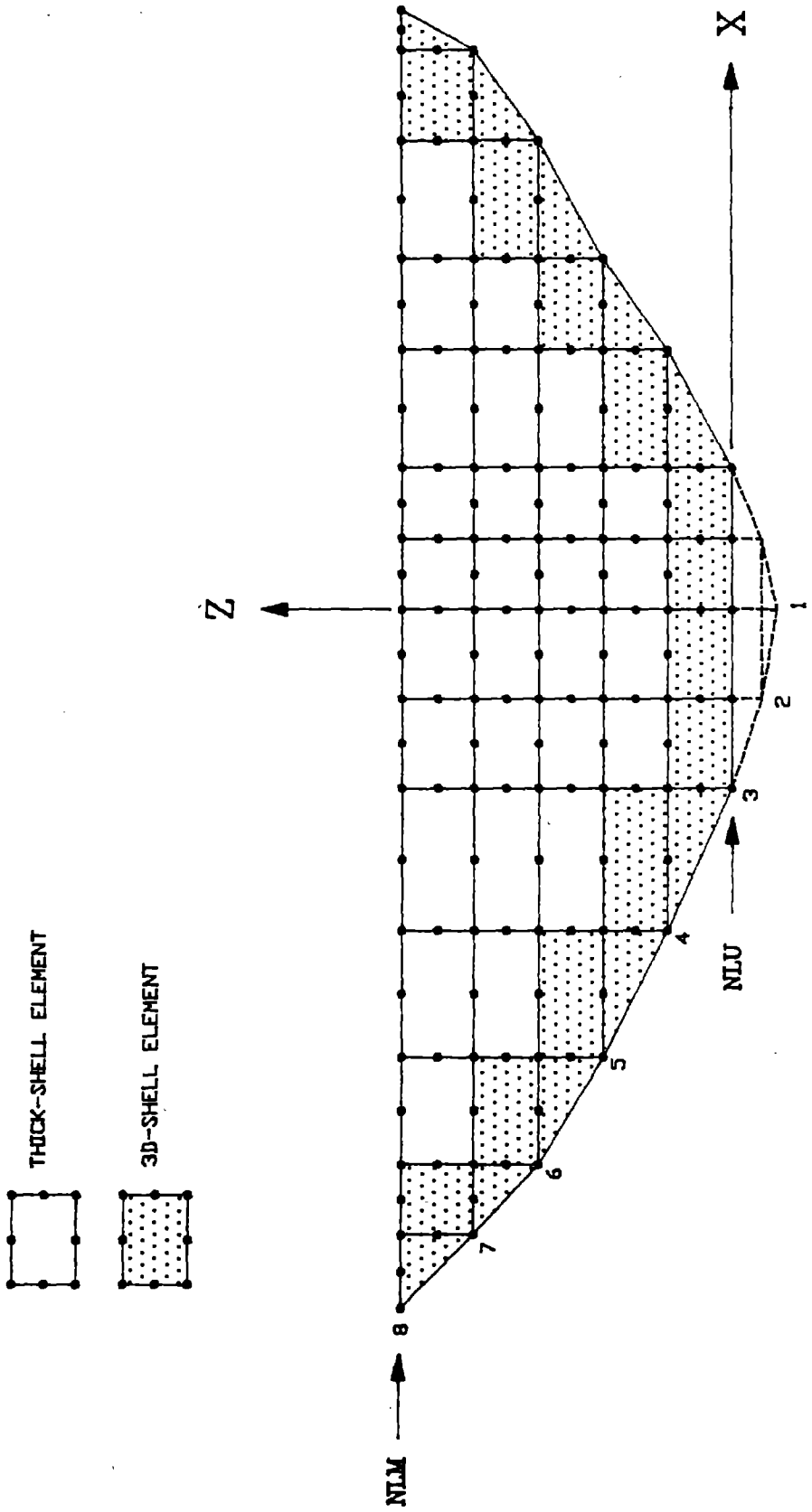

Figure 2.4 Mesh Layout of Thick Shell elements on Developed Reference Surface (U-Shaped Valley)

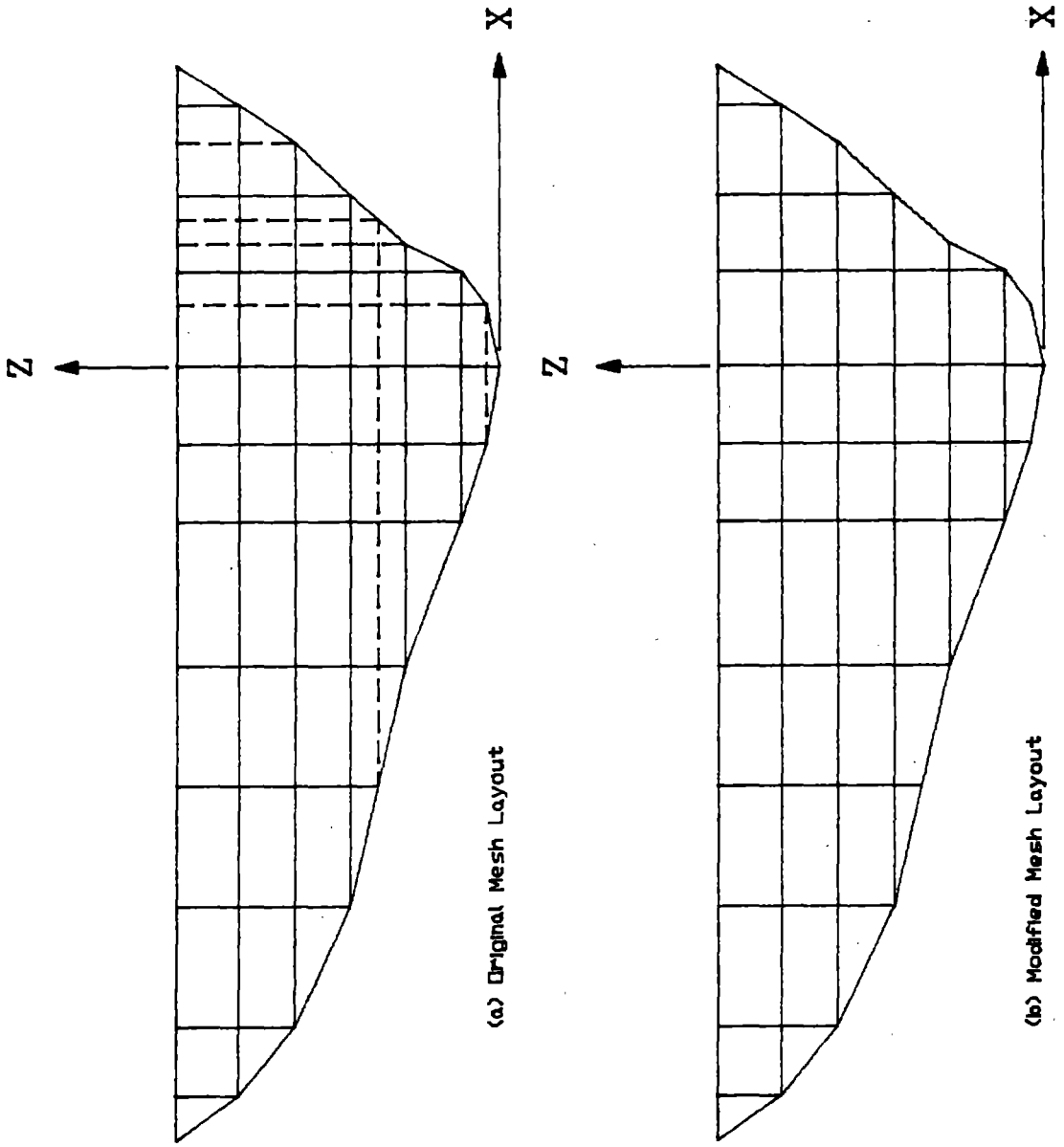

Figure 2.5 Mesh Layout of an Arch Dam with Irregular Geometry

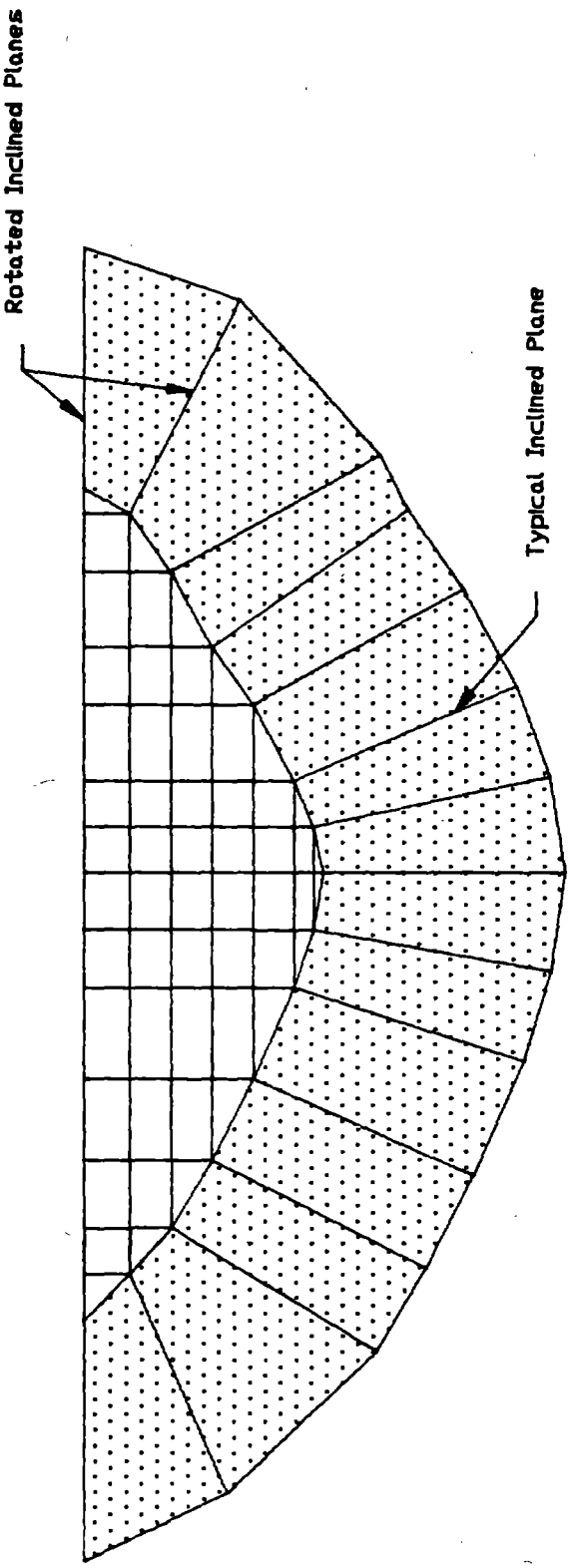

Figure 2.6 Section View of Dam-Foundation System

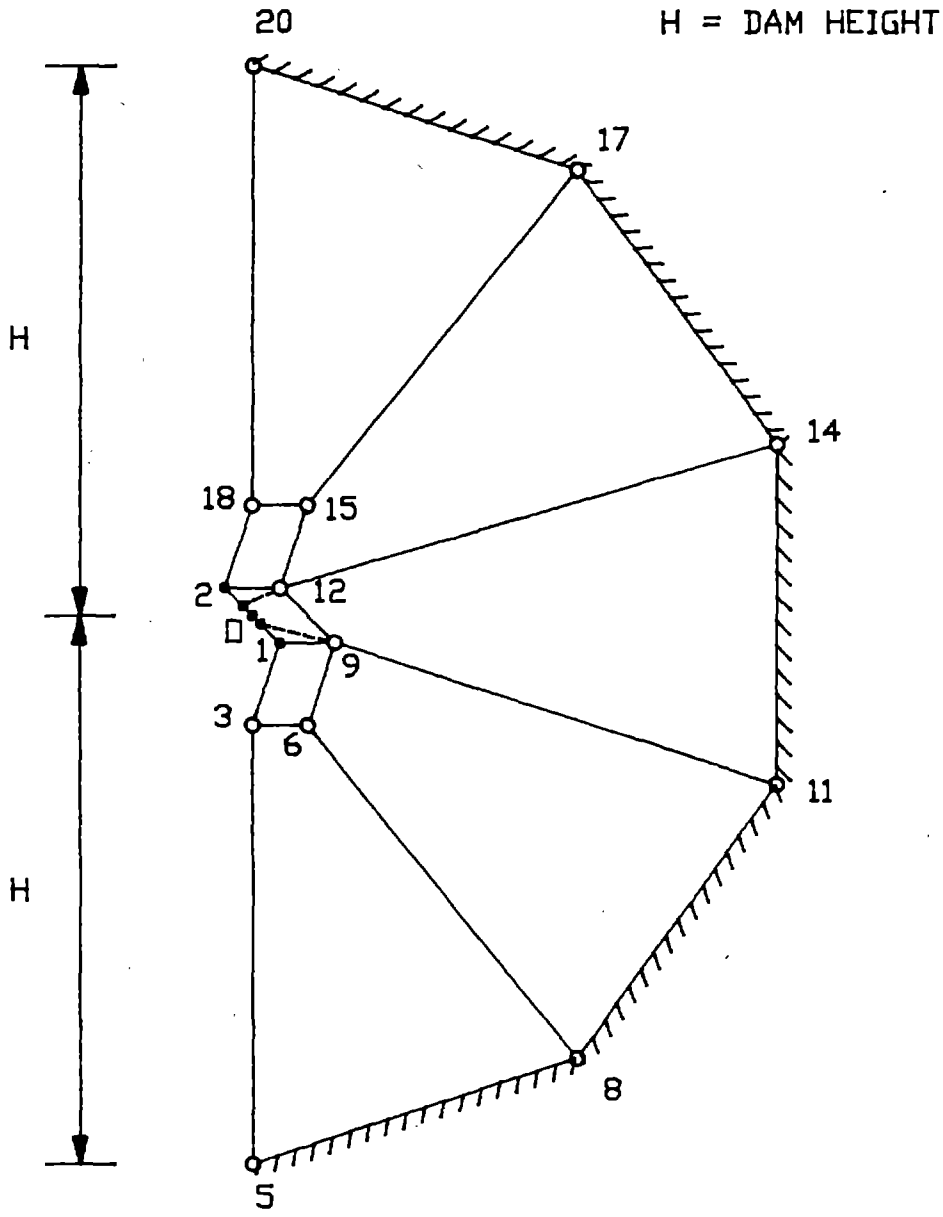

Figure 2.7 Foundation Mesh Type 1 : Sequence of Nodal Points on Inclined Planes

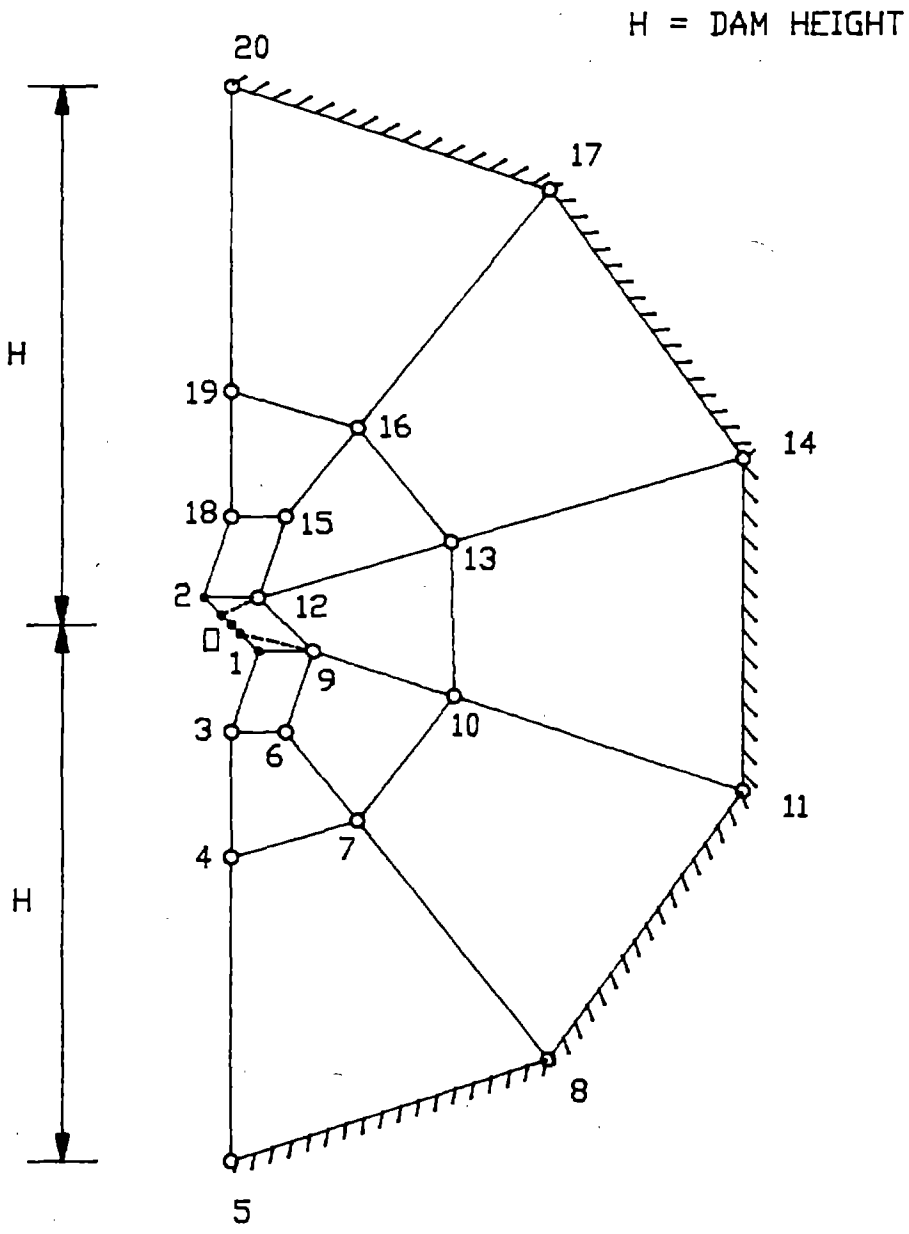

Figure 2.8 Foundation Mesh Type 2 : Sequence of Nodal Points on Inclined Planes

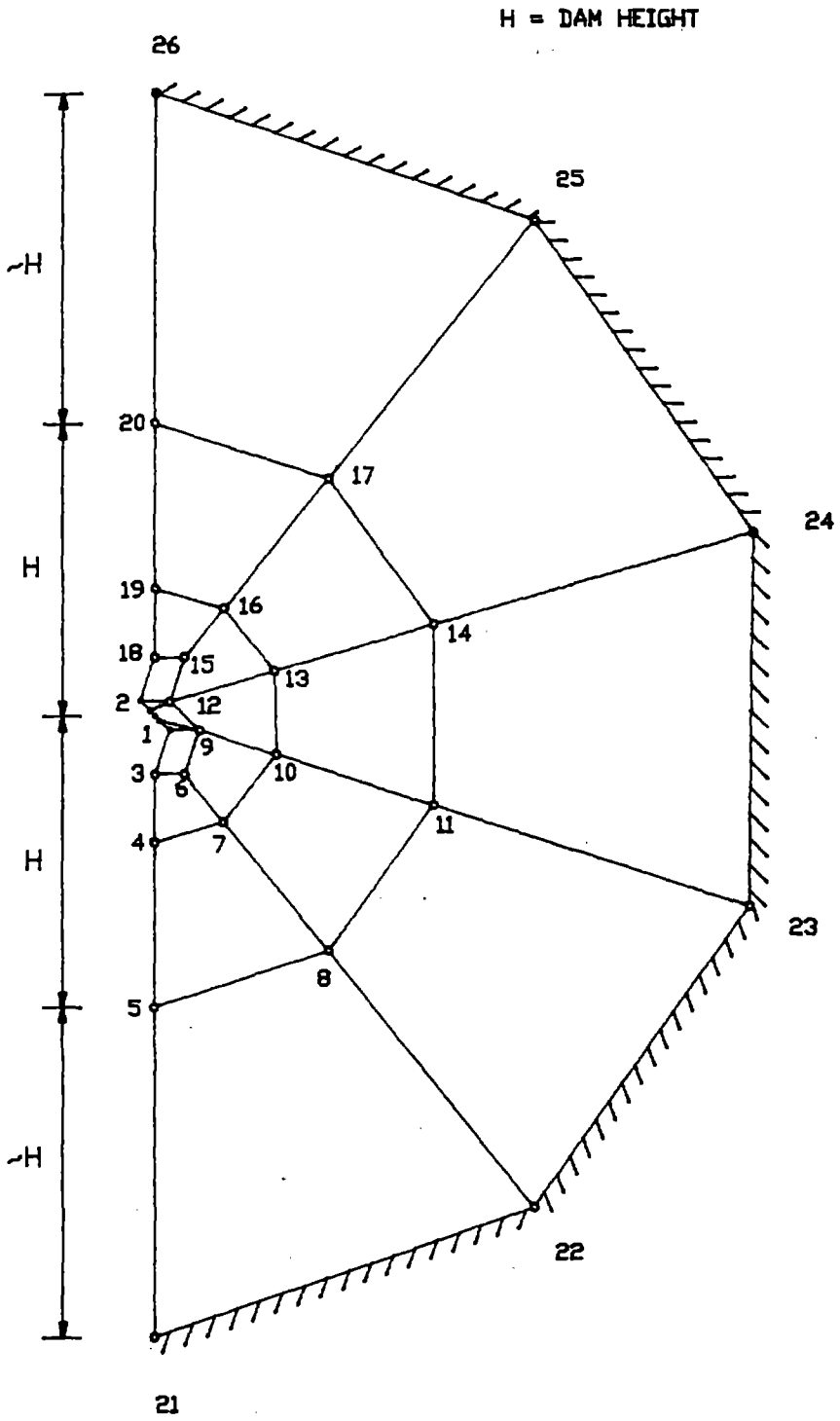

Figure 2.9 Foundation Mesh Type 3: Sequence of Nodal Points on Inclined Planes

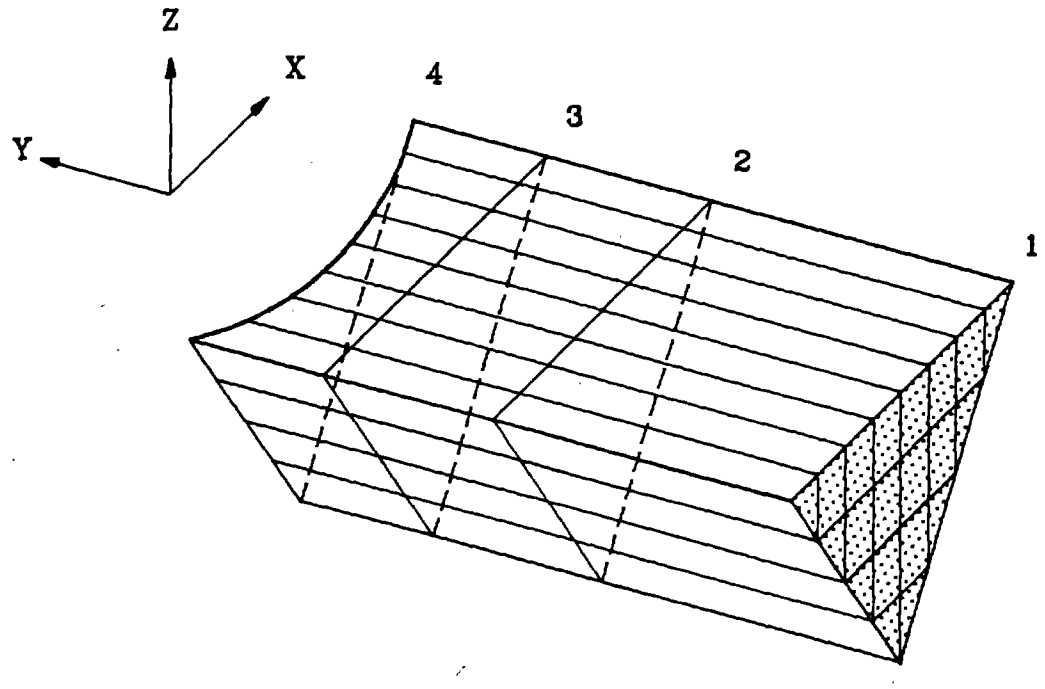

(a) Isometric View of Prismatic Reservoir

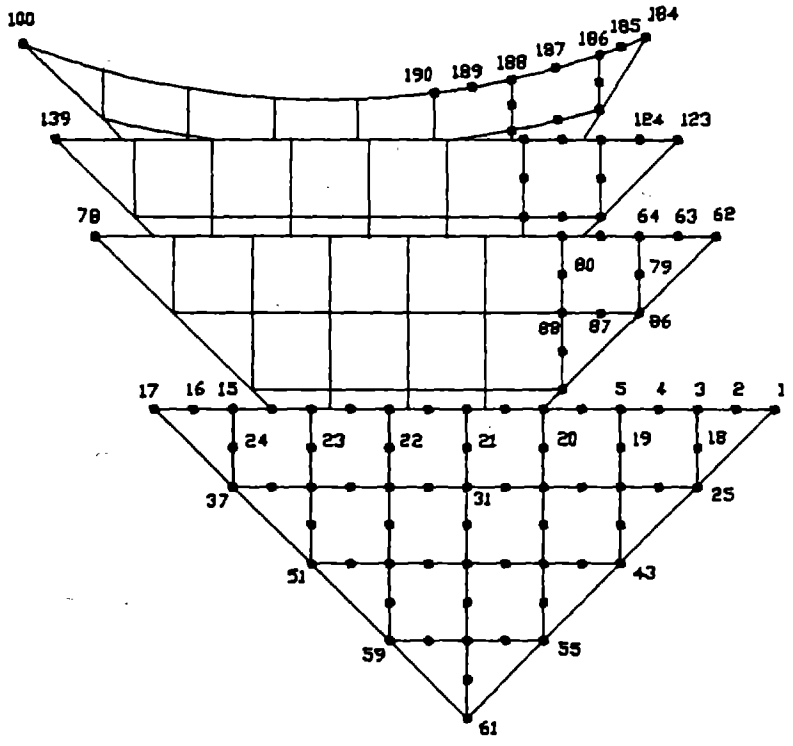

(b) Section View of Liquid Element Meshes in Reservoir
(Looking Downstream)

Figure 2.10 Finite Element Mesh of Reservoir Water

3. DESCRIPTION OF FINITE ELEMENTS

The EADAP program includes three different solid element types for idealizing the dam-foundation system and two liquid element types for modeling the reservoir water. Each element type is briefly discussed below and appropriate references are cited that provide further details.

3.1 Eight-Node Solid Element

A typical eight-node solid element defined with respect to a local curvilinear coordinate system r, s, t is shown in Figure 3.1. The node numbering indicated in this figure shows the order in which the actual node numbers must be input. The element is based on linear isoparametric interpolation and is derived in Reference [6] using the standard description given in Reference [7]. However, the present element employs additional incompatible deformation modes for improved efficiency. These elements generally are used to represent the foundation rock, but they can also be used in the dam in a mesh with three elements through the thickness.

Each nodal point includes three translational degrees of freedom which are defined with respect to global X, Y, Z Cartesian coordinates. The element loading consists of temperature, surface pressure, and inertia loads in three directions. Elastic orthotropic material properties can be specified for this element with the axes of orthotropy coinciding with the global axes. Thus the element can be used to represent a foundation with different mechanical properties in three global directions (vertical, downstream, and cross canyon directions).

Stresses may be computed at two points in each element, at the center of the element and at the center of an individual face. Stresses at the center of the element are calculated in the global X, Y, Z coordinates, while stresses at the face point are given with reference to a local axes (x, y, z) individually defined for each face. Let nodal points I, J, K, and L be the four corners of the element face (Figure 3.1). Then x is specified by LK-IJ, where LK and IJ are mid-points of sides L-K and I-J; z

is normal to the element face and is directed outward from the element; y is normal to x and z, to complete the right-handed system.

When the mesh generator is used to model the dam by eight-node solid elements, the stresses at the free face of the elements of the upstream and downstream layers of the dam are defined such that the x-axis passes through the mid-points of the lower and upper horizontal sides and is directed upward. Thus the x-axis is nearly vertical and σ_{xx}, σ_{yy}, and σ_{xy} components at the face stress points represent the cantilever, arch, and shear stresses, respectively. The stress axes at the face stress point of a six-node solid element are specified similarly, by considering that the lower horizontal side of the element face has degenerated into a single point. Thus, for the six-node elements, the x-axis is not nearly vertical and the stress components σ_{xx}, σ_{yy}, and σ_{xy} cannot be interpreted as the cantilever, arch, and shear stresses, respectively.

3.2 Three-Dimensional Thick Shell Element (3DSHEL)

The three-dimensional thick shell element is a 16-node isoparametric element developed in Reference [8]. The element uses quadratic geometry and displacement interpolation functions in the dam face directions, but only a linear interpolation in the thickness direction. In addition, it includes incompatible deformation modes, which improve its bending behavior. The element is shown in Figure 3.2 with respect to a set of local axes; the element nodes are located at the corners and at the mid-sides of each exterior face. The actual node numbers should follow the numbering order indicated in this figure. Assuming that these elements are mapped into X, Y, Z space such that t is in the negative Y direction, then, to an observer located on the upstream of the dam, the nodes should be numbered counter-clockwise. The element may be degenerated into a triangular form. In that case only 12 nodes are required to define the element (Figure 3.2b). Also any mid-side node can be eliminated by introducing a linear kinematic constraint along that side. This provides a convenient

means for connecting the 8-node elements of the foundation to the three-dimensional shell elements of the dam.

The element loads consist of hydrostatic loads, inertia loads in three directions, and the temperature loads. The temperature distribution within the element is calculated from the nodal temperatures using the same displacement interpolation functions described above. The material properties of a 3DSHEL element are restricted to elastic isotropy. Stresses are given at ten points located at the inner and outer surfaces of the element; locations of these points are shown in Figure 3.3. At any stress point, six stress components are calculated with respect to an orthogonal, right-handed local coordinate system (x, y, z). The local axes are defined such that the x-axis is horizontal and tangent to the face of the dam and the z-axis is normal to the face of the dam, while the y-axis is perpendicular to the x and z-axes. Thus σ_{xx}, σ_{yy}, and σ_{xy} components at each stress point, represent the arch, cantilever and the shear stresses, respectively. For the 12-node degenerated elements the same rules apply, except that the lower horizontal edge of the element degenerates into a single point and the stress points 7 and 8 do not exist.

3.3 Thick Shell Element (THKSHEL)

The thick shell element is described in Reference [9] and is used to represent the central part of the concrete arch. It is based on the same isoparametric interpolation functions described for the 3D shell elements, but its 16 surface nodes are reduced to 8 mid-surface nodes, each having five degrees of freedom; three translations and two rotations. A typical thick shell element is shown in Figure 3.4. Nodes 1 to 8 located at the surface $t=+1$ (corresponding to the dam upstream face) are referred to as the primary nodes and the corresponding nodes on the opposite surface are called the adjacent nodes. Both the primary and adjacent nodes and their locations are actual input data that are provided by the user to describe the element geometry. The same primary node numbers are then used to identify the mid-surface nodes; their coordinates are calculated by averaging the coordinates of the primary and

adjacent nodes on the two opposite surfaces. The boundary conditions and the concentrated loads for each mid-surface node are actually specified for the primary nodes; the corresponding adjacent nodes should be assumed to be fixed. Similarly, the calculated displacements associated with a primary node actually indicate those of the corresponding mid-surface node. The primary nodes should always be numbered first; the actual node numbering of the element should follow the order indicated in Figure 3.4. Thick shell elements are mapped into X, Y, Z space such that local the axis t is in the negative Y direction. Thus, to an observer located on the upstream of the dam, the nodes should be numbered clockwise.

Connection of the thick shell element to any three-dimensional solid element is made possible by transforming the shell element into a transition element. The solid element may be representing either the foundation rock or an adjacent portion of the dam. A transition element has essentially the same characteristics as the thick shell element, except that the five degrees-of-freedom of each mid-surface node along the interface are transformed to the six degrees-of-freedom of the corresponding nodes on the upstream and downstream faces. This transformation is based on the assumption that displacements vary linearly through the element thickness. The transition element is compatible with the eight-node solid elements of the foundation if the mid-side nodes of the transition element at the interface are eliminated. Transition elements are automatically generated by the program based on the boundary condition data provided by the user.

The element loads include hydrostatic loads, inertia in three directions, and the temperature loads. The temperature distribution within the element follows the same interpolation functions that relate the local and global coordinates; thus it is linear in the thickness direction and quadratic in the surface directions. The stresses for the thick shell and transition elements are calculated at eight Gauss Quadrature points located on the two opposite faces of the element (Figure 3.5). At each integration point, five stress components are calculated (the σ_{zz} stress component is assumed to be zero) with reference to a local x,y,z coordinate system which is defined identical to that described for

the 3DSHEL elements. Thus, a total of 40 (8x5) stress components will be obtained for each thick shell element.

3.4 Liquid Elements

Liquid elements used to represent the incompressible reservoir water are formulated as described in Reference [4]. They result from the numerical solution of the pressure wave equation with the nodal hydrodynamic pressures being the unknowns. Two types of elements are employed to represent the dam-water interface and the body of impounded water. The dam-water interface (Mesh-1) is descretized by 8-node curvilinear two-dimensional elements, whereas the impounded water (Mesh-2) is represented by 16-node three-dimensional elements. Both elements are based on isoparametric formulation and use quadratic interpolations in the surface directions; 3D liquid elements use linear interpolation along the element length (channel direction). These elements are shown in Figure 3.6. The nodal points are located at the corners and at the mid-sides of the element surfaces. Triangular elements can be obtained by degenerating an element side into a single point. Any mid-side node may also be eliminated by assuming a zero node number at the location. The liquid elements are mapped into the global X-Y-Z space in such a way that the local t axis is pointing in the negative Y direction. Thus, to an observer looking downstream, nodes should be numbered counter-clockwise.

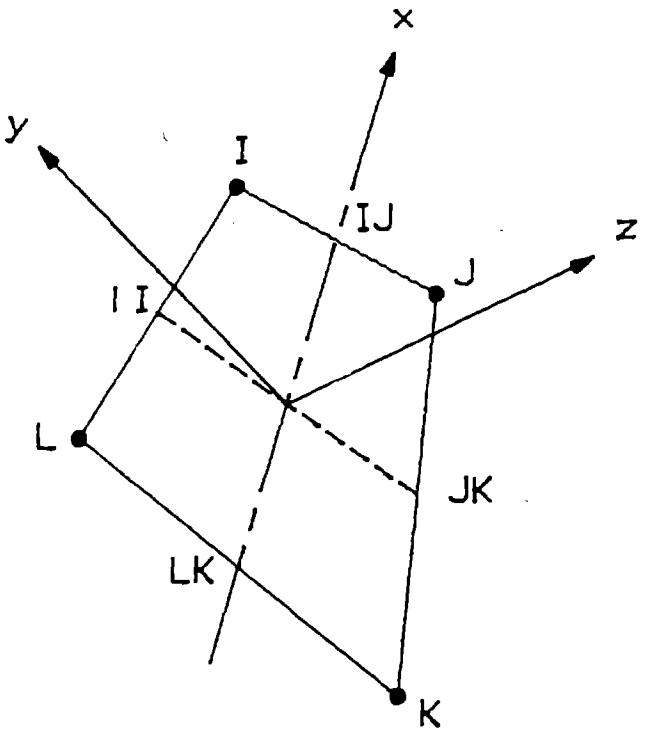

FACE NUMBER	CORNER NODAL POINTS			
	I	J	K	L
1	1	2	6	5
2	4	3	7	8
3	2	3	7	6
4	1	4	8	5
5	5	6	7	8
6	1	2	3	4

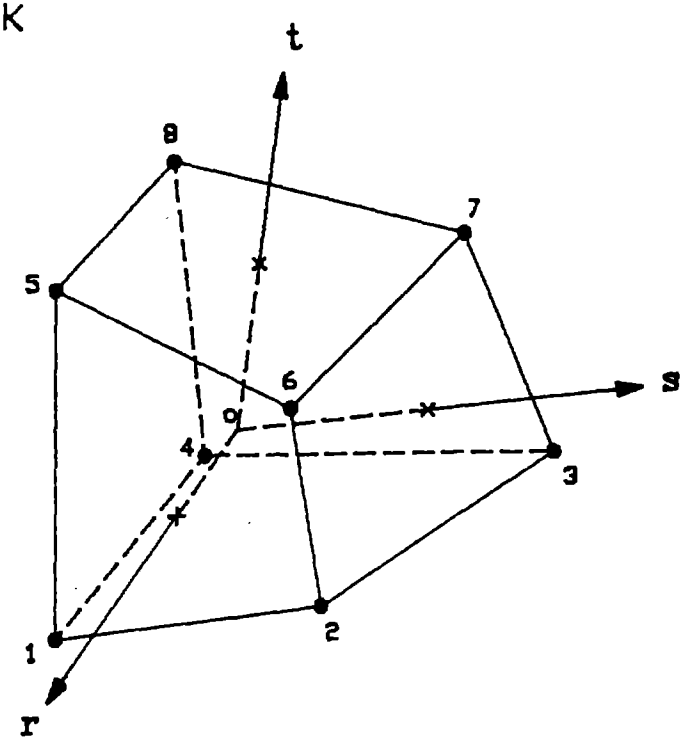

Figure 3.1 Node and Element Face Numbering of 3D Solid Element

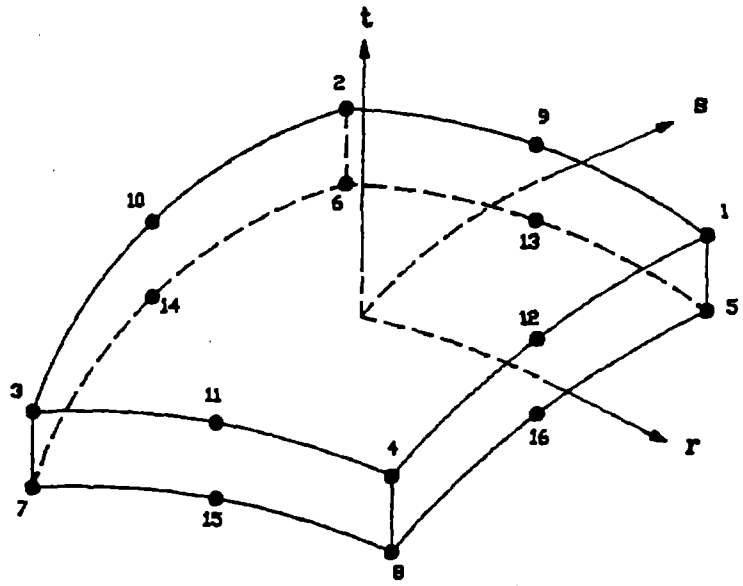

(a) 16-Node 3D Shell Element

FACE NUMBER	CORNER NODAL POINTS			
1	1	4	8	5
2	2	3	7	6
3	5	6	2	1
4	8	7	3	4
5	1	2	3	4
6	5	6	7	8

(c) Element Face Numbering of 3D Shell Element

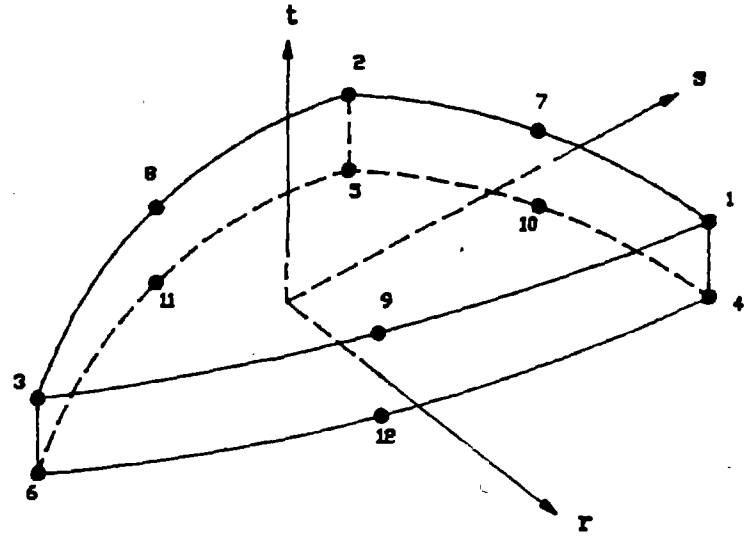

(b) 12-Node Degenerated 3D Shell Element

Figure 3.2 Node and Element Face Numbering of of 3D Shell Element

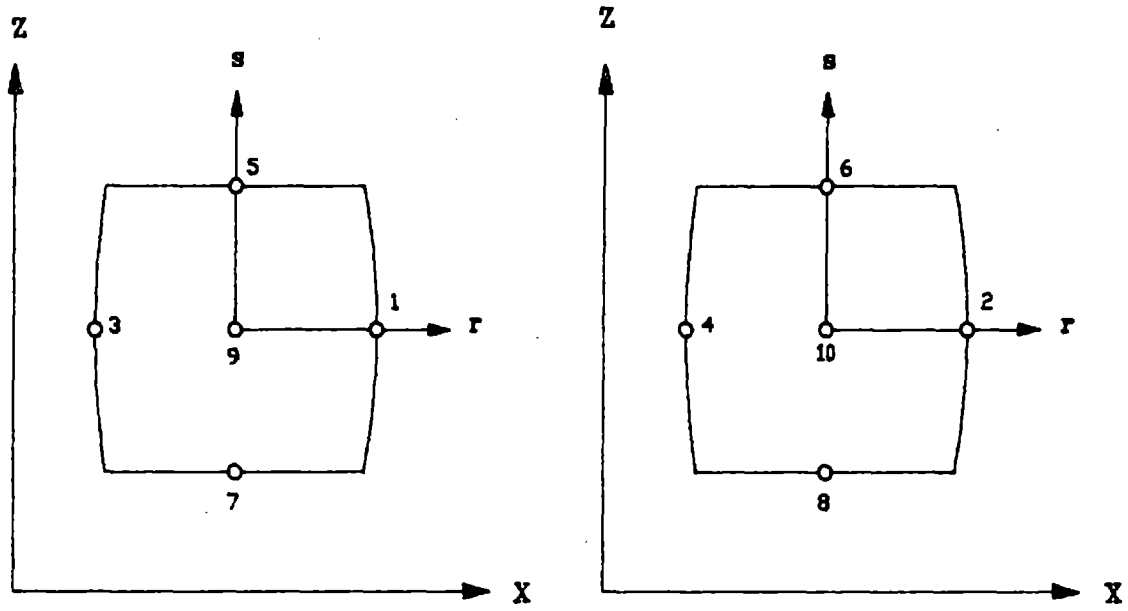

(a) Upstream Face

(b) Downstream Face

Stress Point	r	s	t	Corresponding Node Number	
				16-Node Element	12-Node Element
1	+1	0	+1	12	9
2	+1	0	-1	16	12
3	-1	0	+1	10	8
4	-1	0	-1	14	11
5	0	+1	+1	9	7
6	0	+1	+1	13	10
7	0	-1	-1	11	NONE
8	0	-1	+1	15	NONE
9	0	0	-1		
10	0	0	+1		

(c) Location of Stress Points

Figure 3.3 Location of Stress Points of 3D Shell Elements

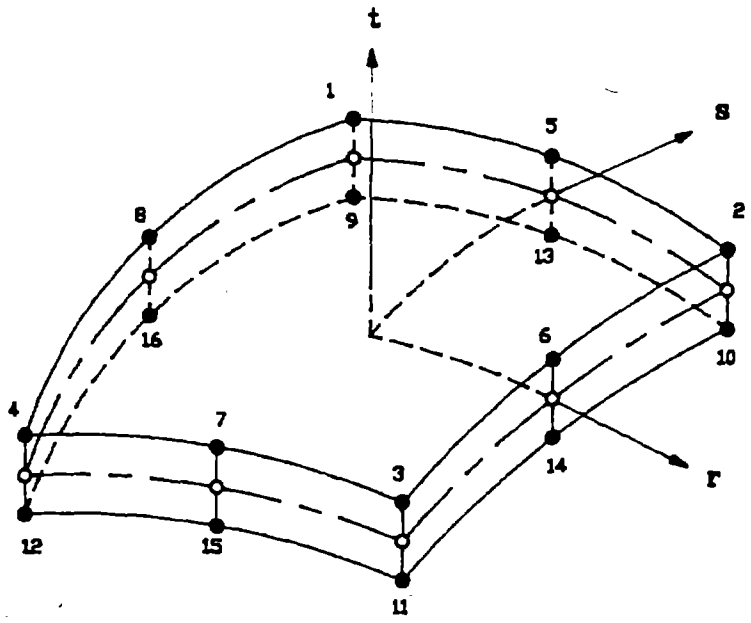

(a) 16-Node Thick-Shell Element

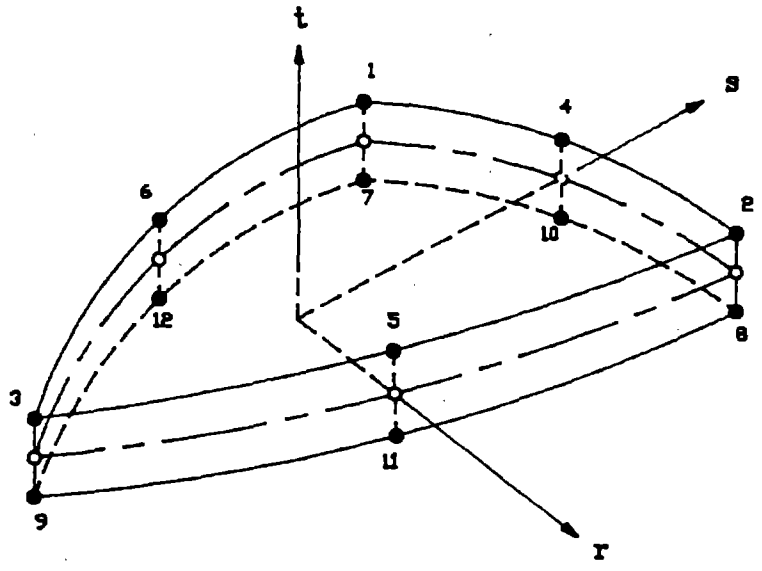

(b) Degenearted Thick Shell Element

Figure 3.4 Node Numbering of Thick-Shell Elements

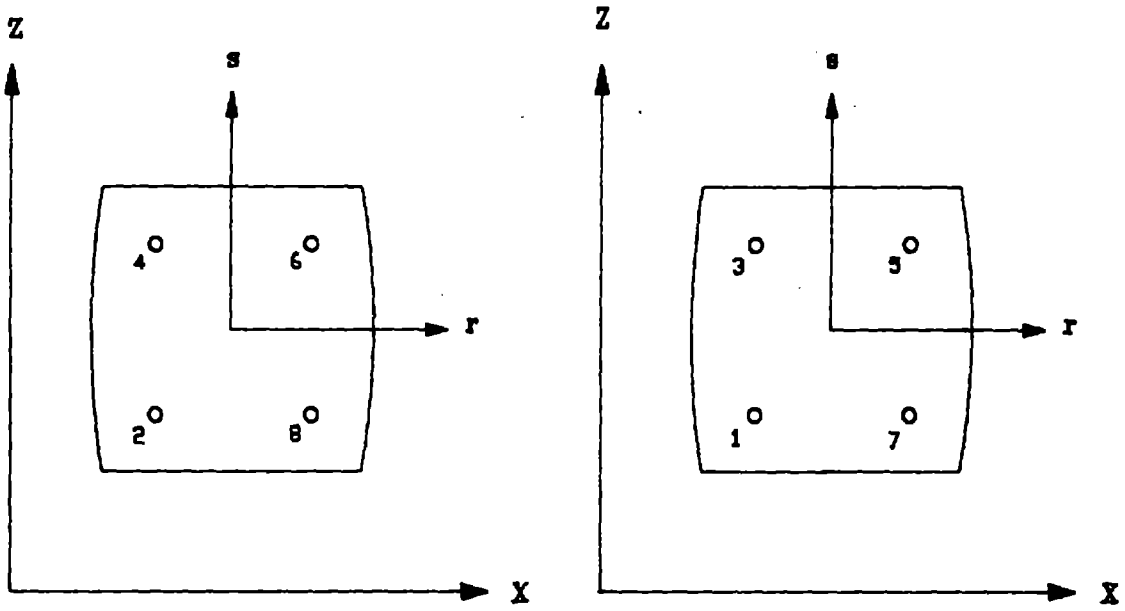

(a) Upstream Face

(b) Downstream Face

Stress Point	r	s	t
1	-0.5774	-0.5774	-1
2	-0.5774	-0.5774	+1
3	-0.5774	+0.5774	-1
4	-0.5774	+0.5774	+1
5	+0.5774	-0.5774	-1
6	+0.5774	-0.5774	+1
7	+0.5774	+0.5774	-1
8	+0.5774	+0.5774	+1

(c) Location of Stress Points

Figure 3.5 Location of Stress Points of Thick-Shell Elements

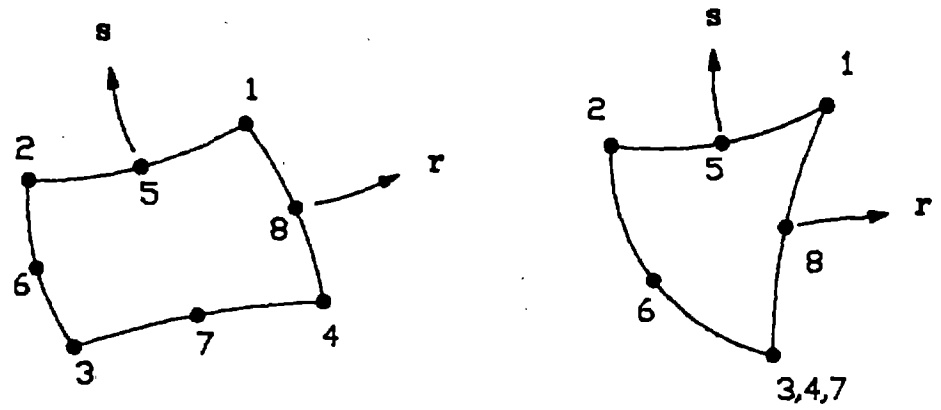

(a) 2D Interface Elements

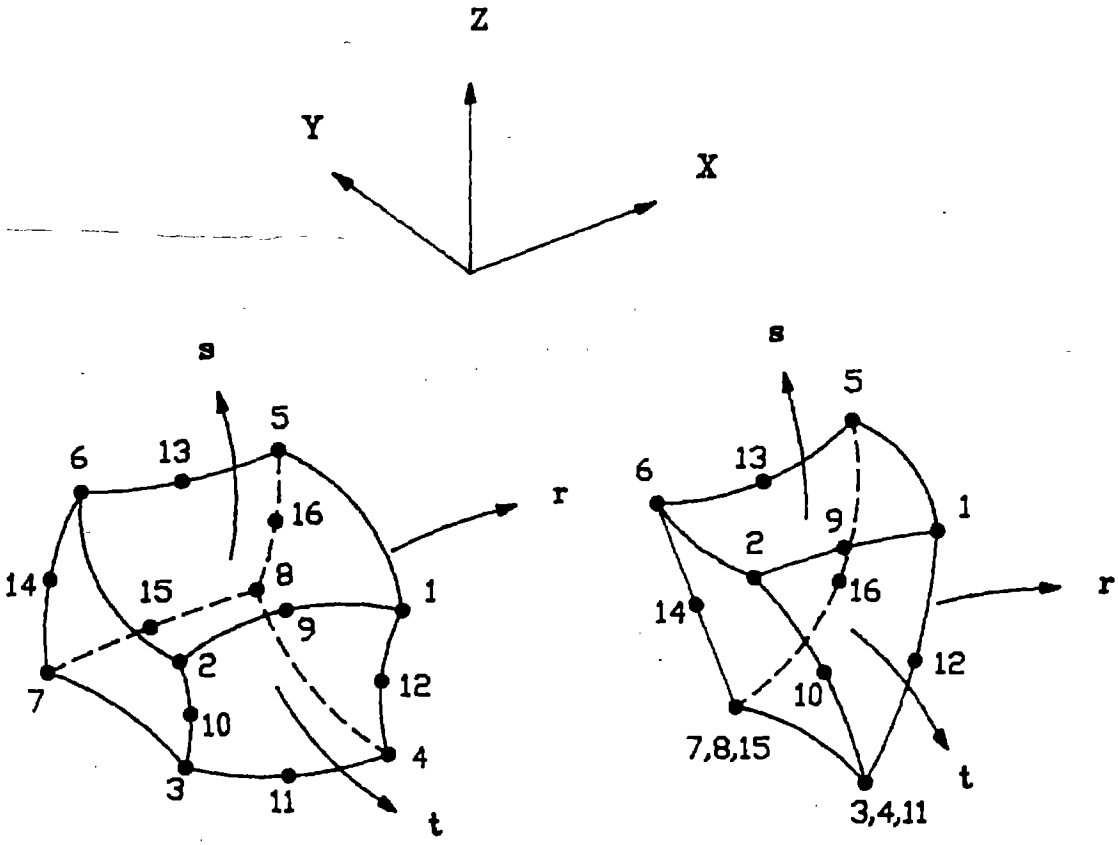

(b) 3D Liquid Elements

Figure 3.6 2D and 3D Liquid Elements

4. OUTLINE OF STATIC ANALYSIS PROCEDURE

The EADAP program performs linear static analyses of any arbitrary arch dam-foundation system. The dam-foundation system is idealized as an assemblage of finite elements as described in the previous chapters. The input data including the geometric and element data are specified using the mesh generation capabilities of the program. However, for more complex geometries, several mesh layouts may be combined manually, in order to obtain an appropriate mesh which is a realistic representation of the dam-foundation system. Linearly elastic material properties are assumed for both the concrete and the foundation rock. Shell elements in the concrete arch are assumed to be isotropic, but orthotropic properties may be specified for the eight-node solid elements representing the foundation rock. Different material properties may be specified for each element. However, only one property type is assigned to each individual element.

The static loads to be considered include concentrated forces or moments at the nodal points and the consistent forces due to the distributed element loads. The element load types consist of the gravity, hydrostatic pressures, silt pressures, and the temperature changes. These loads may be applied separately or as an arbitrary combination together with an arbitrary set of concentrated loads. The following is a brief description of the various static loads.

4.1 Gravity Load

Gravity loads due to the weight of the concrete may be applied with or without the effects of the construction joints. When the construction joints are ignored, the arch dam is treated as a continuous shell and the weight is applied at one instant to the entire structure. However, in the actual arch dam construction process, cantilever monoliths are free standing until the joints are grouted. Thus each cantilever supports its own gravity load without any arch action. The analysis for this situation is handled in two steps. In the first step the gravity loads are applied to alternate cantilevers by assuming zero modulus of elasticity for the remaining cantilevers. The second step is performed

similarly, except that the alternate cantilevers are switched. The stress results from the two steps are then superimposed.

4.2 Water Load

Water loads are applied in the form of hydrostatic pressures acting on appropriate faces of the dam and foundation elements. When mesh generation is used, only the water level needs to be specified; the elements subjected to the hydrostatic pressures are automatically identified by the program. However, in the manual input mode, the user must specify not only the water level, but also the elements and the faces on which the hydrostatic pressures are acting.

4.3 Temperature Load

Various temperature changes including uniform, differential, and linear temperature changes may be specified by the mesh generator. Temperature changes may vary with elevation and in the direction of dam thickness, but they are assumed to be constant across the arch sections. Temperature values at each mesh elevation are obtained by cubic interpolation from the user specified values at the design elevations. The nodal temperature values at all concrete nodes are then calculated based on the uniform temperature assumption across the arch sections. No temperature change is considered for the foundation. The nodal temperature values generated according to the above rules may be over-ridden by supplying the desired values as the input data. Thus, it is possible to consider temperature changes across the arch sections by directly supplying them as the input nodal temperature values.

4.4 Silt Load

The pressure exerted by the saturated silt load on the face of a dam may be assumed to be equivalent to that of a fluid with an appropriate weight per unit volume. Thus the static analyses due to silt loads are carried out exactly the same as those of the water loads.

4.5 Ice Load

Ice loads may be considered by treating them as equivalent concentrated loads applied at the upstream face of the dam.

4.6 Results of Static Analysis

The results of static analysis include nodal point displacements and element stresses due to the applied loads. The displacements of each thickshell node consist of five components, three translations in the direction of global axes and two rotations about the local rotation axes. All other element types have only three global translations per node.

For each element, stresses are calculated at several points referred to as stress points and are presented with respect to a set of local axes, except at the center of eight-node solid elements where the stresses are given in reference to the global axes. The stress points and stress axes for each element type were described earlier in Chapter 3. The element stresses are given on the upstream and downstream faces of the dam and include the arch, cantilever, shear, and the minor and major principal stresses together with the angle defining the principal directions.

5. OUTLINE OF DYNAMIC ANALYSIS PROCEDURE

Dynamic analysis involves solving the equations of motion assembled for the dam-foundation-reservoir system, and includes the interaction effects of both the foundation rock and reservoir water. The equations of motion of the system can be written as:

$$(\mathbf{M}+\mathbf{M_a})\,\ddot{\mathbf{U}} + \mathbf{C}\,\dot{\mathbf{U}} + \mathbf{K}\,\mathbf{U} = -\,(\mathbf{M}+\mathbf{M_a})\,\mathbf{r}\,\ddot{\mathbf{U}}_g$$

where,

- $\mathbf{M}$ = Mass matrix of the concrete arch system
- $\mathbf{M_a}$ = Added-mass of the reservoir system
- $\mathbf{C}$ = Viscous damping matrix
- $\mathbf{K}$ = Stiffness matrix of the dam-foundation system
- $\mathbf{U}$ = Nodal displacement vector
- $\dot{\mathbf{U}}$ = Nodal velocity vector
- $\ddot{\mathbf{U}}$ = Nodal acceleration vector
- $\ddot{\mathbf{U}}_g$ = Vector of earthquake accelerations
- $\mathbf{r}$ = Influence coefficient matrix

Note that the foundation rock is assumed to be massless, and thus does not contribute to the mass matrix. The solution is obtained using the mode-superposition method of dynamic analysis [12]. In this method, first the equations of motion are transformed to the uncoupled modal coordinate form using the free vibration mode shapes of the system (including added reservoir mass). Then the response for each uncoupled equation is computed and these modal responses are superimposed to obtain the total response of the structure. Two types of mode-superposition method are provided in the program: the response spectrum and the response history methods. In both methods three translational components of the ground motion may be applied simultaneously in the analysis. In the following sections, the procedures used in evaluating the added-mass of the reservoir, the system frequencies and mode shapes, the response spectrum, and the response history analysis are discussed.

5.1 Added-Mass of Water

The added-mass of the incompressible water is obtained from the hydrodynamic pressures along the face of the dam by solving the Helmholtz pressure wave equation. The solution is based on the finite-element formulation which takes full account of the very significant effects resulting from the geometry and flexibility of the dam as well as the natural topography of the reservoir. The finite-element formulation for the added-mass calculation is given in Reference [4]. A brief description of the solution procedures as applied in the INCRES program is presented here.

In this approach, the reservoir water is descretized by 2D and 3D liquid elements and is bounded on the upstream by a vertical plane located at a distance from the dam of about three times the dam height. The hydrodynamic pressures at the element nodal points are the unknowns: one degree of freedom for each node below the water free surface. The bottom and side walls of the incompressible reservoir and the vertical plane at the upstream end are assumed to be rigid. The hydrodynamic pressures at nodal points on the reservoir free surface are set to zero, and thus the effects of surface waves are neglected. Furthermore, the pressures along the dam-reservoir interface are related to the total nodal accelerations in the direction normal to the dam face.

The finite-element descretization of the wave equation with the above boundary conditions leads to a symmetric system of equations with the nodal pressures as unknowns. The hydrodynamic pressures acting on the face of the dam are determined by solving the resulting system of equations for the dam-reservoir interface degrees of freedom only; all nodal pressures within the body of the reservoir are eliminated by static condensation. In the INCRES program, the degrees of freedom corresponding to the interface nodal points are numbered last to facilitate the reduction process. The calculated hydrodynamic pressures on the face of the dam are then converted into equivalent nodal forces using a consistent lumping process. Since the hydrodynamic forces, like the pressures, are proportional to the accelerations at nodal degrees of freedom on the face of the dam, this conversion leads to the added-mass coefficient matrix. The added-mass coefficient matrix is then rearranged with respect to

the degrees of freedom of the concrete nodes on the upstream dam face and is stored on a disk file for later use by the EADAP program. The rearranged added-mass matrix in the binary form is supplied as additional input data, so that its contribution to the mass of the concrete can be accounted for in the eigenproblem or the earthquake response analyses.

5.2 Mode Shapes and Frequencies

The first step in the mode-superposition method of dynamic analysis is evaluation of a limited number of the lower natural frequencies and mode shapes of undamped free vibration of the system. The mode shapes and frequencies give great insight into the dynamic response behavior of the structure, and are used to uncouple and reduce the number of equilibrium equations of the system. The free vibration problem is solved using the subspace iteration technique [13] which is especially effective for large structural systems such as arch dams. It should be noted that the EADAP subroutines related to this algorithm have been modified to handle the non-diagonal mass matrices of the concrete and the reservoir water. The eigenvalue problem is solved for the dam-foundation-reservoir system considering only the flexibility (no mass) of the foundation and including the added-mass of the reservoir water . Other conditions such as an empty reservoir and a rigid foundation may be analyzed as special cases.

The results of the free vibration analysis include a limited number of the lower frequencies and mode shapes of the system. The desired number of modes should be specified by the user and depends both on the properties of the structural system and the frequency content of the earthquake ground motion. In the program output, the frequencies are tabulated and the mode shapes are printed in the form of nodal displacements. In addition, the calculated mode shapes and frequencies in binary forms are stored on restart files for use in the subsequent response spectrum or response history analyses.

5.3 Response Spectrum Analysis

The earthquake response spectrum provides an approximate mode-superposition method for calculating the maximum response of structures. The maximum response in each natural mode of vibration is first computed based on the spectral acceleration of the specified earthquake motion, corresponding to the vibration period and the damping ratio of the mode. The modal maxima computed for each mode and for each component of the earthquake motion, are then combined by the square-root-of-the-sum-of-the-squares (SRSS) method to obtain the total response of the structure. For a linear-elastic response, only a few modes are needed to express the essential dynamic behavior.

The previously calculated vibration mode shapes and frequencies, the added-mass of the reservoir water, and the spectral acceleration values of the specified earthquake motion are the input to the program. The results of the response spectrum analysis are the estimated maximum nodal displacements and the element stresses of the dam structure. These results are printed out in the same way as was described for the static analysis.

5.4 Response History Analysis

In the response history analysis, the uncoupled equations of motion expressed in modal coordinates, are solved by the linear acceleration step-by-step integration method [13]. The resulting modal displacements and stresses at each time step are then superimposed to obtain the total response history of the structure. The same integration time step and the same modal damping ratio are specified for all modes. However, the integration time step should be selected small enough to obtain accuracy in the integration of all modal responses which significantly contribute to the total structural response. In general, a time step at least 5 to 10 times less than the lowest period in the system, will provide good accuracy for all modes that are considered in the analysis. To assure stability and

accuracy of the solution, the program EADAP automatically filters the high mode response, for which the period of vibration is less than 5 times the integration step.

The free vibration mode shapes and frequencies and the added-mass of the reservoir are read from the restart files as input to the program. The seismic input includes the acceleration time histories that are assumed to be applied at the foundation rock boundary points. Any single component of a selected accelerogram or all three accelerogram components may be specified by the user as input. The results of the analysis include the displacement and stress histories of the nodes and elements prescribed by the user as part of the input data; response histories may be requested for all or selected nodes and stress components. The output also includes the maximum and minimum displacements and stress components developed at any time during the earthquake (the so-called envelope values) and the times at which they occur. In addition, the maximum and minimum modal values of the displacements and stress components of those modes included in the analysis are also provided. This provides information regarding the relative influence of each mode of vibration on the various stress and displacement components.

6. EXAMPLE STATIC AND DYNAMIC ANALYSES OF MONTICELLO DAM

This section presents results of static and dynamic analyses of Monticello Dam which was selected as an example structure to demonstrate the use of the EADAP and INCRES programs. Input data files for each analysis are provided in the floppy diskette containing the source programs. The finite-element models of the Monticello dam-foundation-reservoir system, static loads, material properties, and the seismic input are described, and selected response results are presented.

A graphics pre- and post-processing package described in an appendix was used extensively, to prepare all the 3D and 2D figures presented in this report, and to display the results of the example analyses.

6.1 Finite Element Models

Monticello Dam is a 304 ft high concrete arch which was designed by the U.S. Bureau of Reclamation and was completed in 1957 [14]. It has a crest length of 1,025 ft, a crest thickness of 12 ft, and a maximum thickness of 86 ft at the base of the dam. The dam is located on Putah Creek about 30 miles west of Sacramento, California

The finite element models of the dam and foundation rock were automatically generated by the mesh generator of EADAP, and the reservoir model was constructed based on the procedures described above. A perspective view of the finite element models is shown in Figure 2.1, and the mesh layout of the arch structure on the developed reference surface is depicted in Figure 2.3. The concrete arch model includes 8 mesh elevations and consists of 26 3D-shell and 30 thick-shell elements (Figure 6.1); node numbers on the upstream face of the dam are given in Figure 6.2 for reference purposes. The foundation rock which was idealized by the mesh type-1, includes 112 eight-node solid elements. The prismatic finite-element mesh of the reservoir in section view along the channel is shown in Figure

6.3. It consists of three liquid layers including 168 three-dimensional and 56 two-dimensional liquid elements, and extends upstream to a distance equal to three times the dam height (873 ft).

6.2 Material Properties

The following material properties are assumed for the static and dynamic analyses:

Material Property		Static	Dynamic
Concrete Unit Weight	*(pcf)*	150	150
Concrete Modulus of Elasticity	*(psi)*	$3x10^6$	$4x10^6$
Concrete Poisson's Ratio		0.2	0.2
Rock Modulus of Elasticity	*(psi)*	$3x10^6$	$4x10^6$
Rock Poisson's Ratio		0.2	0.2
Water Unit Weight	*(pcf)*	62.4	62.4

6.3 Static Analysis

Static analysis was performed for the separate and the combined action of the gravity and water loads. The water surface was assumed at elevation 420 ft and the gravity loads were applied to the grouted dam. The input data file for this analysis is STATIC.IN which includes three load cases, gravity alone, hydrostatic alone , and the gravity and hydrostatic loads combined. The results of the analysis for the combined loading case are given in Figures 6.4 and 6.5. These are the arch and cantilever stress contours plotted on the upstream and downstream faces of the dam. Stresses are given in units of psi with positive and negative values representing tension and compression, respectively.

6.4 Reservoir Added-mass

In dynamic analysis with full reservoir, the added-mass of the reservoir water was calculated separately by the program INCRES. The input data file (INCRES.IN) for the finite-element reservoir model was constructed according to the descriptions given in Chapters 2 and 8. The resulting added-mass matrix in binary form is stored in TAPE12.DAT for use in the frequency and dynamic response analyses. It should be noted that the added-mass data in TAPE12.DAT is defined with respect to the degrees of freedom of the nodes on the upstream face of the dam, and thus it can be directly used as input to the EADAP program in the subsequent analyses.

6.5 Vibration Frequencies and Mode Shapes

The free vibration analysis of Monticello Dam was carried out for the empty and full reservoirs. In both analyses, EIGEN.IN was the standard input data; for the full reservoir case, the added-mass matrix (TAPE12.DAT) was supplied as additional input. Seven frequencies and mode shapes were calculated. The natural frequencies are given in the table below, and the mode shapes for the full reservoir case are plotted along arch sections in Figure 6.6.

Natural Frequencies of Dam-Foundation System
With Empty and Full Reservoirs (Hz)

Mode No.	Empty Reservoir	Full Reservoir
1	3.70	3.22
2	4.02	3.63
3	5.13	4.75
4	6.20	5.86
5	7.51	6.88
6	8.14	7.19
7	8.94	8.52

In the vibration analysis, in addition to the standard output file, the mode shapes and frequencies and the structural properties are saved in binary output files that are used as input in the earthquake response analysis. This information is as follows:

File Name	Description
TAPE1.DAT	*Stress Matrices of Elements*
TAPE8.DAT	*Nodal Point Data*
TAPE9.DAT	*Structure Mass Matrix*
TAPE10.DAT	*Mode Shapes and Frequencies*

6.6 Seismic Input

The ground motion recorded at Morgan Hill, California, in April 1984 [15] was selected as the ground acceleration applied for this example analysis. The ground acceleration time histories for the upstream, cross-stream, and the vertical directions are shown in Figure 6.9. The maximum peak ground acceleration for the upstream component is 0.34 g. The response spectra calculated from these input motions are supplied as input data for the response spectrum analysis. It should be noted that the earthquake motion and the material properties have been selected arbitrarily, and thus the results of the earthquake analysis presented here should not be used for evaluation of the safety of Monticello Dam.

6.7 Response Spectrum Analysis

RSPEC.IN is the standard input data provided for the response spectrum analysis of Monticello Dam. It contains response spectra for three components of the earthquake motion that are applied simultaneously. The structural data and mode shapes are read from the restart files generated in the

free vibration analysis; the added-mass of the reservoir stored on TAPE12.DAT is also provided as input. A damping ratio of 5% is assumed for all modes.

The results of the analysis include nodal displacements for each mode of vibration, the SRSS nodal displacements, and the SRSS stresses for all elements. The SRSS stress results are given with respect to the element local coordinate system, and thus represent the arch, cantilever, and shear stresses. The arch and cantilever stress contours plotted on the upstream and downstream faces of the dam are shown in Figures 6.7 and 6.8.

6.8 Response History Analysis

The standard input data for the response history analysis is provided in TIMHIST.IN file. This file includes acceleration records for the three components of the Morgan Hill earthquake motion (Figure 6.9). Similar to the response spectrum analysis, a modal damping ratio of 5% is assumed and the three components of the earthquake motion are applied simultaneously. The same restart files consisting of the structural data, mode shape and frequencies, and the added-mass of the reservoir are supplied as additional input.

A complete response history analysis of Monticello Dam was performed using the EADAP program. Displacement response histories for an upstream crown node at the crest (Node 323) are shown in Figure 6.10. The maximum arch and cantilever stresses occurred on the upstream faces of thick-shell elements 11 and 14, respectively. Time histories of the arch and cantilever stresses at these locations and at the corresponding opposite points on the downstream face are presented in Figures 6.11 and 6.12. In addition, the envelope of maximum arch and cantilever stresses due to the earthquake loads alone are presented in Figures 6.13 and 6.14, respectively. These are the maximum stresses that in general would occur at different time steps; they may be directly compared with the results of the response spectrum analysis.

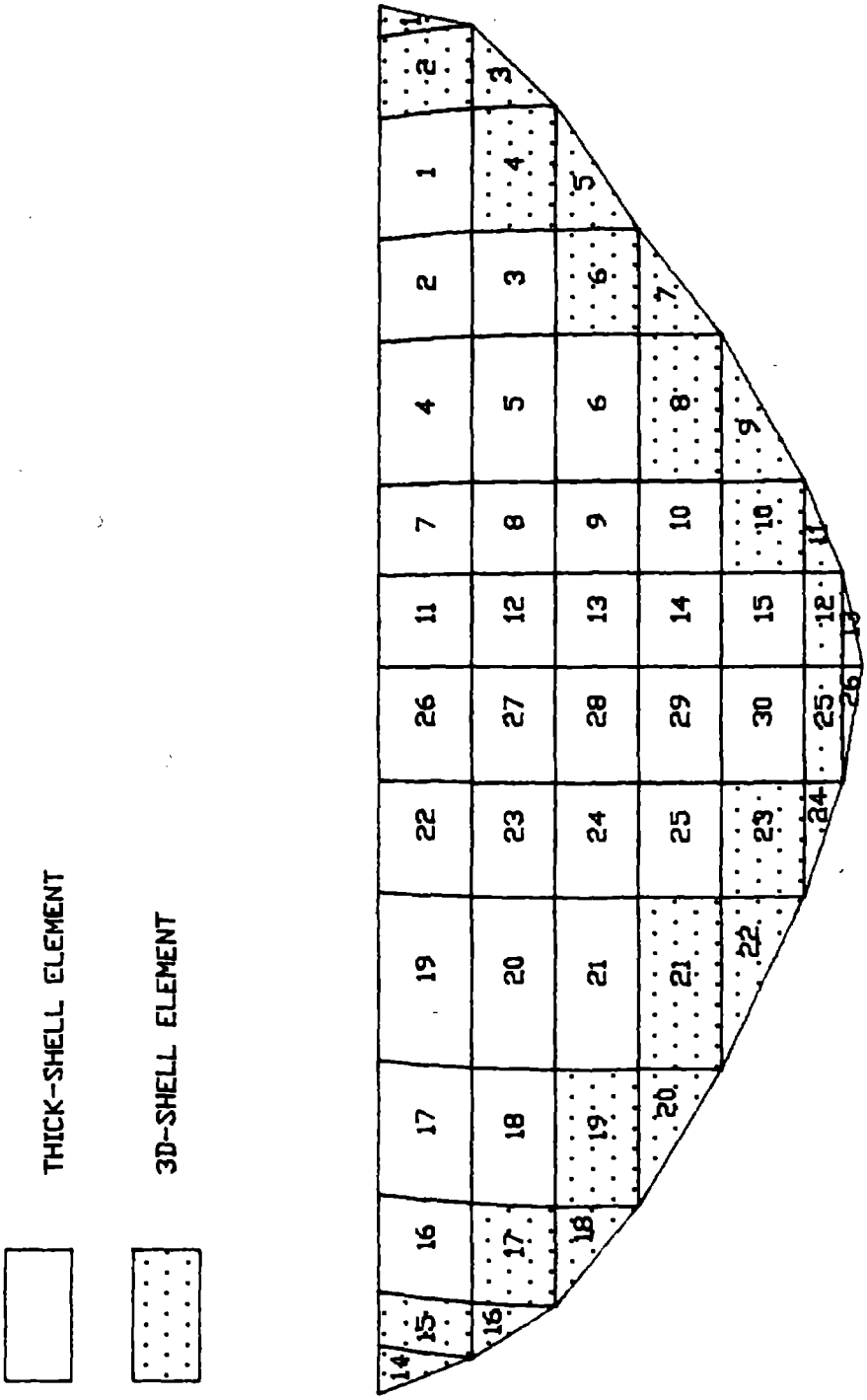

Figure 6.1 Element Numbers of Monticello Dam Model

Preceding Page Blank

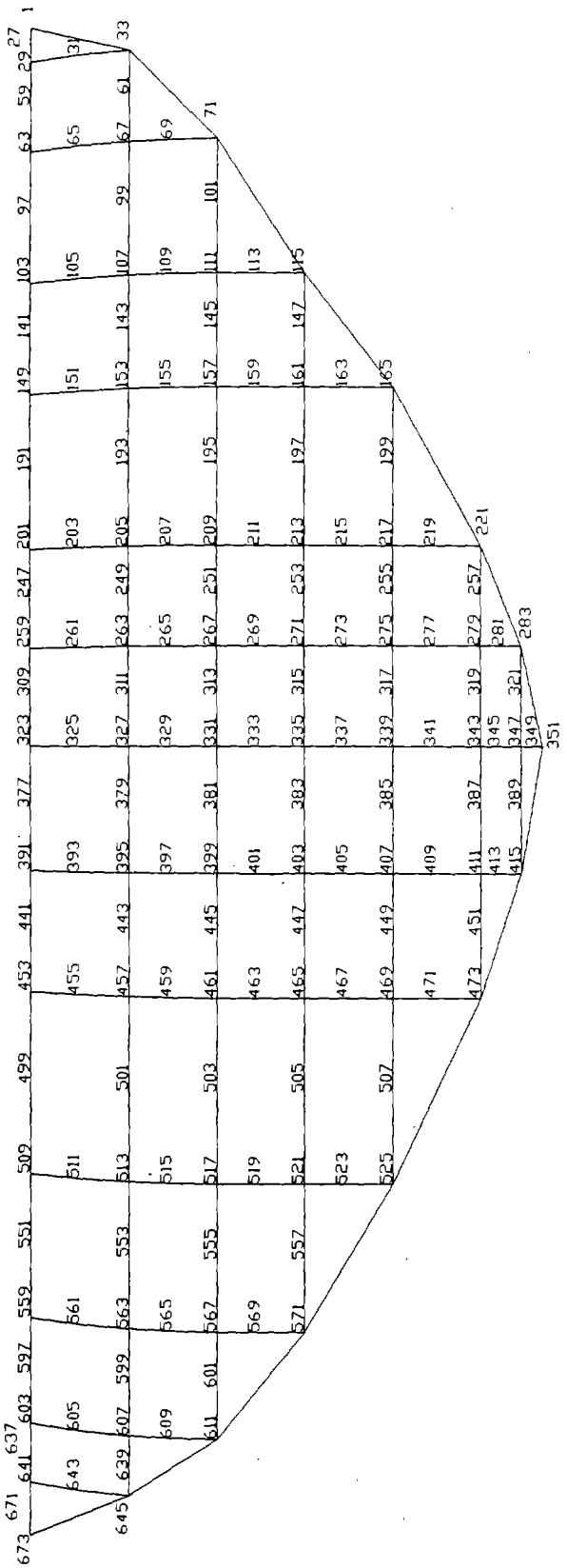

Figure 6.2 Upstream Node Numbers of Finite Element Mesh

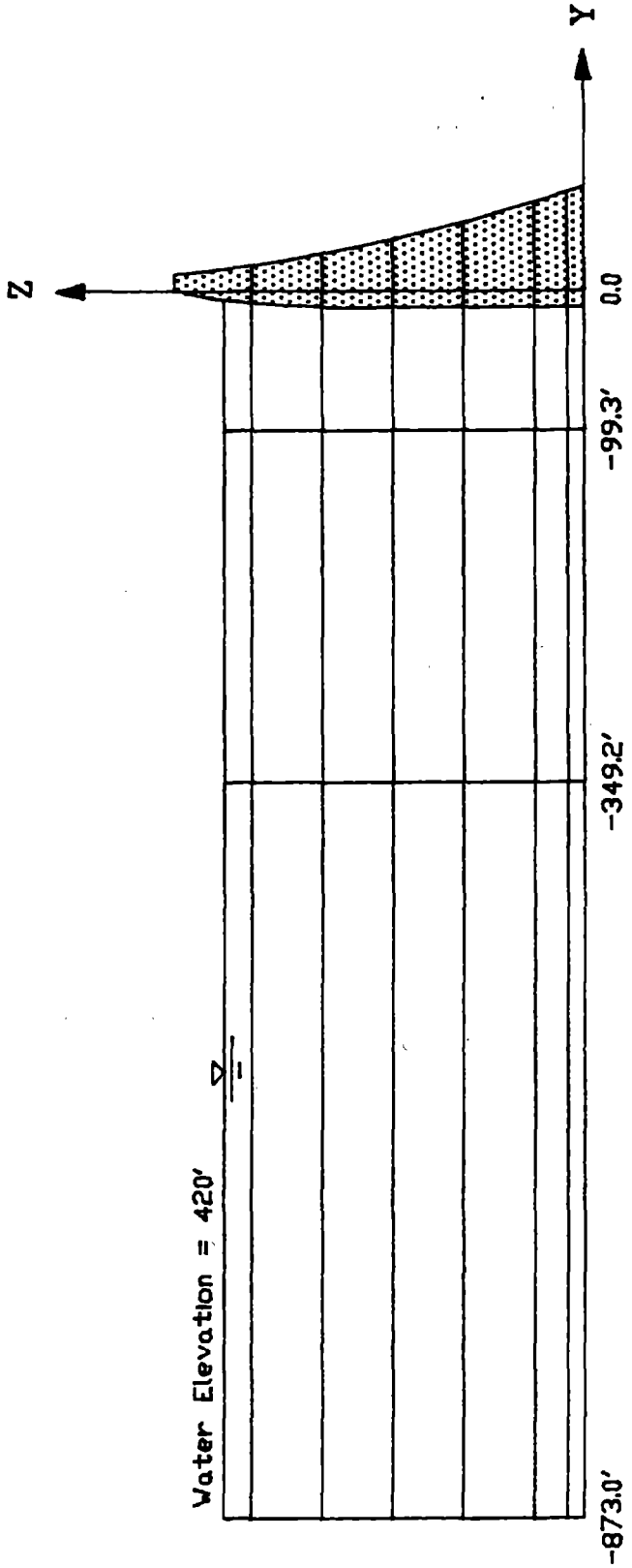

Figure 6.3 Section View of Finite Element Reservoir Model

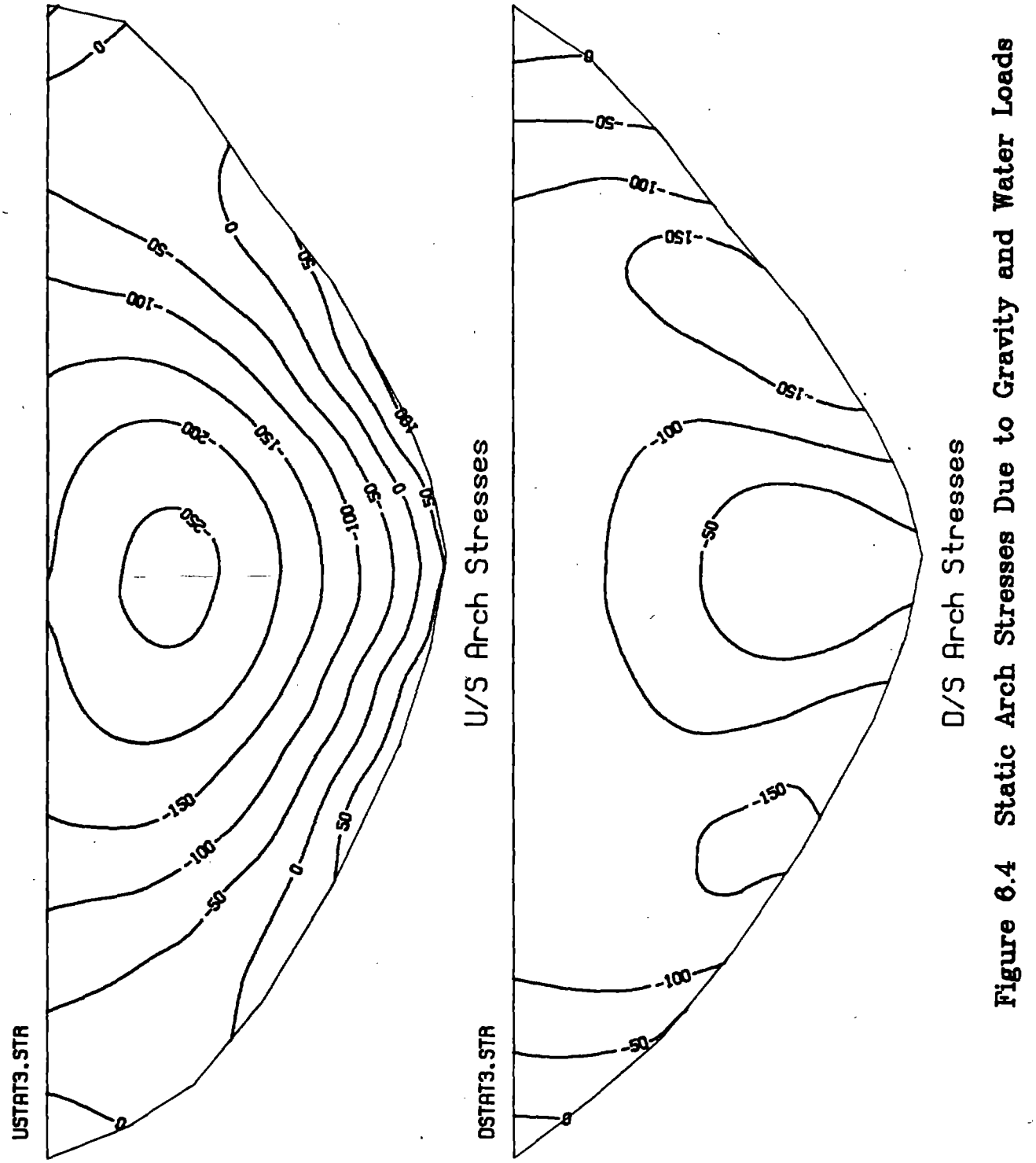

Figure 6.4 Static Arch Stresses Due to Gravity and Water Loads

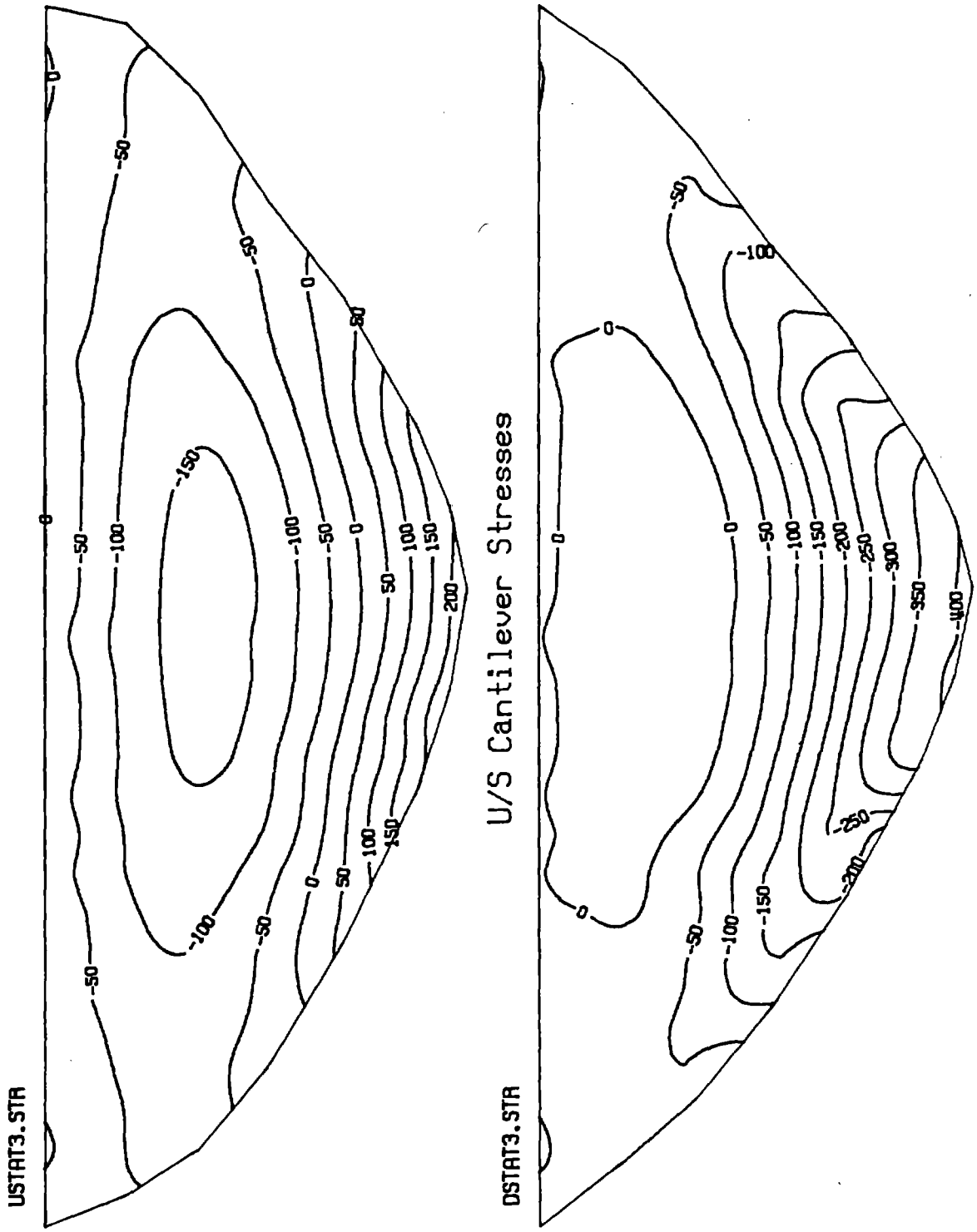

Figure 6.5 Static Cantilever Stresses Due to Gravity and Water Loads

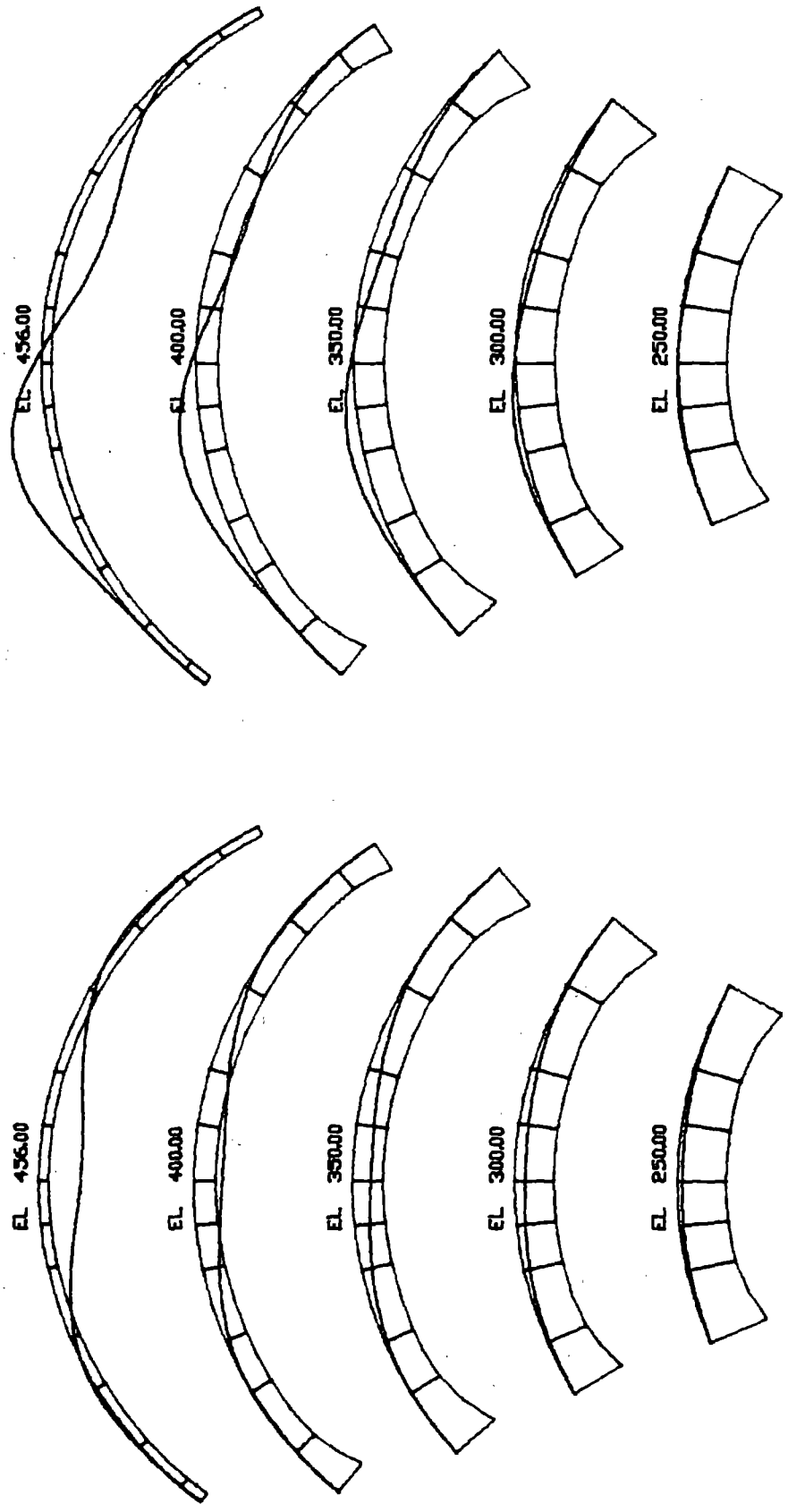

Figure 8.6 Mode Shapes of Dam–Foundation–Reservoir System

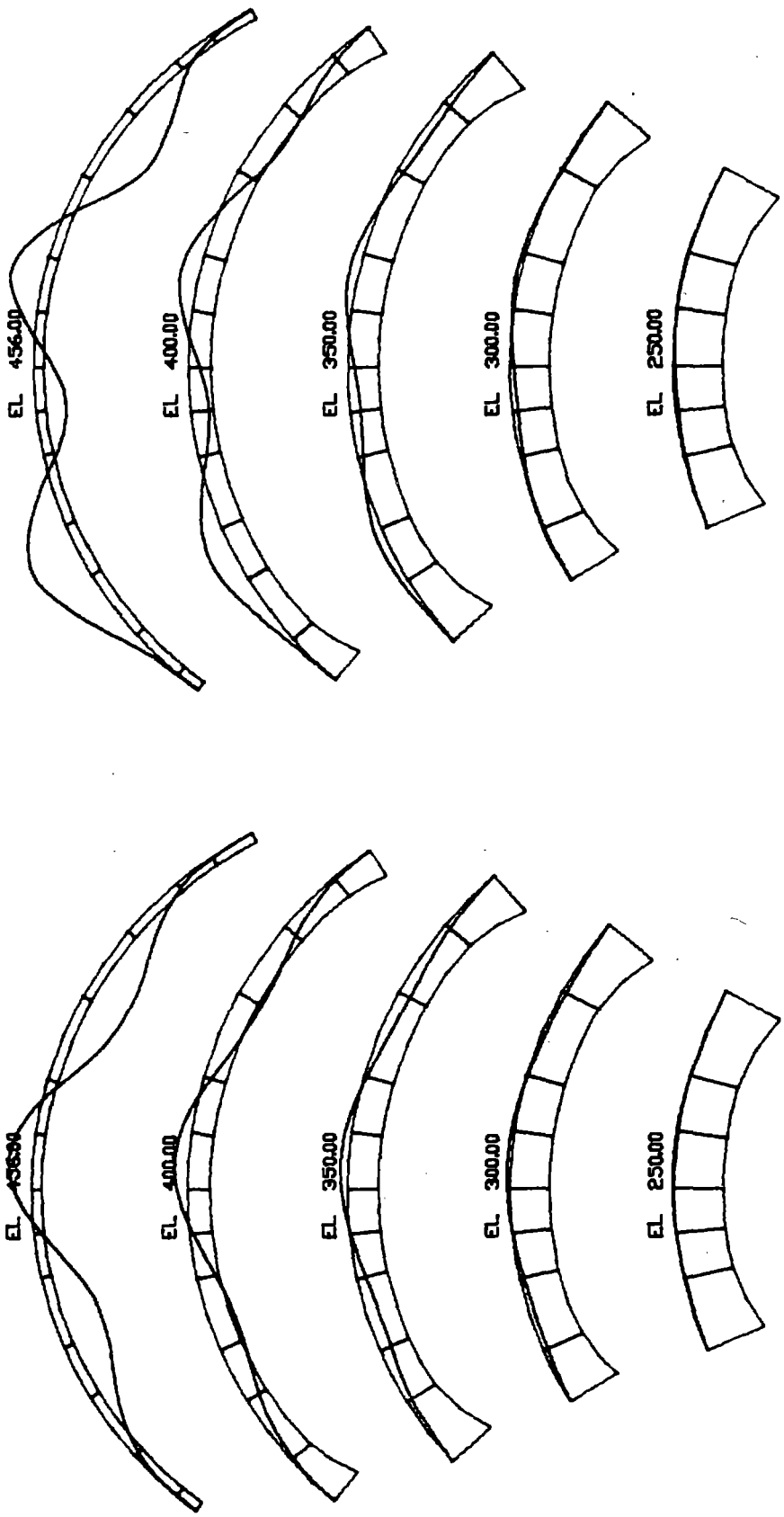

Mode 4
f = 5.86 Hz

Mode 3
f = 4.75 Hz

Figure 6.6 Cont'd

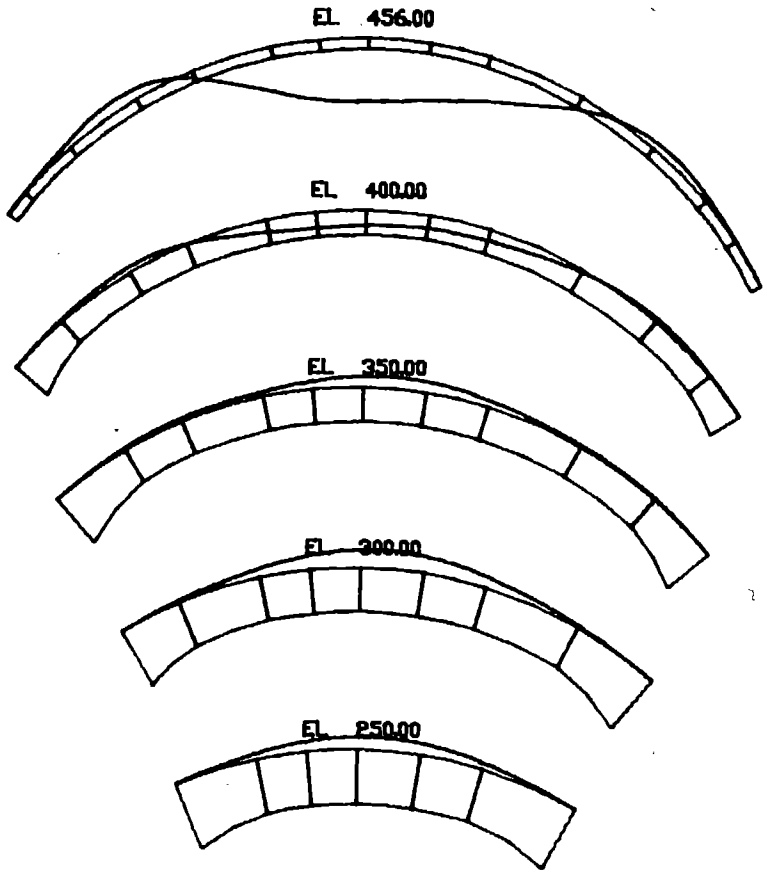

Mode 5
f = 6.88 Hz

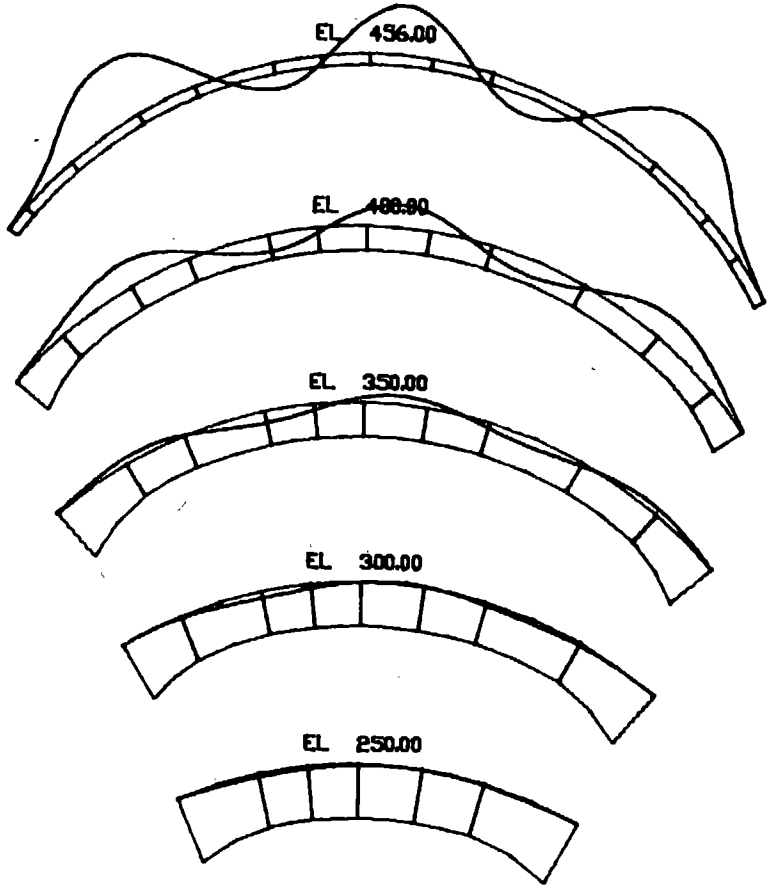

Mode 6
f = 7.19 Hz

Figure 6.6 Cont'd

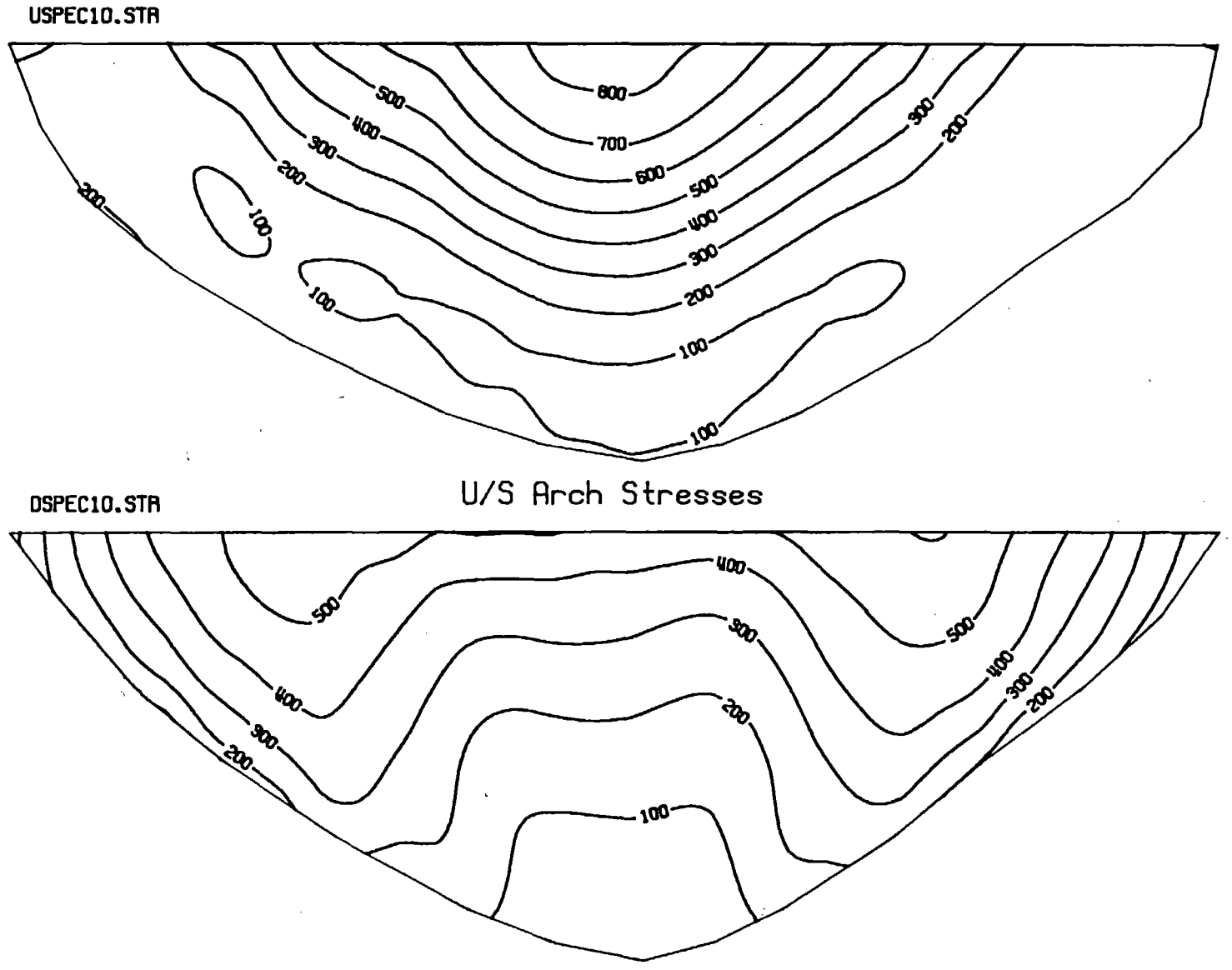

Figure 6.7 Envelope Earthquake Arch Stresses (Response Spectrum)

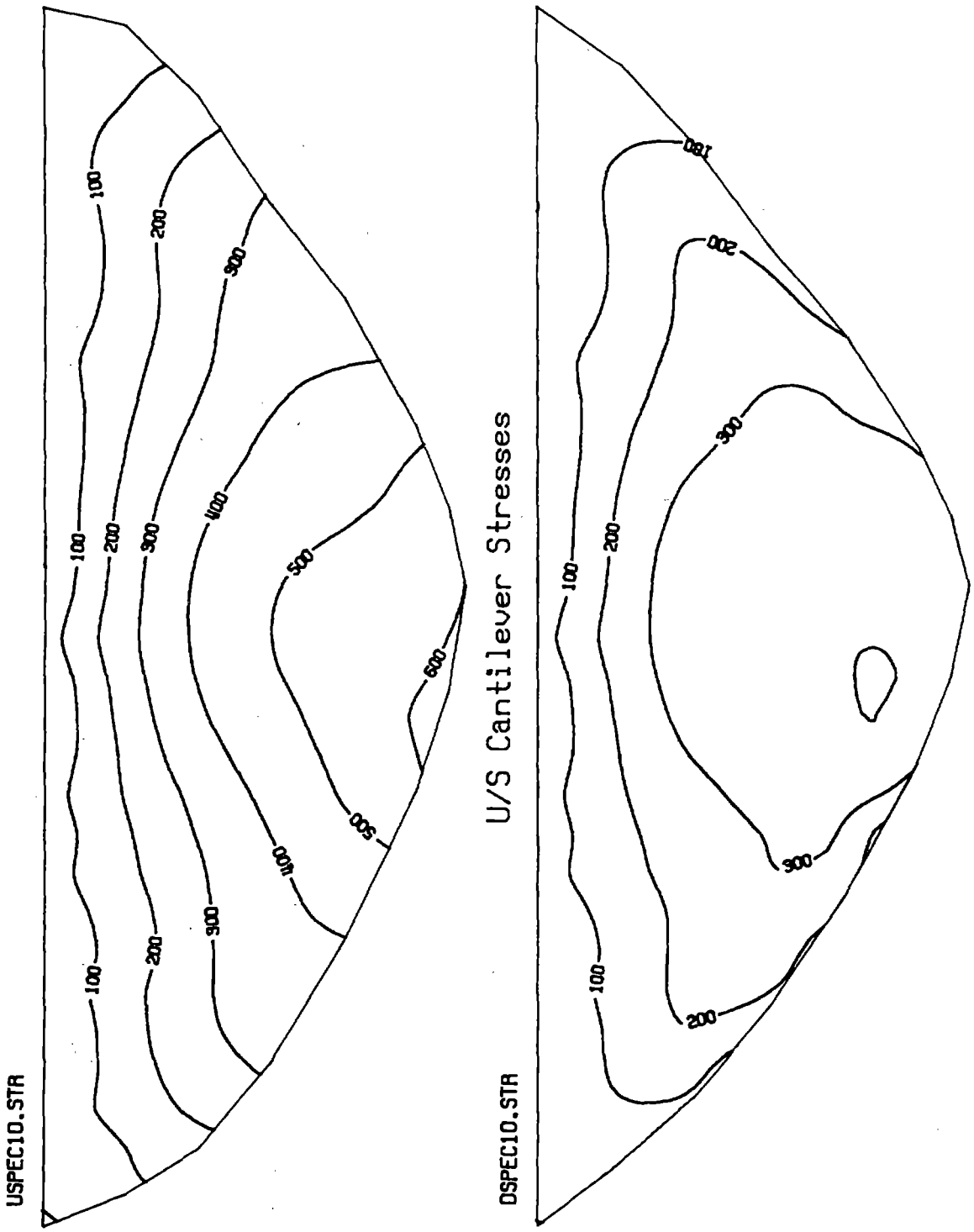

Figure 6.8 Envelope Earthquake Cantilever Stresses (Response Spectrum)

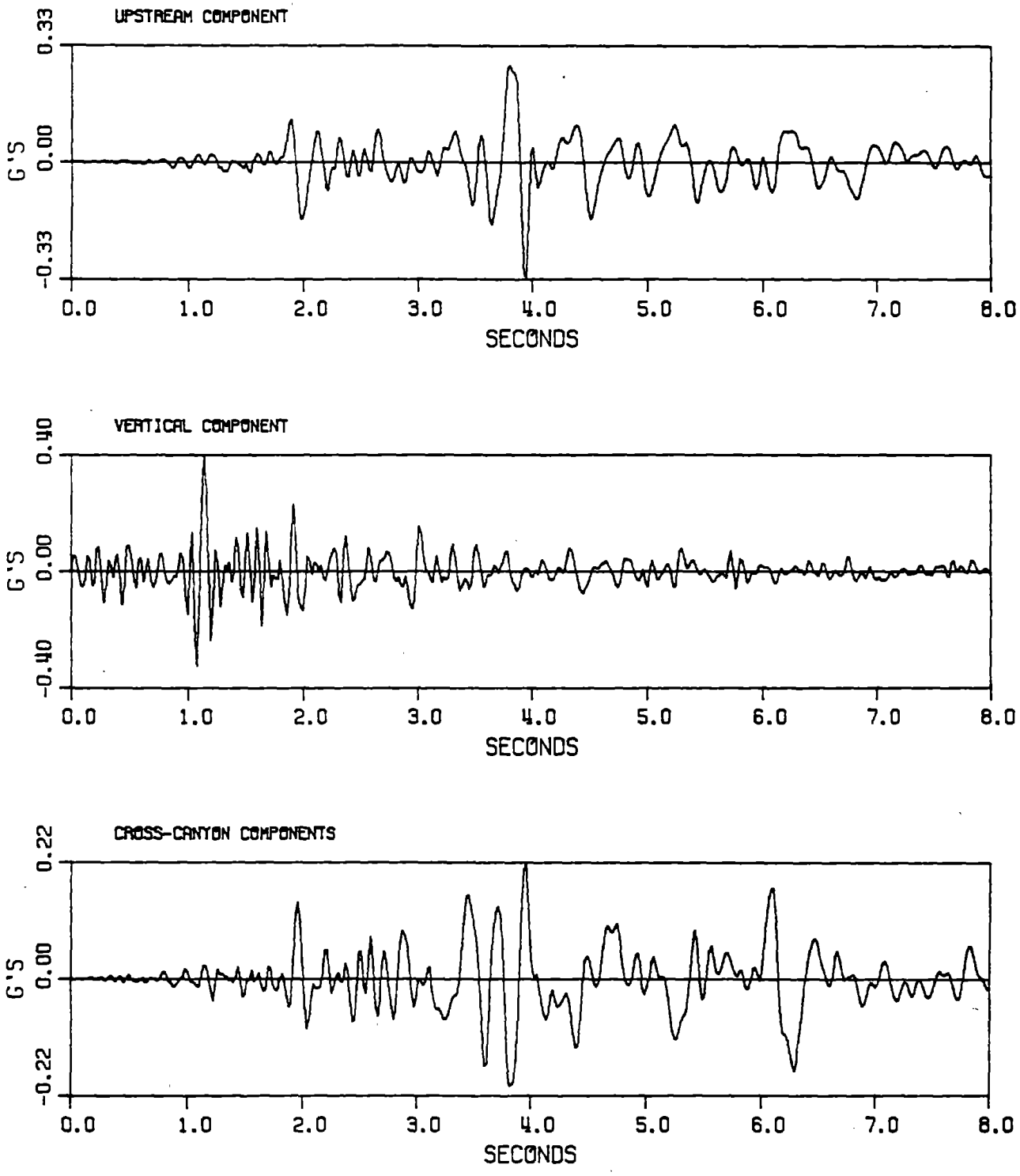

Figure 6.9 Ground Motion Recorded at Morgan Hill, California Earthquake of 24 April 1984

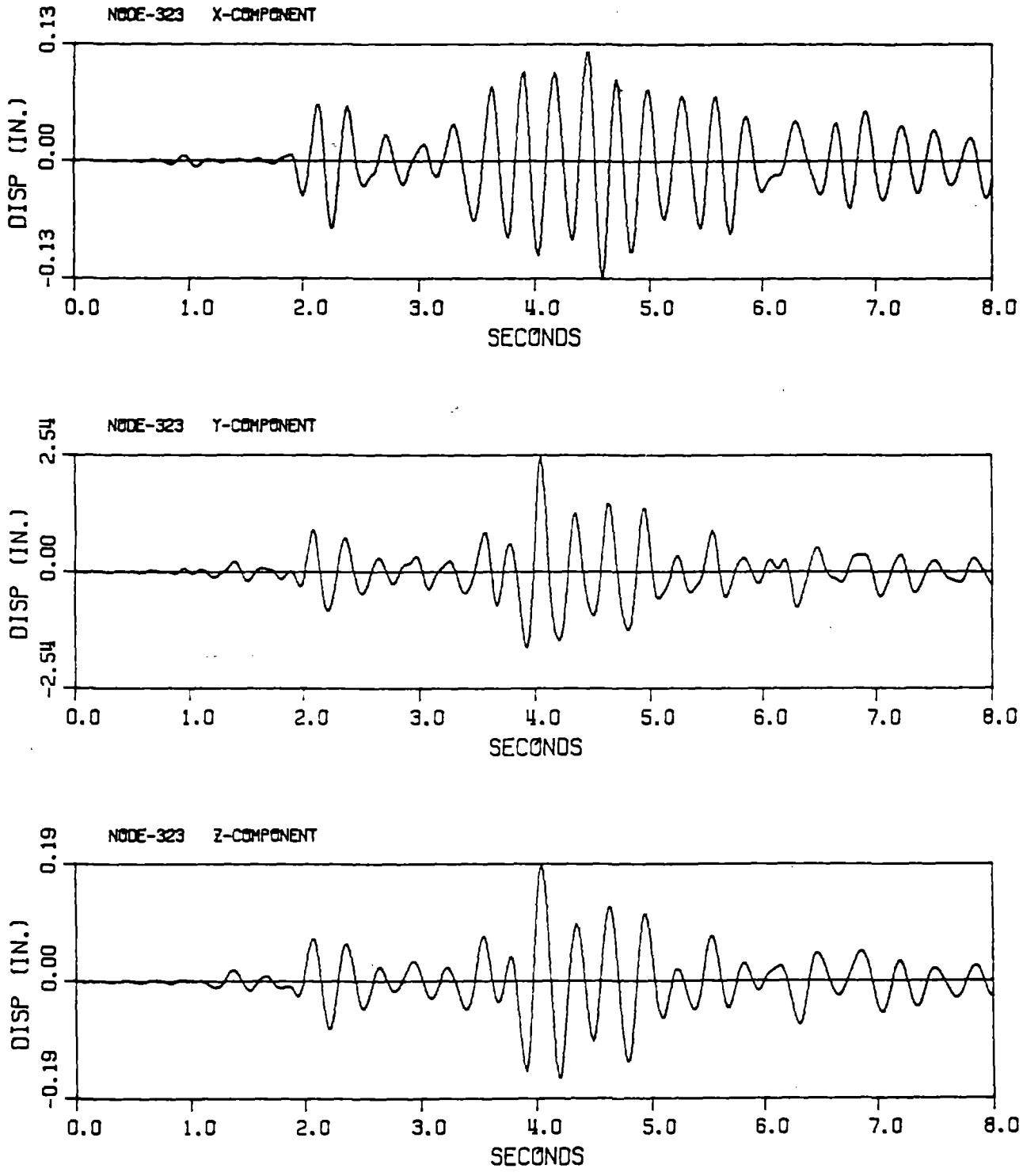

Figure 6.10 Displacement Response of Monticello Dam–Foundation–Reservoir System to Morgan Hill Earthquake

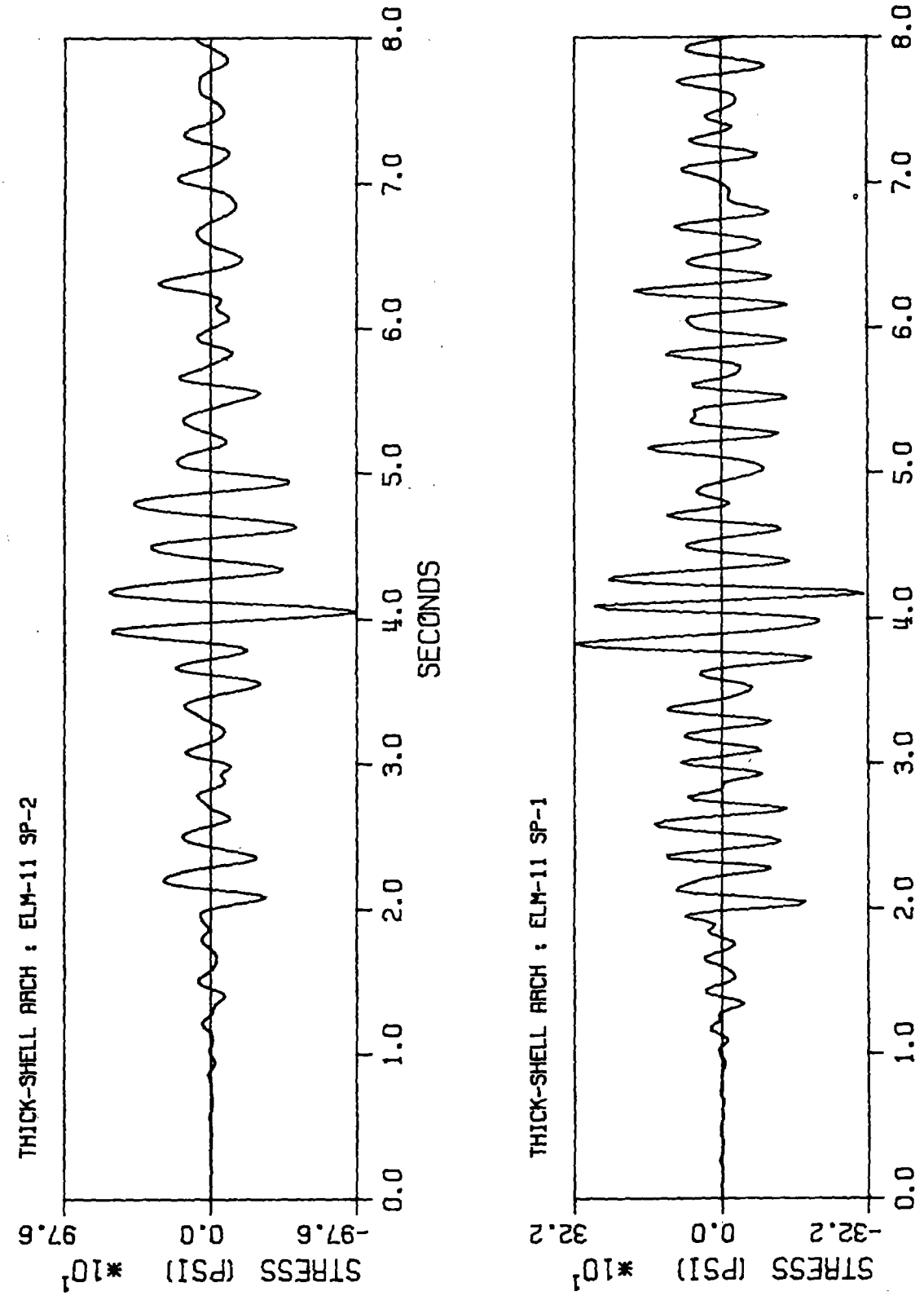

Figure 6.11 Time History of Earthquake Arch Stresses at Two Opposite Points on U/S and D/S faces of Thick-shell No. 11

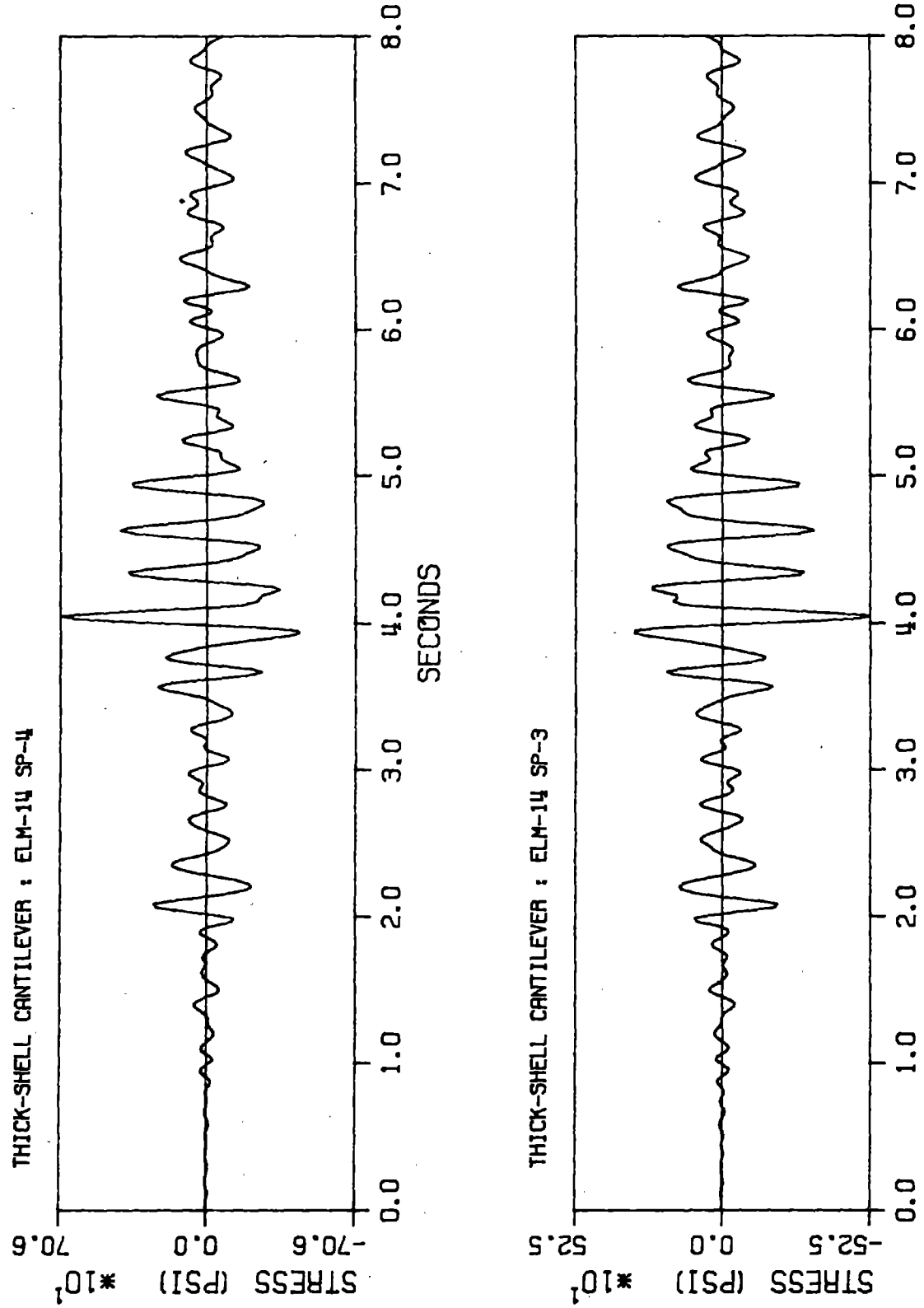

Figure 6.12 Time History of Earthquake Cantilever Stresses at Two Opposite Points on U/S and D/S Faces of Thick-shell No. 14

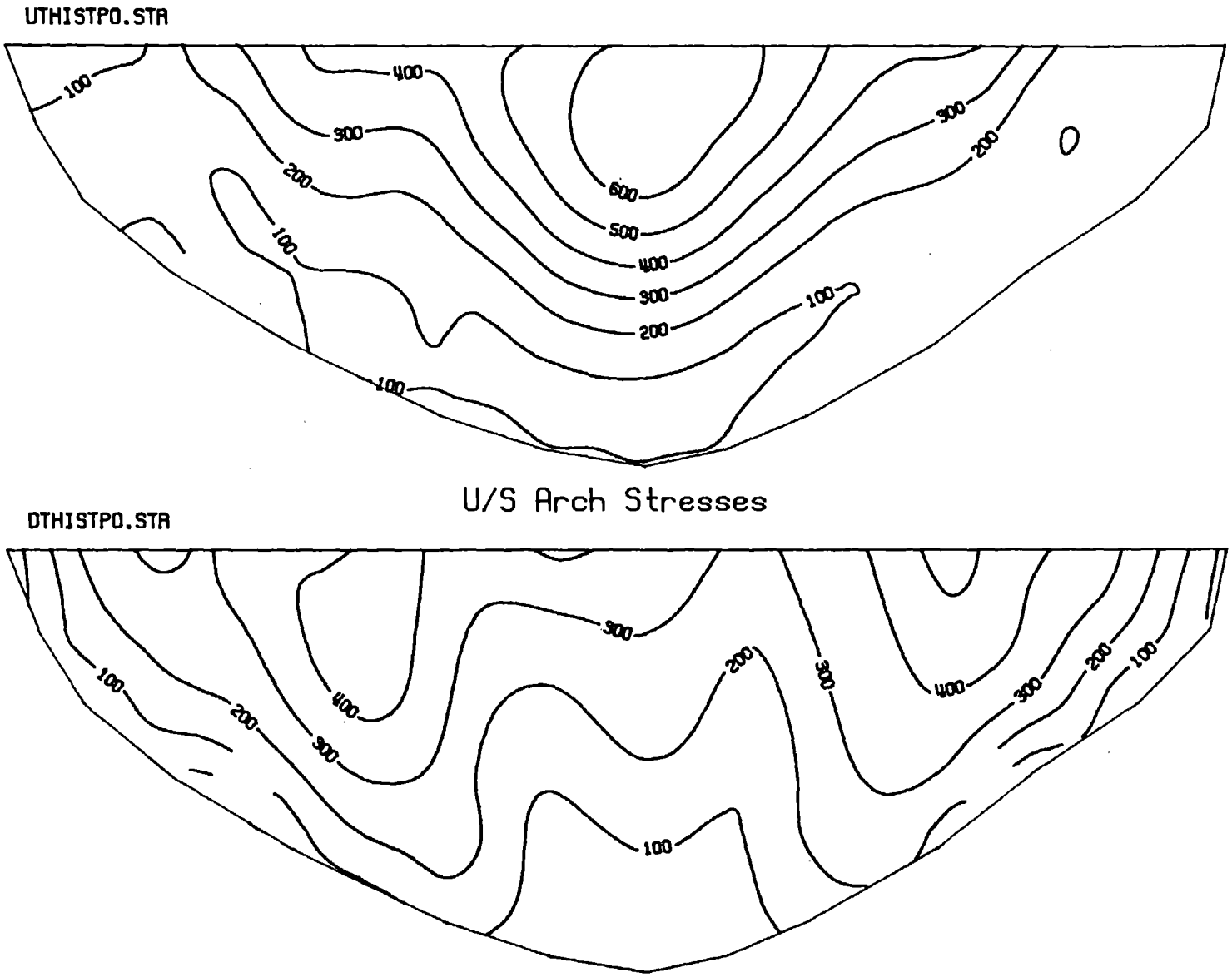

Figure 6.13 Envelope Earthquake Arch Stresses (Time History)

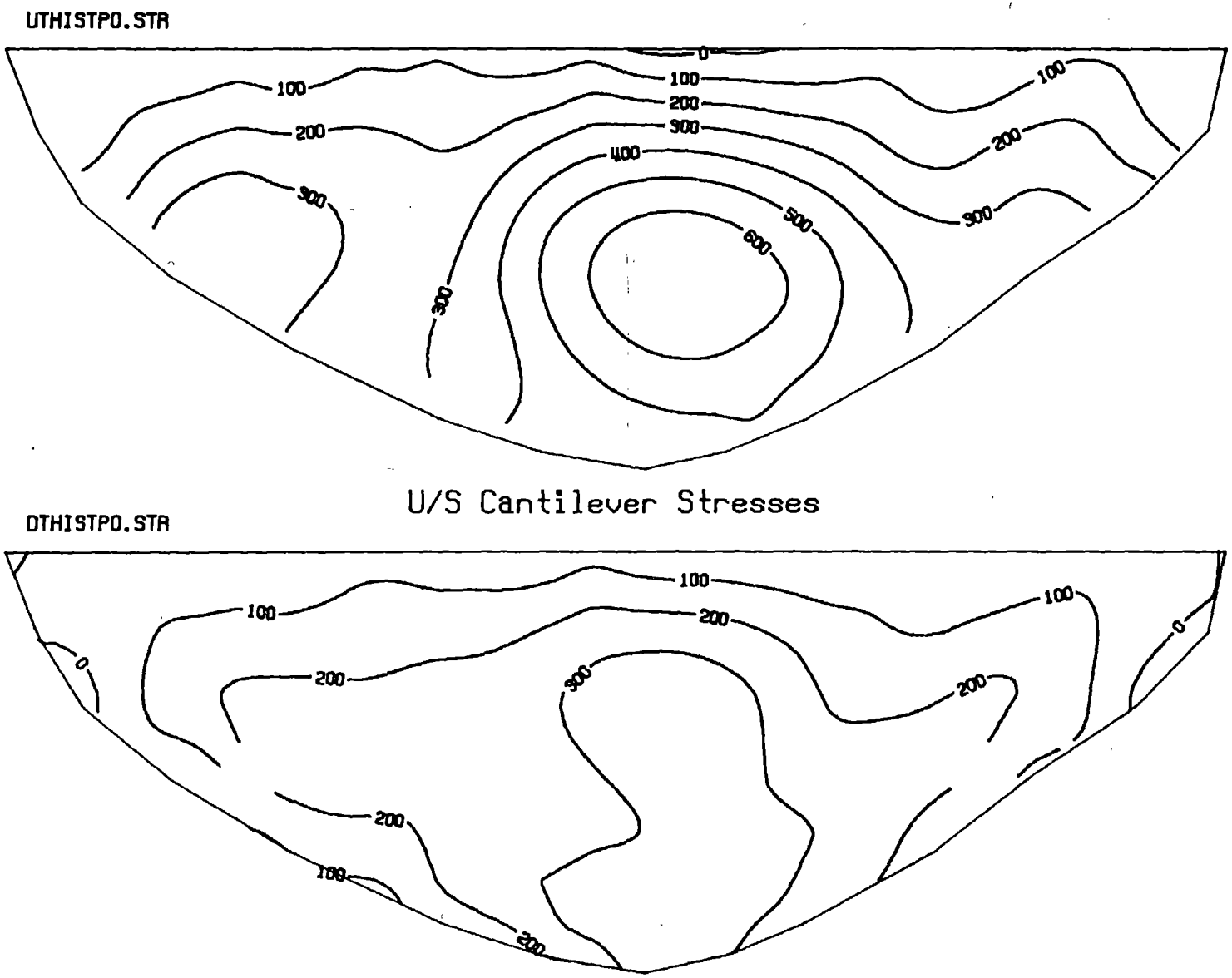

Figure 6.14 Envelope Earthquake Cantilever Stresses (Time History)

7. DESCRIPTION OF INPUT DATA FOR EADAP PROGRAM

EADAP INPUT DATA

The input data for the computer program EADAP are prepared according to the format described in this section. Each card contains one or several fields identified by column numbers and one of three data-types: (I), integer; (F), floating point; or (A), character string.

A. TITLE CARD

1 -72 (A)	TITLE	Information to be printed as the output header.

B. MASTER CONTROL CARDS

One or both of the following cards will be required depending on the type of input data.

Card Set B.1 - Model Definition and Analysis Type

This card is always required.

1 - 4 (I)	NUMNP	Total number of nodal points. Enter zero if Mesh Generator (MG) is used (See Note-a below).
5 -10 (I)	MTOT	Size of the available blank **COMMON** block (Note-b).
11-15 (I)	NELTYP	Number of different element types to be used (Note-c).
16-20 (I)	LL	Number of static load cases. Enter zero in dynamic analysis.
21-25 (I)	NF	Number of frequencies to be calculated in vibration analysis. It is also number of modes to be considered in response history or response spectrum analysis in which previously calculated mode shapes are read from restart tape.
26-30 (I)	NDYN	Analysis code: = 0, static analysis; = 1, vibration analysis to calculate frequency and mode shapes; = 2, response history analysis; = 3, response spectrum analysis.
31-33 (I)	NLM	Number of mesh elevations. Enter zero if MG is not used.
33-35 (I)	NLU	Mesh elevation number associated with the bottom elevation of a U-shaped valley (see Figure 2.4). Enter zero for V-shaped valley.
36-40 (I)	NEQEST	Estimated number of degrees of freedom. Enter zero if no estimate is available. The execution halts if the estimated and computed dof's do not match (Note-d).
41-45 (I)	IMODE	Restart option for dynamic analysis: = 1, Element stress matrices, nodal point data, structural mass, and frequencies and mode shapes are stored or read from restart files; = 0, otherwise

46-50 (I)	**IPRM**	Option for mode shape print-out in dynamic analysis: = 0, mode shapes are printed; = 1, no mode-shape print-out.
51-60 (F)	**ESTVOL**	Estimated total volume of all elements with 10E-4 accuracy. Enter zero if no estimate of element volumes is available. The execution halts if estimated and computed volumes do not match within the above accuracy (Note-e).
61-62 (I)	**MESH**	Dam mesh type when mesh generator is used: = 1, dam is modeled by combination of 3D-shell and thick-shell elements (one element through the dam thickness); = 3, dam is modeled by 8-node solid elements, three elements through the dam thickness. Enter zero if mesh generator is not used.
63-64 (I)	**MESHFN**	Foundation mesh type when MG is used: = 0, no foundation (rigid); = 1 foundation mesh *type 1*; = 2, foundation mesh *type 2*; = 3, foundation mesh *type 3.* Enter zero when MG is not used.
65-66 (I)	**IADMAS**	Code for added-mass in dynamic analysis: = 0, static analysis, or dynamic analysis with empty reservoir; = 2, dynamic analysis with finite-element added-mass. The added-mass previously calculated by the program INCRES is read from TAPE12.DAT file.
67-73 (F)	**WATL**	Z-coordinate of the water level.
74-80 (F)	**WDEN**	Water weight density.

Card Set B.2 - Dynamic Analysis with Restart Option

This card set is required for dynamic response calculation for which mode-shapes, frequencies, and structural data are read from the restart files. The following parameters are retrieved from the output of the free vibration analysis that generated the restart files.

1 - 5 (I)	**MBAND**	1/2 bandwidth of the system of equilibrium equations.
5 -10 (I)	**NUMEL**	Total number of elements (dam plus foundation).
11-15 (I)	**NEQ**	Number of equations or degrees of freedom.
16-20 (I)	**N3DDAM**	Number of 3-D solid elements in dam.
21-25 (I)	**N3DFN**	Number of 3-D solid elements in foundation.
26-30 (I)	**NSHEL2**	Number of 3-D shell elements.
31-35 (I)	**NSHEL3**	Number of Thick-shell elements.

Notes:

a) When mesh generator is used, NUMNP is automatically calculated by the program and consists of the nodal points for the dam with foundation mesh type-3. Otherwise the exact number of nodal points should be provided by the user. For thick-shell and transition elements all 16 surface nodes are considered.

b) MTOT controls the number of blocks and number of equations in each block for the out-of-core solution. Smaller MTOT values result in larger number of blocks with smaller number of equations per block. Depending on available hardware resources, it could be set to any number in the range of 10,000-200,000.

c) Maximum of three element types can be specified.

8-Node solid : element type-1
3D-Shell : element type-2
Thickshell : element type-3

d) NEQEST may be used for checking the generated data. If set to a non-zero value other than the actual number of dof's, structural data including the nodal coordinates, ID array, and the element data are generated and then the execution stops.

e) ESTVOL may be used for further examination of the generated element data to identify any excessive element distortions. If set to a non-zero value other than the actual total volume of all elements, stiffness and mass matrix for each element are calculated, the element data such as the volumes and connectivity data are printed out, and the execution stops without the structural response being calculated.

C. MESH GENERATION INPUT DESCRIPTION

Skip this section if mesh generation is not used or this run is a dynamic response calculation for which mode-shapes, frequencies, and structural data are read from the restart files.

Card Set C.1 - Reference Surface Data

1 -10 (F)	**RI**	Radius of the inner portion of the reference surface (Figure 2.2).
11-20 (F)	**RO(1)**	Radius of the right outer-portion of the reference surface.
21-30 (F)	**RO(2)**	Radius of the left outer-portion of the reference surface.
31-35 (I)	**NL**	Number of design elevations.
36-40 (I)	**IEL**	= 1 Same compounding angles are specified at all elevations; = 0 Compounding angles differ for each elevation.
41-45 (I)	**IRL**	= 1 Same compounding angles are specified for the right and left portions of the dam; = 0 Otherwise.
45-50 (I)	**IIE**	= 1 Same compounding angles are specified for the intrados and extrados faces of the dam; = 0 Otherwise.
51-55 (I)	**NRL**	= 1 Same radius is specified for the right and left portions of the intrados and extrados arcs; = 0 Otherwise.
56-60 (I)	**IPLOT**	Not used; leave blank
61-65 (I)	**ISYM**	= 0 Non-symmetric dam; = 1 Symmetric dam with symmetric B.C's along the crown section; =-1 Symmetric dam with anti-symmetric B.C's along the crown section.

Card Set C.2 - Compounding Angles and Angles to Abutments

One card is required for each design elevation. The sequence of cards corresponds to increasing order of elevations. For the definition of the angles refer to Figure 2.2.

1 -10 (F)	**EL(I)**	Elevation i
11-20 (F)	**FCI(I,1)**	Compounding angle of the right-intrados arc at elevation i.
21-30 (F)	**FCI(I,2)**	Compounding angle of the left-intrados arc at elevation i.
31-40 (F)	**FCE(I,1)**	Compounding angle of the right-extrados arc at elevation i.
41-50 (F)	**FCE(I,2)**	Compounding angle of the left-extrados arc at elevation i.
51-60 (F)	**FA(I,1)**	Angle to the right abutment at elevation i.
61-70 (F)	**FA(I,2)**	Angle to the left abutment at elevation i.

Notes:

1. If IEL = 1 (Card Set C.1), only compounding angles for the first elevation are required.
2. If IRL = 1 (Card Set C.1), only compounding angles for the right arcs are required.
3. If IIE = 1 (Card Set C.1), only compounding angles of the intrados are required.

Card Set C.3 - Temperature Data

Two sets of data cards are required to specify the temperature data at the design elevations. The first set corresponds to the upstream face. Eight values are given on each card and as many cards as required should be supplied. Temperature values are specified in the sequence of increasing elevations. The second set of cards corresponds to the downstream face. Starting on columns 1-10 of the first card of the second set, temperature values are specified in exactly the same way as described above.

Blank cards should be provided, when temperature variation is not considered in the analysis.

Card Set C.4 - Mesh Elevations

Mesh elevations are specified in increasing sequence; eight values are given on each card and as many cards as required should be supplied. A maximum of 20 mesh elevations may be specified.

Card Set C.5 - Intrados and Extrados Arcs

One card is required for each design elevation to specify the radius and Y-coordinate of the center of each arc. The sequence is according to the increasing order of the elevations.

1 -10 (F)	**YII**	Y-coordinate of center of intrados inner-arc (Figure 2.2).
11-20 (F)	**YEI**	Y-coordinate of center of extrados inner-arc.
21-30 (F)	**RII**	Radius of intrados inner-arc.
31-40 (F)	**REI**	Radius of extrados inner-arc.
41-50 (F)	**RIO(1)**	Radius of intrados right-outer-arc.
51-60 (F)	**REO(1)**	Radius of extrados right-outer-arc.
61-70 (F)	**RIO(2)**	Radius of intrados left-outer-arc.
71-80 (F)	**REO(2)**	Radius of extrados left-outer-arc.

Notes:

If NRL = 1 (Card Set C.1), radii of the left-outer-arc for intrados and extrados may be omitted.

Card Set C.6 - X-Coordinate of Center of Inner-Arcs

Two sets of cards are required to specify the X-coordinate of the center of inner-arcs at the design elevations.

The first set corresponds to the intrados inner-arc. Eight values are given on each card and as many cards as required should be supplied. Coordinate values are specified in the sequence of increasing elevations.

The second set of cards specifies the X-coordinates of the center of the extrados inner-arc. Same procedures mentioned above apply to this set.

Card Set C.7 - Material Property of Elements

The following set of cards specifies the material property identification numbers for each element type.

Card Set C.7.1 - Eight-node Solid Elements of Dam

For mesh *type-1* (MESH=1, Card Set B.1), no card is required.

For mesh *type-3* (MESH=3), when all eight-node solid elements of dam have the same material properties (i.e. homogeneous concrete), a blank card should be supplied. In this case material type number-1 will be assigned to all eight-node solid elements of dam.

For mesh *type-3*, when eight-node solid elements of dam have different material properties, one card should be assigned to each group of elements having the same material properties according to the following format:

1- 5 (I)	**NLL**	Element number.
6-10 (I)	**MATT**	Material identification number.

Note:

The sequence of cards should correspond with increasing order of the element numbers. If a group of successive elements have the same material numbers, only a material card for the first element in the group is needed. The sequence of cards should be terminated by a blank card, unless the material number for the last element is supplied.

Card Set C.7.2 - Eight-node Solid Elements of Foundation

For the case with rigid foundation (MESHFN=0), no card is needed.

For MESHFN > 0 and both concrete arch dam and foundation rock are assumed to be homogeneous a blank card should be supplied. In this case material number 1 (if MESH = 1) or 2 (if MESH = 3) is assigned to eight-node brick elements of the foundation.

For MESHFN > 0 and either concrete arch dam or foundation rock is not homogeneous, a set of cards should be supplied to specify the material numbers of different foundation elements. These cards follow the same format described above (Card Set C.7.1).

Card Set C.7.3 - 3D Shell Elements

For the MESH not equal to 1, no card is required.

For MESH = 1 and all 3D shell elements having the same material properties, a blank card is supplied; and the material number 1 is assumed for all 3D shell elements.

For MESH = 1 and 3D shell elements having different material properties, one card is supplied for each group of elements having identical material properties. These data are prepared according to the format described above (Card Set C.7.1).

Card Set C.7.4 - Thick Shell Elements

Follow the procedure presented for the 3D shell elements.

D. DESCRIPTION OF MANUAL INPUT OF NODAL DATA

Skip this section if mesh generation is used. Otherwise, one card per node is required unless some nodes are to be generated.

Card Set D.1 - Nodal Coordinates and Temperature Values

1- 5 (I)	**NODE**	Node number
6-15 (F)	**COORD(NODE,1)**	X-coordinate
16-25 (F)	**COORD(NODE,2)**	Y-coordinate
26-35 (F)	**COORD(NODE,3)**	Z-coordinate
36-45 (f)	**COORD(NODE,4)**	Temperature value

These cards are supplied in increasing node number sequence. However, if a group of cards is omitted, the coordinates of the corresponding nodes are generated at equal intervals on a straight line connecting two nodes for which coordinates have been supplied.

Card Set D.2 - Boundary Conditions and Adjacent Node Data

One card per node is supplied, unless for some nodes the adjacent nodes and boundary conditions are to be generated.

1- 5 (I)	**NODE**	Node number
6-10 (I)	**NADJ**	Adjacent node number
11-15 (I)	**ID(NODE,1)**	X-translation fixity code
16-20 (I)	**ID(NODE,2)**	Y-translation fixity code
21-25 (I)	**ID(NODE,3)**	Z-translation fixity code
26-30 (I)	**ID(NODE,4)**	X-rotation fixity code
31-35 (I)	**ID(NODE,5)**	Z-rotation fixity code = 0 ; free = 1 ; fixed

If NADJ $\leq$ 0, columns 26-35 may be left blank. These cards are supplied in increasing node number sequence. However, if a group of cards is omitted between a pair of non-consecutive nodes, the missing information is generated by the program as follows:

1. The fixity conditions will be the same as those on the first card of the pair.

2. The adjacent node numbers will be generated by linear interpolation between adjacent node numbers on the given pair of cards.

E. MODIFICATION OF NODAL POINT DATA

The previously generated nodal coordinates, temperature values, and the fixity data may be modified by supplying the following information.

Card Set E.1 - Control Data

1- 5 (I)	**MODC**	Number of nodes for which coordinates are to be modified.
6-10 (I)	**MODB**	Number of nodes for which fixity and adjacent node numbers are to be modified.
11-15 (I)	**MODT**	Number of nodes for which temperature values are to be modified.
16-20 (I)	**IPPR**	Code for print-out of nodal data: = 0 nodal coordinates, fixity, and temperature values are printed; = 1 no print-out.

Supply one blank card when no modification is required.

Card Set E.2 - Coordinate Modification

A total of MODC cards is required. These data override previously generated or read in nodal coordinates. Each card corresponds to one nodal point. Arbitrary sequence may be used.

1- 5 (I)	**NODE**	Node number
6-15 (F)	**COORD(NODE,1)**	X-coordinate
16-25 (F)	**COORD(NODE,2)**	Y-coordinate
26-30 (F)	**COORD(NODE,3)**	Z-coordinate

Card Set E.3 Temperature Modification

A total of MODT cards is required. These data override previously generated or read in temperature values. Each card corresponds to one nodal point. Arbitrary sequence may be used.

1- 5 (I)	**NODE**	Node number
6-15 (f)	**COORD(NODE,4)**	Temperature value

Card Set E.4 - Modification of Fixity and Adjacent Nodes

A total of MODB cards are used to override previously generated fixity conditions and adjacent node data. One card is needed for each node; arbitrary node sequence may be used.

1- 5 (I)	**NODE**	Node number
6-10 (I)	**NADJ**	Adjacent node number
11-15 (I)	**ID(NODE,1)**	X-translation fixity code
16-20 (I)	**ID(NODE,2)**	Y-translation fixity code
21-25 (I)	**ID(NODE,3)**	Z-translation fixity code
26-30 (I)	**ID(NODE,4)**	Local x-rotation fixity code
31-35 (I)	**ID(NODE,5)**	Local z-rotation fixity code = 0 ; free = 1 ; fixed

If NADJ $\leq$ 0, columns 26-35 may be left blank.

F. THICKNESS CHANGE

The program can handle a condition where thick-shell elements of different thicknesses are connected as shown below. In that case the total nodes in the structure includes all surface nodes of thick-shell elements. The mid-surface nodes of each pair of elements along the thickness change are assumed to coincide at points marked by x in the figure. In the input data, fixity condition and concentrated loads associated with primary nodes of one of the elements, say i, j, and k, will refer to those of the mid-surface. The primary nodes of the other element, l, m, and n, will be fixed.

One card is required for each mid-surface node along the thickness change. Fixed and free nodal points are selected such that J > I. This set of cards must be terminated by a blank card.

1- 5 (I)	I	Corresponding fixed primary node
6-10 (I)	J	Corresponding free primary node

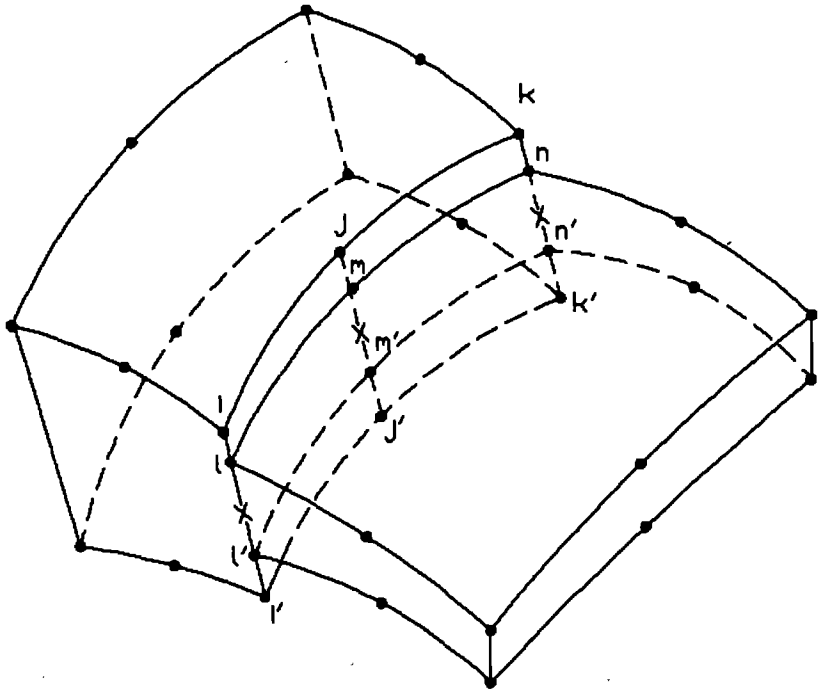

Connection of Thick-shell Elements Along Thickness Discontinuity

G. 8-NODE SOLID ELEMENTS

This section is not required in a dynamic analysis with restart option. Otherwise, the following cards are needed when 8-node solid elements are used in the finite-element model.

Card Set G.1 - Control Data

1- 5 (I)	**MTYPE**	Element type number: Enter 1 for 8-node solid elements
6-10 (I)	**NBRK8**	Total number of elements. Leave blank if MG is used.
11-15 (I)	**NMAT**	Number of different material types.
16-20 (I)	**NLD**	Number of different surface loads. Leave blank if MG is used.

Card Set G.2 - Modulus of Elasticity and Poisson's Ratio

1- 5 (I)	**N**	Material identification number
6-10 (I)	**ISOT**	= 0 isotropic material; = 1 orthotropic material
11-20 (F)	**EE(1)**	Modulus of elasticity E_{xx}
21-30 (F)	**EE(2)**	Modulus of elasticity E_{yy}*
31-40 (F)	**EE(3)**	Modulus of elasticity E_{zz}*
41-50 (F)	**EE(4)**	Poisson's ratio ν_{xy}
51-60 (F)	**EE(5)**	Poisson's ratio ν_{xz}*
61-70 (F)	**EE(6)**	Poisson's ration ν_{yz}*

Card Set G.3 - Shear Modulus and Thermal Coefficients

1-10 (F)	**EE(7)**	Shear modulus G_{xy}*
11-20 (F)	**EE(8)**	Shear modulus G_{yz}*
21-30 (F)	**EE(9)**	Shear modulus G_{zx}*
31-40 (F)	**EE(10)**	Coefficient of thermal expansion α_x
41-50 (F)	**EE(11)**	Coefficient of thermal expansion α_y*
51-60 (F)	**EE(12)**	Coefficient of thermal expansion α_z*
61-70 (F)	**EE(13)**	Weight density of the material

* Leave blank for isotropic material.

Card Set G.4 - Surface Loads

This card is not needed if mesh generation is used.

1- 5 (I)	**N**	Surface load identification number
6-10 (I)	**KTYPE**	Surface pressure type: = 1 uniform pressure; = 2 hydrostatic pressure.
11-20 (F)	**PR**	Pressure value if KTYPE = 1, Weight density of water if KTYPE = 2.
21-30 (F)	**ZREF**	Z-coordinate of the water level. Leave blank for KTYPE = 1.
31-35 (I)	**NFACE**	Element face number upon which pressure acts (Figure 3.1).

Card Set G.5 - Reference Temperature and Gravity Acc.

1-10 (F)	**REFT**	Stress free temperature
11-20 (F)	**GRAV**	Gravitational acceleration

Card Set G.6- Element Data

No card is needed if mesh generation is used. Eight-node solid elements are numbered from one to NBRK8. One card is required for each element except for those that are to be generated.

1- 5 (I)	**NEL**	Element number
6-10 (I)	**NP(1)**	Node - 1
.		
.		
.		
41-45 (I)	**NP(8)**	Node - 8
46-50 (I)	**NINT**	Integration order: = 2 for regular shapes; = 3 for irregular shapes.
51-55 (I)	**MAT**	Material number
56-60 (I)	**INC**	Generation parameter
61-65 (I)	**MLD**	Surface pressure number (zero means no surface pressure)
66-70 (I)	**ISP(1)**	Stress point number 1: If set to zero, stresses at the center of the element are calculated.
71-75 (I)	**ISP(2)**	Stress point number 2: Set to a prescribed element face number to calculate stresses at the center of that face. If set to zero, only stresses at ISP(1) as set above are calculated.

H. 3D SHELL ELEMENTS

Skip this section for a dynamic response calculation with the restart option. Otherwise, the following cards are supplied if 3D shell elements are used in the finite-element model.

Card Set H.1 - Control Data

1- 5 (I)	**MTYPE**	Element type number: Enter 2 for 3D shell.
6-10 (I)	**N3DEL**	Total number of elements. Leave blank if MG is used.
11-15 (I)	**NMAT**	Number of material types.
16-20 (I)	**NLD**	Number of surface load types. Leave blank if MG is used.

Card Set H.2 - Material Properties

1- 5 (I)	**N**	Material identification number
6-15 (F)	**EE**	Modulus of elasticity
16-25 (F)	**ENU**	Poisson's ratio
26-35 (F)	**RHO**	Weight density of material
36-45 (F)	**ALPT**	Coefficient of thermal expansion

Card Set H.3 - Surface Loads

This card is not needed when mesh generation is used.

1- 5 (I)	**N**	Surface pressure ID number
6-10 (I)	**KTYPE**	Surface pressure type: = 1 uniform pressure; = 2 hydrostatic pressure.
11-20 (F)	**PR**	Pressure value if KTYPE = 1. Weight density of water if KTYPE = 2.
21-30 (F)	**ZREF**	Z-coordinate of the water level. Leave blank if KTYPE = 1.
31-35 (I)	**NFACE**	Element face number upon which pressure acts (Figure 3.2).

Card Set H.3 - Reference Temperature and Gravity Acc.

1-10 (F)	**REFT**	Stress free temperature
11-20 (F)	**GRAV**	Gravitational acceleration

Card Set H.4 - Element Data

Skip this card set if mesh generator is used.

Two cards are required for each element except for those that are to be generated.

Card Set H.4.1 - Control Data

1- 5 (I)	**NEL**	Element number
6-10 (I)	**NINT**	Integration order: = 3 for regular shape; = 4 for irregular shape.
11-15 (I)	**MAT**	Material type number
16-20 (I)	**INC**	Generation increment
21-25 (I)	**MLD**	Surface pressure number
75-80 (I)	**IGG**	= 0 for 16-node elements; = 1 for 12-node elements.

Card Set H.4.2 - Element Connectivity

1- 5 (I)	**NP(1)**	Node 1
	.	(see Figure 3.2)
	.	
	.	
76-80 (I)	**NP(16)**	Node 16

I. THICK SHELL ELEMENTS

Skip this section for a dynamic response analysis using the restart files. Otherwise, the following data cards should be supplied if thick shell elements are used in the finite-element model.

Card Set I.1 - Control Data

1- 5 (I)	**MTYPE**	Element type number: Enter 3 for thick-shell elements.
6-10 (I)	**NUMEL**	Total number of elements. Leave blank if MG is used.
11-15 (I)	**NMAT**	Number of material types.

Card Set I.2 - Material Properties

1- 5 (I)	**MAT**	Material identification number
6-15 (F)	**EE**	Modulus of elasticity
16-25 (F)	**NU**	Poisson's ratio
26-35 (F)	**RO**	Mass density of the material
36-45 (F)	**GRAV**	Weight density of the material
46-55 (F)	**THERM**	Coefficient of thermal expansion

Card Set I.3 - Water and Temperature Data

1-10 (F)	**ROWATER**	Weight density of water
11-20 (F)	**REFT**	Stress free temperature

Card Set I.4 - Element Data

Skip this card set if mesh generator is used.

Two cards are required for each element and they must be numbered in increasing sequence.

Card Set I.4.1 - Connectivity Data

1- 5 (I)	**NN2**	Element number
6-10 (I)	**IX2(1)**	Node 1
	.	
	.	
	.	
41-45 (I)	**IX2(8)**	Node 8

Card Set I.4.2 - Material and Pressure Types

1- 5 (I)	**MAT**	Material Identification number.
6-15 (F)	**PRESS(1)**	Uniform normal pressure acting on face t = -1.
16-25 (F)	**PRESS(2)**	Uniform normal pressure acting on face t = +1.

J. STATIC ANALYSIS

The following cards are required in static analysis only.

Card Set J.1 - Concentrated Nodal Loads

For each nodal point at which concentrated forces or moments are applied a number of cards are required. This number is equal to the number of load cases in which concentrated loads are acting at that nodal point. The data cards are provided according to the nodal number sequence and should be terminated by a blank card. Each data card contains the following information:

1- 5 (I)	**N**	Node number
6-10 (I)	**L**	Load case number
11-20 (F)	**R(1)**	Force in X-direction
21-30 (F)	**R(2)**	Force in Y-direction
31-40 (F)	**R(3)**	Force in Z-direction
41-50 (F)	**R(4)**	Moment about local x-axis
51-60 (F)	**R(5)**	Moment about local z-axis

Card Set J.2 - Element Loads

For each load case, one card is supplied to specify the element loads to be considered in the analysis. There are total of LL load cases as specified in Section B.2.

1- 5 (I)	**IA**	Gravity load multiplier: = 1 include gravity load; = 0 otherwise.
6-10 (I)	**IB**	Water load multiplier, same rules are applied.
11-15 (I)	**IC**	Temperature load multiplier.

K. RESPONSE HISTORY ANALYSIS

The following cards are needed in response history analysis only.

Card Set K.1 - Response Control Data

1- 5 (I)	**NFN**	Number of components of ground motion.
6-10 (I)	**NT**	Total number of time steps.
11-15 (I)	**NOT**	Time interval for print-out of nodal displacements and stresses, expressed as a multiple of the integration time step.
16-25 (F)	**DT**	Integration time step.
26-35 (F)	**DAMP**	Modal damping ratio to be applied to all modes.

Card Set K.2 - Ground Motion Control Data

1- 5 (I)	**JFN(1)**	Identification number for the ground motion in the x-direction.
6-10 (I)	**JFN(2)**	Identification number for the ground motion in the y-direction.
11-15 (I)	**JFN(3)**	Identification number for the ground motion in the z-direction.

Card Set K.3 - Ground Motion

The following set of cards is required for each component of the ground motion. The sequence should correspond to ground motion identification numbers in increasing order.

Card Set K.3.1 - Control Data

1- 5 (I)	**NLP**	Number of acceleration data points
6-15 (F)	**SFTR**	Scale factor multiplier (default = 1). It is also used to convert input accelerations into consistent units.
16-80 (A)	**HETD**	Print-out heading for the input motion

Card Set K.3.2 - Acceleration Data

1-10 (F)	**T**	Time value at point 1
11-20 (F)	**P**	Acceleration value at point 1
	.	
	.	
	.	

Six pairs of time and acceleration values are supplied on each card. As many cards as required are provided to specify NLP pairs of data points.

Card Set K.4 - Displacement Output

The following set of cards is required to specify the displacement output results.

Card Set K.4.1 - Control Data

1- 5 (I)	**KKK**	Code for output type: = 1 Print-out of displacement histories and maxima; = 2 Not used; = 3 Print-out of displacement maxima only.

Card Set K.4.2 - Displacement Components

One card is required for each node for which displacement print-out is requested. The set of cards is in increasing order of nodal numbers. One blank card is supplied to terminate the sequence of cards. Up to five displacement components may be requested for the thick shell nodes and up to three components for all other nodes.

1- 5 (I)	**NP**	Node number
10 (I) 15 (I) 20 (I) 25 (I) 30 (I)	**IC**	Displacement component: = 1 X-component = 2 Y-component = 3 Z-component = 4 Local x-rotation = 5 Local z-rotation

First zero or blank on these columns terminates the sequence of displacement components of the node.

Card Set K.5 - Stress Output

The following cards are required to specify the stress output.

Card Set K.5.1 - Control Data

1- 5 (I)	**KKK**	Code for output type: = 1 Print-out of stress histories and maxima; = 2 Not used; = 3 Print-out of stress maxima only.

Card Set K.5.2 - Stress Components

For each element type used one set of cards is required. The order of 8-node solid, 3D shell, and thick-shell should be followed. In each set, four cards are supplied for each element for which stress output is requested. Each set is terminated by a blank card. For example if stress output is requested for N 8-node elements, 4N+1 cards are supplied with the last one being a blank card. The four sets of cards for each element are prepared as follows:

Card -1 :

1- 5 (I)	NEL	Element number

Cards 2, 3, and 4:

Contain numbers associated with the requested stress components of the elements. They are entered on columns 4, 8, ..., 80 as (20I4) format. The first zero or blank on these columns will terminate the request of the stress components of the element. Up to 12, 60, and 40 stress components may be requested for 8-node solid, 3D shell, and thick-shell elements, respectively. Stress components for each element type are summarized in the tables below.

Table 7.1 Stress Components in 8-Node Solid Elements

Stress Components	Face Center / or Centroid, Point 1	Face Center Point 2
σ_{xx}	1	7
σ_{yy}	2	8
σ_{zz}	3	9
σ_{xy}	4	10
σ_{yz}	5	11
σ_{zx}	6	12

Table 7.2 Stress Components in 3D-Shell Elements

Stress Components	Stress Points 1	2	3	4	5	6	7	8	9	10
σ_{xx}	1	7	13	19	25	31	37	43	49	55
σ_{yy}	2	8	14	20	26	32	38	44	50	56
σ_{zz}	3	9	15	21	27	33	39	45	51	57
σ_{xy}	4	10	16	22	28	34	40	46	52	58
σ_{yz}	5	11	17	23	29	35	41	47	53	59
σ_{zx}	6	12	18	24	30	36	42	48	54	60

Table 7.3 Stress Components in Thick-shell Elements

Stress Components	1	2	3	4	5	6	7	8
σ_{xx}	1	6	11	16	21	26	31	36
σ_{yy}	2	7	12	17	22	27	32	37
σ_{xy}	3	8	13	18	23	28	33	38
σ_{yz}	4	9	14	19	24	29	34	39
σ_{zx}	5	10	15	20	25	30	35	40

L. RESPONSE SPECTRUM ANALYSIS

The following cards are required only in a response spectrum analysis:

Card Set L.1 - Control Data

1- 5 (I)	**MGM**	Number of components of the ground motion (1, 2, or 3).
6-10 (I)	**IPD**	Code for Displacement output: = 1 Print-out of modal and SRSS displacements; = 0 no displacement print-out.
11-15 (I)	**IPS**	Code for stress output: = 0 compute and print stresses; = 1 do not compute stresses.

Card Set L.2 - Acceleration Spectrum Data

The following set of cards should be supplied for each component of the ground motion (follow the X, Y, and Z order). If no ground motion is to be considered in a particular direction, two blank cards should be supplied instead.

Card Set L.2.1 - Header Information

1-72 (A)	**HED**	Ground motion heading information.

Card Set L.2.2 - Control Data

1- 5 (I)	**NP**	Number of points specifying the acceleration spectrum.
6-15 (F)	**SFTR**	Scale factor; use to scale spectral accelerations or to convert them into consistent units.

Card Set L.2.3 - Response Spectrum Data

1-10 (F)	**T**	Period value of point 1
11-20 (F)	**S**	Spectral acc. value at point 1
	.	
	.	
	.	

Four pairs of period and acceleration spectrum values are specified on each card. Supply as many cards as required to define all NP points. Linear interpolation is used in the program to calculate spectrum values for the periods between the specified input points.

M. TERMINATION CARD

Two blank cards should be supplied to terminate the program execution.

8. DESCRIPTION OF INPUT DATA FOR INCRES PROGRAM

INCRES INPUT DATA

The input data for the INCRES program is described in this section.

A. TITLE

1 -80 (A)		Information to be printed as the output header.

B. CONTROL DATA

1 - 5 (I)	**NUMNP**	Total fluid nodal points.
6 -10 (I)	**NUMNS**	Number of fluid nodal points on the dam-reservoir interface.
11-15 (I)	**N3DEL**	Number of 3D fluid elements.
16-20 (I)	**N2DEL**	Number of 2D interface fluid elements.
21-30 (F)	**WMASS**	Mass density of water.
31-40 (F)	**GA**	Gravity acceleration.
41-50 (F)	**WATL**	Z-coordinate of water level.
51-55 (I)	**ICOMP**	Code for comparison between the finite element and Westergaard solutions; = 0, no comparison is made; ≠ 0, A comparison is made by subjecting the dam face to a pattern of unit g uniform accelerations in the ICOMP direction. (ICOMP = 1, 2, or 3, corresponding to the x, y, and z directions)

Note:

The comparison between the finite element and the Westergaard is made only for a simple pattern of unit g accelerations that are applied in the global x, y, or z direction. This is essentially equivalent to a rigid body motion of the dam, and thus does not consider the flexibility of the arch structure. The resulting hydrodynamic pressures acting on the face of the dam, and the equivalent nodal forces for each method are printed out in the output files.

C. NODAL COORDINATES AND BOUNDARY CONDITIONS

One card per nodal point is required to specify the coordinates and the boundary conditions.

1 - 5 (I)	**N**	Node number*
6 -15 (F)	**XYZ(1,N)**	X-coordinate
16-25 (F)	**XYZ(2,N)**	Y-coordinate
26-35 (F)	**XYZ(3,N)**	Z-coordinate
36-40 (I)	**IBC(N)**	Boundary condition codes: = 0 Non-interface below-the- surface-nodes = 1 Non-interface surface-nodes =-2 Interface surface-nodes =-1 Interface below-the-surface-nodes

* Reservoir nodal points should be numbered according to Figure 2.10. Each reservoir section is numbered across the channel and from water surface to bottom.

D. 2D ELEMENT DATA

One or both of the following data cards specify each 2D element on the interface. The sequence of data is such that the absolute values of the element numbers are in increasing order.

D.1 Element Connectivity

This card is always required.

1 - 5 (I)	**NEL**	Element number: For an element that its nodes at the water surface do not coincide with the corresponding concrete nodes, NEL is entered as a negative number.
6 -10 (I)	**NCON(1)**	Element nodal point 1*
	.	
	.	
	.	
41-45 (I)	**NCON(8)**	Element nodal point 8
46-50 (I)	**NINT**	Integration order: 2, or 3 (2 is usually sufficient).

* Degenerated nodal points and the omitted mid-side nodes of a degenerated element should be set to zero. For example the element connectivity for the triangular 2D element in Figure 3.6a is 1, 2, 3, 0, 5, 6, 0, 8.

D.2 Z-coordinates of Surface Elements

This card is required when NEL is negative. That is when the water surface does not coincide with the upper edge of the concrete elements.

1 -10 (F)	**Z2**	Z-coordinate of the nodes on the upper side of the corresponding dam element.
11-20 (F)	**Z0**	Z-coordinate of the nodes on the mid-height of the corresponding dam element.
21-30 (F)	**Z1**	Z-coordinate of the nodes on the lower side of the corresponding dam element.

Note: Water level always lies between Z2 and Z1.

E. 3D ELEMENT DATA

Two cards are required for each 3D fluid element. The sequence of cards is in increasing order of the element numbers.

E.1 Element Identification

1 - 5 (I)	**NE**	Element number
6 -10 (I)	**NINT**	Integration order: 2, or 3(usually 2 is sufficient).

E.2 Element Connectivity

1 - 5 (I)	**NP(1)**	Element nodal number 1*
	.	
	.	
	.	
76-80 (I)	**NP(16)**	Element nodal number 16

* Degenerated nodal points and omitted mid-side nodes of a degenerated 3D fluid element should be set to zero. For example element numbering of the triangular 3D element in Figure 3.6b is 1, 2, 3, 0, 5, 6, 7, 0, 9, 10, 0, 12, 13, 14, 0, 16.

F. ADDED-MASS MATRIX

The following cards are supplied to convert the calculated added-mass defined with respect to the reservoir dof's into a mass matrix consistent with the dam dof's. The resulting mass matrix is a full square matrix with a dimension equal to the number of dof's of the dam, and is blocked similar to the concrete mass matrix. It should be noted that only those terms corresponding to the upstream nodes of the dam (wet nodes) are non-zero. This resequenced added-mass matrix which is saved in binary form on TAPE12.DAT, is later used as an input to EADAP program to account for the interaction with the reservoir in dynamic analysis.

F.1 Resequencing Option

1 - 5 (I)	**ISEQ**	Code for resequencing the added-mass: EQ. 0, Do not resequence NE. 0, Resequence

F.2 Blocking Information

When resequencing is requested, the following information is provided for storing the added-mass in block forms.

1 - 5	**NEQB**	Number of equations per block for the dam-foundation system. NEQB is obtained from a previous EADAP dynamic analysis.
6 -10	**NBLOCK**	Number of blocks for the dam- foundation system.
11-15	**NLL**	Number of dof's of the interface nodes (no. of nodes on interface multiplied by 3).

F.3 DOF's of Dam Interface Nodes

The following set of cards are supplied to resequence the added-mass.

Degrees-of-freedom of the dam interface-nodes are provided according to the node numbering sequence of the reservoir interface-nodes. For each node only three translational degrees-of-freedom are considered. Degrees-of-freedom of the concrete nodes are obtained from the ID array of the dam-foundation system which is included in the output-file of any EADAP analysis. Thus, for every reservoir interface-node, a corresponding concrete node is identified and its dof's are retrieved from the ID array.

Sixteen values are provided in each card (16I5 format), and as many cards as needed are supplied to define all dof's of all interface-nodes.

G. TERMINATION CARD

Two blank cards terminate the program execution.

9. REFERENCES

1. R. W. Clough, K.-T. Chang, et al. "*Dynamic Response Behavior of Xiang Hong Dian Dam,*" Report No. UCB/EERC 84/02, Earthquake Engineering Research Center, University of California, Berkeley, April 1984.

2. R. W. Clough, K.-T. Chang, et al. "*Dynamic Response Behavior of Quan Shui Dam,*" Report no. UCB/EERC 84/20, Earthquake Engineering Research Center, University of California, Berkeley, November 1984.

3. R. W. Clough, J. M. Raphael, and S. Mojtahedi, "*ADAP - A Computer Program for Static and Dynamic Analysis of Arch Dams,*" Report NO. UCB/EERC 73/14, Earthquake Engineering Research Center, University of California, Berkeley, June 1973.

4. J. S.-H. Kuo, "*Fluid-Structure Interactions: Added-Mass Computations for Incompressible Fluid,*" Report No. UCB/EERC 82/09, Earthquake Engineering Research Center, University of California, Berkeley, August 1982.

5. R. W. Clough, Y. Ghanaat, and X.-F. Qiu "*Dynamic Reservoir Interaction with Monticello Dam,*" Report No. UCB/EERC 87/21, Earthquake Engineering Research Center, University of California, Berkeley, December 1987.

6. E. L. Wilson, "*SAP, A General Structural Analysis Program*", Report No. UC/SESM 70-20, Structural Engineering Laboratory, University of California, Berkeley, September 1970.

7. O.C. Zienkiewics, Y.K. Cheung, "*The Finite Element Method in Structural and Continuum Mechanics*", McGraw- Hill, 1967.

8. J. Ghaboussi, E.L. Wilson, and R.L. Taylor, "*Isoparametric Finite Elements with Incompatible Deformation Modes*", Proceedings of O.N.R. Symp., University of Illinois, Urbana, Sept. 8-10, 1971.

10. S.F. Pawsey, "*The Analysis of Moderately Thick to Thin Shells by the Finite Element Method*", Report NO. UC/SESM 70-12, Structural Engineering Laboratory, University of California, Berkeley, August 1970.

11. S. Ahmad, B.M. Irons, and O.C. Zienkiewicz, "*Curved Thick Shell and Membrane Elements with Particular Reference to Axisymmetric Problem*", Proceedings of the Second Conference on Methods in Structural Mechanics, Wright Patterson Army Air Force Base, Ohio, 1968.

12. R.W. Clough, J. Penzien, Dynamics of Structures, McGraw Hill Book Company, New York, N.Y., 1975.

13. K.-J. Bathe, E.L. Wilson, Numerical Methods In Finite Element Analysis, Prentice-Hall, Inc., Englewood Cliffs, NJ, 1976.

14. U.S. Department of Interior, Bureau of Reclamation, Design of Arch Dams, Denver, Colorado, 1977 (pp 422 and 423).

15. A.F. Shakal, M.J. Huang, et al., "*Processed Data from the Strong Motion Records of the Morgan Hill Earthquake of 24 April 1984 -- Part-I. Ground Response Records,*" California Department of Conservation, Division of Mines and Geology Report No. OSMS 85-04, May 1986.

APPENDIX

PRE- AND POST-PROCESSING CAPABILITIES

The present EADAP program can automatically generate finite element meshes for the concrete arch dam and the foundation rock. But the mesh generation is limited to regular geometries and the program does not include any pre- and post-processing graphics capabilities.

QUEST Structures, a consulting engineering company in Emeryville, California, has enhanced and extended the program EADAP further and has developed pre- and post- processing graphics capabilities for the program. The QUEST version of the program, which is called GDAP, for Graphics-based Dam Analysis Program, was used extensively to prepare all the 3D and 2D pictures presented in this report and to display the results of the example analyses.

The program GDAP and its associated pre- and post-processors run on 386-based microcomputers under the UNIX operating system and share graphics and data files with the MS-DOS environment. It can easily be installed on any mini-computer or graphics workstation that has MS-DOS capabilities. An outline of this commercial package offered by QUEST Structures is provided here for information purposes.

Pre-Processor

The pre-processor automatically generates finite-element meshes for the dam, foundation rock, and the reservoir water from either the ADSAS (US Bureau of Reclamation's Arch Dam Stress Analysis System) or GDAP input data. Depending on the options selected, the pre-processor generates various 3D and 2D graphics for presentation or examination of the accuracy of various aspects of the generated finite-element models. Following is a list of available features:

- *Automatic mesh generation of the dam, foundation, and the reservoir models for arch dams located in narrow, wide, regular, or irregular canyons.*
- *Accepting ADSAS data files as input.*

- *3D plots of the dam, foundation, and reservoir models with hidden lines removed.*
- *3D "shrink" plots of the dam and foundation to check element connectivities.*
- *2D plots of the upstream and downstream faces of the dam to examine node numbers, and element numbers.*
- *Plot of crown cantilever with Line of Centers (LOC) for comparison with design layouts.*
- *Plan view of arch sections to check curvatures and angles to the abutments.*

Post-Processor

The post-processor of the GDAP program transforms the results of the static and dynamic analyses into appropriate plots and contours for easy review and evaluation. In particular, it includes evaluation criteria for analyzing the large amount of data produced in a typical response history analysis. It automatically retrieves the envelope of the maximum and minimum stress values, identifies all significant concurrent stresses, recovers stress histories at all critical locations, provides statistics regarding the number of stress cycles exceeding the allowable stress, and calculates the excursion time of stress cycles beyond the allowable values. A list of available features follows:

- *Plot of nodal displacements and mode shapes along each arch section.*
- *Contour plots of the static, dynamic, and the static plus dynamic arch and cantilever stresses.*
- *Vector plots of static, dynamic, and static plus dynamic principal stresses.*
- *Contour plots of the envelope arch and cantilever stresses due to the dynamic only and the dynamic plus static loads.*
- *Contour plots of concurrent stresses at critical instants of time.*
- *Time history plots of the input earthquake motions and the critical nodal displacements and element stresses.*
- *Statistics on number of stress cycles exceeding allowable stress and the corresponding excursions of these stress cycles beyond specified limits.*

EARTHQUAKE ENGINEERING RESEARCH CENTER REPORT SERIES

EERC reports are available from the National Information Service for Earthquake Engineering(NISEE) and from the National Technical Information Service(NTIS). Numbers in parentheses are Accession Numbers assigned by the National Technical Information Service; these are followed by a price code. Contact NTIS, 5285 Port Royal Road, Springfield Virginia, 22161 for more information. Reports without Accession Numbers were not available from NTIS at the time of printing. For a current complete list of EERC reports (from EERC 67-1) and availablity information, please contact University of California, EERC, NISEE, 1301 South 46th Street, Richmond, California 94804.

UCB/EERC-80/01 "Earthquake Response of Concrete Gravity Dams Including Hydrodynamic and Foundation Interaction Effects," by Chopra, A.K., Chakrabarti, P. and Gupta, S., January 1980, (AD-A087297)A10.

UCB/EERC-80/02 "Rocking Response of Rigid Blocks to Earthquakes," by Yim, C.S., Chopra, A.K. and Penzien, J., January 1980, (PB80 166 002)A04.

UCB/EERC-80/03 "Optimum Inelastic Design of Seismic-Resistant Reinforced Concrete Frame Structures," by Zagajeski, S.W. and Bertero, V.V., January 1980, (PB80 164 635)A06.

UCB/EERC-80/04 "Effects of Amount and Arrangement of Wall-Panel Reinforcement on Hysteretic Behavior of Reinforced Concrete Walls," by Iliya, R. and Bertero, V.V., February 1980, (PB81 122 525)A09.

UCB/EERC-80/05 "Shaking Table Research on Concrete Dam Models," by Niwa, A. and Clough, R.W., September 1980, (PB81 122 368)A06.

UCB/EERC-80/06 "The Design of Steel Energy-Absorbing Restrainers and their Incorporation into Nuclear Power Plants for Enhanced Safety (Vol 1a): Piping with Energy Absorbing Restrainers: Parameter Study on Small Systems," by Powell, G.H., Oughourlian, C. and Simons, J., June 1980.

UCB/EERC-80/07 "Inelastic Torsional Response of Structures Subjected to Earthquake Ground Motions," by Yamazaki, Y., April 1980, (PB81 122 327)A08.

UCB/EERC-80/08 "Study of X-Braced Steel Frame Structures under Earthquake Simulation," by Ghanaat, Y., April 1980, (PB81 122 335)A11.

UCB/EERC-80/09 "Hybrid Modelling of Soil-Structure Interaction," by Gupta, S., Lin, T.W. and Penzien, J., May 1980, (PB81 122 319)A07.

UCB/EERC-80/10 "General Applicability of a Nonlinear Model of a One Story Steel Frame," by Sveinsson, B.I. and McNiven, H.D., May 1980, (PB81 124 877)A06.

UCB/EERC-80/11 "A Green-Function Method for Wave Interaction with a Submerged Body," by Kioka, W., April 1980, (PB81 122 269)A07.

UCB/EERC-80/12 "Hydrodynamic Pressure and Added Mass for Axisymmetric Bodies.," by Nilrat, F., May 1980, (PB81 122 343)A08.

UCB/EERC-80/13 "Treatment of Non-Linear Drag Forces Acting on Offshore Platforms," by Dao, B.V. and Penzien, J., May 1980, (PB81 153 413)A07.

UCB/EERC-80/14 "2D Plane/Axisymmetric Solid Element (Type 3-Elastic or Elastic-Perfectly Plastic)for the ANSR-II Program," by Mondkar, D.P. and Powell, G.H., July 1980, (PB81 122 350)A03.

UCB/EERC-80/15 "A Response Spectrum Method for Random Vibrations," by Der Kiureghian, A., June 1981, (PB81 122 301)A03.

UCB/EERC-80/16 "Cyclic Inelastic Buckling of Tubular Steel Braces," by Zayas, V.A., Popov, E.P. and Mahin, S.A., June 1981, (PB81 124 885)A10.

UCB/EERC-80/17 "Dynamic Response of Simple Arch Dams Including Hydrodynamic Interaction," by Porter, C.S. and Chopra, A.K., July 1981, (PB81 124 000)A13.

UCB/EERC-80/18 "Experimental Testing of a Friction Damped Aseismic Base Isolation System with Fail-Safe Characteristics," by Kelly, J.M., Beucke, K.E. and Skinner, M.S., July 1980, (PB81 148 595)A04.

UCB/EERC-80/19 "The Design of Steel Energy-Absorbing Restrainers and their Incorporation into Nuclear Power Plants for Enhanced Safety (Vol.1B): Stochastic Seismic Analyses of Nuclear Power Plant Structures and Piping Systems Subjected to Multiple Supported Excitations," by Lee, M.C. and Penzien, J., June 1980, (PB82 201 872)A08.

UCB/EERC-80/20 "The Design of Steel Energy-Absorbing Restrainers and their Incorporation into Nuclear Power Plants for Enhanced Safety (Vol 1C): Numerical Method for Dynamic Substructure Analysis," by Dickens, J.M. and Wilson, E.L., June 1980.

UCB/EERC-80/21 "The Design of Steel Energy-Absorbing Restrainers and their Incorporation into Nuclear Power Plants for Enhanced Safety (Vol 2): Development and Testing of Restraints for Nuclear Piping Systems," by Kelly, J.M. and Skinner, M.S., June 1980.

UCB/EERC-80/22 "3D Solid Element (Type 4-Elastic or Elastic-Perfectly-Plastic) for the ANSR-II Program," by Mondkar, D.P. and Powell, G.H., July 1980, (PB81 123 242)A03.

UCB/EERC-80/23 "Gap-Friction Element (Type 5) for the Ansr-II Program," by Mondkar, D.P. and Powell, G.H., July 1980, (PB81 122 285)A03.

UCB/EERC-80/24 "U-Bar Restraint Element (Type 11) for the ANSR-II Program," by Oughourlian, C. and Powell, G.H., July 1980, (PB81 122 293)A03.

UCB/EERC-80/25 "Testing of a Natural Rubber Base Isolation System by an Explosively Simulated Earthquake," by Kelly, J.M., August 1980, (PB81 201 360)A04.

UCB/EERC-80/26 "Input Identification from Structural Vibrational Response," by Hu, Y., August 1980, (PB81 152 308)A05.

UCB/EERC-80/27 "Cyclic Inelastic Behavior of Steel Offshore Structures," by Zayas, V.A., Mahin, S.A. and Popov, E.P., August 1980, (PB81 196 180)A15.

UCB/EERC-80/28 "Shaking Table Testing of a Reinforced Concrete Frame with Biaxial Response," by Oliva, M.G., October 1980, (PB81 154 304)A10.

UCB/EERC-80/29 "Dynamic Properties of a Twelve-Story Prefabricated Panel Building," by Bouwkamp, J.G., Kollegger, J.P. and Stephen, R.M., October 1980, (PB82 138 777)A07.

UCB/EERC-80/30 "Dynamic Properties of an Eight-Story Prefabricated Panel Building," by Bouwkamp, J.G., Kollegger, J.P. and Stephen, R.M., October 1980, (PB81 200 313)A05.

UCB/EERC-80/31 "Predictive Dynamic Response of Panel Type Structures under Earthquakes," by Kollegger, J.P. and Bouwkamp, J.G., October 1980, (PB81 152 316)A04.

UCB/EERC-80/32 "The Design of Steel Energy-Absorbing Restrainers and their Incorporation into Nuclear Power Plants for Enhanced Safety (Vol 3): Testing of Commercial Steels in Low-Cycle Torsional Fatigue," by Spanner, P., Parker, E.R., Jongewaard, E. and Dory, M., 1980.

UCB/EERC-80/33 "The Design of Steel Energy-Absorbing Restrainers and their Incorporation into Nuclear Power Plants for Enhanced Safety (Vol 4): Shaking Table Tests of Piping Systems with Energy-Absorbing Restrainers," by Stiemer, S.F. and Godden, W.G., September 1980, (PB82 201 880)A05.

UCB/EERC-80/34 "The Design of Steel Energy-Absorbing Restrainers and their Incorporation into Nuclear Power Plants for Enhanced Safety (Vol 5): Summary Report," by Spencer, P., 1980.

UCB/EERC-80/35 "Experimental Testing of an Energy-Absorbing Base Isolation System," by Kelly, J.M., Skinner, M.S. and Beucke, K.E., October 1980, (PB81 154 072)A04.

UCB/EERC-80/36 "Simulating and Analyzing Artificial Non-Stationary Earth Ground Motions," by Nau, R.F., Oliver, R.M. and Pister, K.S., October 1980, (PB81 153 397)A04.

UCB/EERC-80/37 "Earthquake Engineering at Berkeley - 1980," by , September 1980, (PB81 205 674)A09.

UCB/EERC-80/38 "Inelastic Seismic Analysis of Large Panel Buildings," by Schricker, V. and Powell, G.H., September 1980, (PB81 154 338)A13.

UCB/EERC-80/39 "Dynamic Response of Embankment, Concrete-Gavity and Arch Dams Including Hydrodynamic Interation," by Hall, J.F. and Chopra, A.K., October 1980, (PB81 152 324)A11.

UCB/EERC-80/40 "Inelastic Buckling of Steel Struts under Cyclic Load Reversal.," by Black, R.G., Wenger, W.A. and Popov, E.P., October 1980, (PB81 154 312)A08.

UCB/EERC-80/41 "Influence of Site Characteristics on Buildings Damage during the October 3,1974 Lima Earthquake," by Repetto, P., Arango, I. and Seed, H.B., September 1980, (PB81 161 739)A05.

UCB/EERC-80/42 "Evaluation of a Shaking Table Test Program on Response Behavior of a Two Story Reinforced Concrete Frame," by Blondet, J.M., Clough, R.W. and Mahin, S.A., December 1980, (PB82 196 544)A11.

UCB/EERC-80/43 "Modelling of Soil-Structure Interaction by Finite and Infinite Elements," by Medina, F., December 1980, (PB81 229 270)A04.

UCB/EERC-81/01 "Control of Seismic Response of Piping Systems and Other Structures by Base Isolation," by Kelly, J.M., January 1981, (PB81 200 735)A05.

UCB/EERC-81/02 "OPTNSR- An Interactive Software System for Optimal Design of Statically and Dynamically Loaded Structures with Nonlinear Response," by Bhatti, M.A., Ciampi, V. and Pister, K.S., January 1981, (PB81 218 851)A09.

UCB/EERC-81/03 "Analysis of Local Variations in Free Field Seismic Ground Motions," by Chen, J.-C., Lysmer, J. and Seed, H.B., January 1981, (AD-A099508)A13.

UCB/EERC-81/04 "Inelastic Structural Modeling of Braced Offshore Platforms for Seismic Loading," by Zayas, V.A., Shing, P.-S.B., Mahin, S.A. and Popov, E.P., January 1981, (PB82 138 777)A07.

UCB/EERC-81/05 "Dynamic Response of Light Equipment in Structures," by Der Kiureghian, A., Sackman, J.L. and Nour-Omid, B., April 1981, (PB81 218 497)A04.

UCB/EERC-81/06 "Preliminary Experimental Investigation of a Broad Base Liquid Storage Tank," by Bouwkamp, J.G., Kollegger, J.P. and Stephen, R.M., May 1981, (PB82 140 385)A03.

UCB/EERC-81/07 "The Seismic Resistant Design of Reinforced Concrete Coupled Structural Walls," by Aktan, A.E. and Bertero, V.V., June 1981, (PB82 113 358)A11.

UCB/EERC-81/08 "Unassigned," by Unassigned, 1981.

UCB/EERC-81/09 "Experimental Behavior of a Spatial Piping System with Steel Energy Absorbers Subjected to a Simulated Differential Seismic Input," by Stiemer, S.F., Godden, W.G. and Kelly, J.M., July 1981, (PB82 201 898)A04.

UCB/EERC-81/10 "Evaluation of Seismic Design Provisions for Masonry in the United States," by Sveinsson, B.I., Mayes, R.L. and McNiven, H.D., August 1981, (PB82 166 075)A08.

UCB/EERC-81/11 "Two-Dimensional Hybrid Modelling of Soil-Structure Interaction," by Tzong, T.-J., Gupta, S. and Penzien, J., August 1981, (PB82 142 118)A04.

UCB/EERC-81/12 "Studies on Effects of Infills in Seismic Resistant R/C Construction," by Brokken, S. and Bertero, V.V., October 1981, (PB82 166 190)A09.

UCB/EERC-81/13 "Linear Models to Predict the Nonlinear Seismic Behavior of a One-Story Steel Frame," by Valdimarsson, H., Shah, A.H. and McNiven, H.D., September 1981, (PB82 138 793)A07.

UCB/EERC-81/14 "TLUSH: A Computer Program for the Three-Dimensional Dynamic Analysis of Earth Dams," by Kagawa, T., Mejia, L.H., Seed, H.B. and Lysmer, J., September 1981, (PB82 139 940)A06.

UCB/EERC-81/15 "Three Dimensional Dynamic Response Analysis of Earth Dams," by Mejia, L.H. and Seed, H.B., September 1981, (PB82 137 274)A12.

UCB/EERC-81/16 "Experimental Study of Lead and Elastomeric Dampers for Base Isolation Systems," by Kelly, J.M. and Hodder, S.B., October 1981, (PB82 166 182)A05.

UCB/EERC-81/17 "The Influence of Base Isolation on the Seismic Response of Light Secondary Equipment," by Kelly, J.M., April 1981, (PB82 255 266)A04.

UCB/EERC-81/18 "Studies on Evaluation of Shaking Table Response Analysis Procedures," by Blondet, J. M., November 1981, (PB82 197 278)A10.

UCB/EERC-81/19 "DELIGHT.STRUCT: A Computer-Aided Design Environment for Structural Engineering," by Balling, R.J., Pister, K.S. and Polak, E., December 1981, (PB82 218 496)A07.

UCB/EERC-81/20 "Optimal Design of Seismic-Resistant Planar Steel Frames," by Balling, R.J., Ciampi, V. and Pister, K.S., December 1981, (PB82 220 179)A07.

UCB/EERC-82/01 "Dynamic Behavior of Ground for Seismic Analysis of Lifeline Systems," by Sato, T. and Der Kiureghian, A., January 1982, (PB82 218 926)A05.

UCB/EERC-82/02 "Shaking Table Tests of a Tubular Steel Frame Model," by Ghanaat, Y. and Clough, R.W., January 1982, (PB82 220 161)A07.

UCB/EERC-82/03 "Behavior of a Piping System under Seismic Excitation: Experimental Investigations of a Spatial Piping System supported by Mechanical Shock Arrestors," by Schneider, S., Lee, H.-M. and Godden, W. G., May 1982, (PB83 172 544)A09.

UCB/EERC-82/04 "New Approaches for the Dynamic Analysis of Large Structural Systems," by Wilson, E.L., June 1982, (PB83 148 080)A05.

UCB/EERC-82/05 "Model Study of Effects of Damage on the Vibration Properties of Steel Offshore Platforms," by Shahrivar, F. and Bouwkamp, J.G., June 1982, (PB83 148 742)A10.

UCB/EERC-82/06 "States of the Art and Pratice in the Optimum Seismic Design and Analytical Response Prediction of R/C Frame Wall Structures," by Aktan, A.E. and Bertero, V.V., July 1982, (PB83 147 736)A05.

UCB/EERC-82/07 "Further Study of the Earthquake Response of a Broad Cylindrical Liquid-Storage Tank Model," by Manos, G.C. and Clough, R.W., July 1982, (PB83 147 744)A11.

UCB/EERC-82/08 "An Evaluation of the Design and Analytical Seismic Response of a Seven Story Reinforced Concrete Frame," by Charney, F.A. and Bertero, V.V., July 1982, (PB83 157 628)A09.

UCB/EERC-82/09 "Fluid-Structure Interactions: Added Mass Computations for Incompressible Fluid," by Kuo, J.S.-H., August 1982, (PB83 156 281)A07.

UCB/EERC-82/10 "Joint-Opening Nonlinear Mechanism: Interface Smeared Crack Model," by Kuo, J.S.-H., August 1982, (PB83 149 195)A05.

UCB/EERC-82/11 "Dynamic Response Analysis of Techi Dam," by Clough, R.W., Stephen, R.M. and Kuo, J.S.-H., August 1982, (PB83 147 496)A06.

UCB/EERC-82/12 "Prediction of the Seismic Response of R/C Frame-Coupled Wall Structures," by Aktan, A.E., Bertero, V.V. and Piazzo, M., August 1982, (PB83 149 203)A09.

UCB/EERC-82/13 "Preliminary Report on the Smart 1 Strong Motion Array in Taiwan," by Bolt, B.A., Loh, C.H., Penzien, J. and Tsai, Y.B., August 1982, (PB83 159 400)A10.

UCB/EERC-82/14 "Shaking-Table Studies of an Eccentrically X-Braced Steel Structure," by Yang, M.S., September 1982, (PB83 260 778)A12.

UCB/EERC-82/15 "The Performance of Stairways in Earthquakes," by Roha, C., Axley, J.W. and Bertero, V.V., September 1982, (PB83 157 693)A07.

UCB/EERC-82/16 "The Behavior of Submerged Multiple Bodies in Earthquakes," by Liao, W.-G., September 1982, (PB83 158 709)A07.

UCB/EERC-82/17 "Effects of Concrete Types and Loading Conditions on Local Bond-Slip Relationships," by Cowell, A.D., Popov, E.P. and Bertero, V.V., September 1982, (PB83 153 577)A04.

UCB/EERC-82/18 "Mechanical Behavior of Shear Wall Vertical Boundary Members: An Experimental Investigation," by Wagner, M.T. and Bertero, V.V., October 1982, (PB83 159 764)A05.

UCB/EERC-82/19 "Experimental Studies of Multi-support Seismic Loading on Piping Systems," by Kelly, J.M. and Cowell, A.D., November 1982.

UCB/EERC-82/20 "Generalized Plastic Hinge Concepts for 3D Beam-Column Elements," by Chen, P. F.-S. and Powell, G.H., November 1982, (PB83 247 981)A13.

UCB/EERC-82/21 "ANSR-II: General Computer Program for Nonlinear Structural Analysis," by Oughourlian, C.V. and Powell, G.H., November 1982, (PB83 251 330)A12.

UCB/EERC-82/22 "Solution Strategies for Statically Loaded Nonlinear Structures," by Simons, J.W. and Powell, G.H., November 1982, (PB83 197 970)A06.

UCB/EERC-82/23 "Analytical Model of Deformed Bar Anchorages under Generalized Excitations," by Ciampi, V., Eligehausen, R., Bertero, V.V. and Popov, E.P., November 1982, (PB83 169 532)A06.

UCB/EERC-82/24 "A Mathematical Model for the Response of Masonry Walls to Dynamic Excitations," by Sucuoglu, H., Mengi, Y. and McNiven, H.D., November 1982, (PB83 169 011)A07.

UCB/EERC-82/25 "Earthquake Response Considerations of Broad Liquid Storage Tanks," by Cambra, F.J., November 1982, (PB83 251 215)A09.

UCB/EERC-82/26 "Computational Models for Cyclic Plasticity, Rate Dependence and Creep," by Mosaddad, B. and Powell, G.H., November 1982, (PB83 245 829)A08.

UCB/EERC-82/27 "Inelastic Analysis of Piping and Tubular Structures," by Mahasuverachai, M. and Powell, G.H., November 1982, (PB83 249 987)A07.

UCB/EERC-83/01 "The Economic Feasibility of Seismic Rehabilitation of Buildings by Base Isolation," by Kelly, J.M., January 1983, (PB83 197 988)A05.

UCB/EERC-83/02 "Seismic Moment Connections for Moment-Resisting Steel Frames.," by Popov, E.P., January 1983, (PB83 195 412)A04.

UCB/EERC-83/03 "Design of Links and Beam-to-Column Connections for Eccentrically Braced Steel Frames," by Popov, E.P. and Malley, J.O., January 1983, (PB83 194 811)A04.

UCB/EERC-83/04 "Numerical Techniques for the Evaluation of Soil-Structure Interaction Effects in the Time Domain," by Bayo, E. and Wilson, E.L., February 1983, (PB83 245 605)A09.

UCB/EERC-83/05 "A Transducer for Measuring the Internal Forces in the Columns of a Frame-Wall Reinforced Concrete Structure," by Sause, R. and Bertero, V.V., May 1983, (PB84 119 494)A06.

UCB/EERC-83/06 "Dynamic Interactions Between Floating Ice and Offshore Structures," by Croteau, P., May 1983, (PB84 119 486)A16.

UCB/EERC-83/07 "Dynamic Analysis of Multiply Tuned and Arbitrarily Supported Secondary Systems," by Igusa, T. and Der Kiureghian, A., July 1983, (PB84 118 272)A11.

UCB/EERC-83/08 "A Laboratory Study of Submerged Multi-body Systems in Earthquakes," by Ansari, G.R., June 1983, (PB83 261 842)A17.

UCB/EERC-83/09 "Effects of Transient Foundation Uplift on Earthquake Response of Structures," by Yim, C.-S. and Chopra, A.K., June 1983, (PB83 261 396)A07.

UCB/EERC-83/10 "Optimal Design of Friction-Braced Frames under Seismic Loading," by Austin, M.A. and Pister, K.S., June 1983, (PB84 119 288)A06.

UCB/EERC-83/11 "Shaking Table Study of Single-Story Masonry Houses: Dynamic Performance under Three Component Seismic Input and Recommendations," by Manos, G.C., Clough, R.W. and Mayes, R.L., July 1983, (UCB/EERC-83/11)A08.

UCB/EERC-83/12 "Experimental Error Propagation in Pseudodynamic Testing," by Shiing, P.B. and Mahin, S.A., June 1983, (PB84 119 270)A09.

UCB/EERC-83/13 "Experimental and Analytical Predictions of the Mechanical Characteristics of a 1/5-scale Model of a 7-story R/C Frame-Wall Building Structure," by Aktan, A.E., Bertero, V.V., Chowdhury, A.A. and Nagashima, T., June 1983, (PB84 119 213)A07.

UCB/EERC-83/14 "Shaking Table Tests of Large-Panel Precast Concrete Building System Assemblages," by Oliva, M.G. and Clough, R.W., June 1983, (PB86 110 210/AS)A11.

UCB/EERC-83/15 "Seismic Behavior of Active Beam Links in Eccentrically Braced Frames," by Hjelmstad, K.D. and Popov, E.P., July 1983, (PB84 119 676)A09.

UCB/EERC-83/16 "System Identification of Structures with Joint Rotation," by Dimsdale, J.S., July 1983, (PB84 192 210)A06.

UCB/EERC-83/17 "Construction of Inelastic Response Spectra for Single-Degree-of-Freedom Systems," by Mahin, S. and Lin, J., June 1983, (PB84 208 834)A05.

UCB/EERC-83/18 "Interactive Computer Analysis Methods for Predicting the Inelastic Cyclic Behaviour of Structural Sections," by Kaba, S. and Mahin, S., July 1983, (PB84 192 012)A06.

UCB/EERC-83/19 "Effects of Bond Deterioration on Hysteretic Behavior of Reinforced Concrete Joints," by Filippou, F.C., Popov, E.P. and Bertero, V.V., August 1983, (PB84 192 020)A10.

UCB/EERC-83/20 "Correlation of Analytical and Experimental Responses of Large-Panel Precast Building Systems," by Oliva, M.G., Clough, R.W., Velkov, M. and Gavrilovic, P., May 1988.

UCB/EERC-83/21 "Mechanical Characteristics of Materials Used in a 1/5 Scale Model of a 7-Story Reinforced Concrete Test Structure," by Bertero, V.V., Aktan, A.E., Harris, H.G. and Chowdhury, A.A., October 1983, (PB84 193 697)A05.

UCB/EERC-83/22 "Hybrid Modelling of Soil-Structure Interaction in Layered Media," by Tzong, T.-J. and Penzien, J., October 1983, (PB84 192 178)A08.

UCB/EERC-83/23 "Local Bond Stress-Slip Relationships of Deformed Bars under Generalized Excitations," by Eligehausen, R., Popov, E.P. and Bertero, V.V., October 1983, (PB84 192 848)A09.

UCB/EERC-83/24 "Design Considerations for Shear Links in Eccentrically Braced Frames," by Malley, J.O. and Popov, E.P., November 1983, (PB84 192 186)A07.

UCB/EERC-84/01 "Pseudodynamic Test Method for Seismic Performance Evaluation: Theory and Implementation," by Shing, P.-S.B. and Mahin, S.A., January 1984, (PB84 190 644)A08.

UCB/EERC-84/02 "Dynamic Response Behavior of Kiang Hong Dian Dam," by Clough, R.W., Chang, K.-T., Chen, H.-Q. and Stephen, R.M., April 1984, (PB84 209 402)A08.

UCB/EERC-84/03 "Refined Modelling of Reinforced Concrete Columns for Seismic Analysis," by Kaba, S.A. and Mahin, S.A., April 1984, (PB84 234 384)A06.

UCB/EERC-84/04 "A New Floor Response Spectrum Method for Seismic Analysis of Multiply Supported Secondary Systems," by Asfura, A. and Der Kiureghian, A., June 1984, (PB84 239 417)A06.

UCB/EERC-84/05 "Earthquake Simulation Tests and Associated Studies of a 1/5th-scale Model of a 7-Story R/C Frame-Wall Test Structure," by Bertero, V.V., Aktan, A.E., Charney, F.A. and Sause, R., June 1984, (PB84 239 409)A09.

UCB/EERC-84/06 "R/C Structural Walls: Seismic Design for Shear," by Aktan, A.E. and Bertero, V.V., 1984.

UCB/EERC-84/07 "Behavior of Interior and Exterior Flat-Plate Connections subjected to Inelastic Load Reversals," by Zee, H.L. and Moehle, J.P., August 1984, (PB86 117 629/AS)A07.

UCB/EERC-84/08 "Experimental Study of the Seismic Behavior of a Two-Story Flat-Plate Structure," by Moehle, J.P. and Diebold, J.W., August 1984, (PB86 122 553/AS)A12.

UCB/EERC-84/09 "Phenomenological Modeling of Steel Braces under Cyclic Loading," by Ikeda, K., Mahin, S.A. and Dermitzakis, S.N., May 1984, (PB86 132 198/AS)A08.

UCB/EERC-84/10 "Earthquake Analysis and Response of Concrete Gravity Dams," by Fenves, G. and Chopra, A.K., August 1984, (PB85 193 902/AS)A11.

UCB/EERC-84/11 "EAGD-84: A Computer Program for Earthquake Analysis of Concrete Gravity Dams," by Fenves, G. and Chopra, A.K., August 1984, (PB85 193 613/AS)A05.

UCB/EERC-84/12 "A Refined Physical Theory Model for Predicting the Seismic Behavior of Braced Steel Frames," by Ikeda, K. and Mahin, S.A., July 1984, (PB85 191 450/AS)A09.

UCB/EERC-84/13 "Earthquake Engineering Research at Berkeley - 1984," by , August 1984, (PB85 197 341/AS)A10.

UCB/EERC-84/14 "Moduli and Damping Factors for Dynamic Analyses of Cohesionless Soils," by Seed, H.B., Wong, R.T., Idriss, I.M. and Tokimatsu, K., September 1984, (PB85 191 468/AS)A04.

UCB/EERC-84/15 "The Influence of SPT Procedures in Soil Liquefaction Resistance Evaluations," by Seed, H.B., Tokimatsu, K., Harder, L.F. and Chung, R.M., October 1984, (PB85 191 732/AS)A04.

UCB/EERC-84/16 "Simplified Procedures for the Evaluation of Settlements in Sands Due to Earthquake Shaking," by Tokimatsu, K. and Seed, H.B., October 1984, (PB85 197 887/AS)A03.

UCB/EERC-84/17 "Evaluation of Energy Absorption Characteristics of Highway Bridges Under Seismic Conditions - Volume I and Volume II (Appendices)," by Imbsen, R.A. and Penzien, J., September 1986.

UCB/EERC-84/18 "Structure-Foundation Interactions under Dynamic Loads," by Liu, W.D. and Penzien, J., November 1984, (PB87 124 889/AS)A11.

UCB/EERC-84/19 "Seismic Modelling of Deep Foundations," by Chen, C.-H. and Penzien, J., November 1984, (PB87 124 798/AS)A07.

UCB/EERC-84/20 "Dynamic Response Behavior of Quan Shui Dam," by Clough, R.W., Chang, K.-T., Chen, H.-Q., Stephen, R.M., Ghanaat, Y. and Qi, J.-H., November 1984, (PB86 115177/AS)A07.

UCB/EERC-85/01 "Simplified Methods of Analysis for Earthquake Resistant Design of Buildings," by Cruz, E.F. and Chopra, A.K., February 1985, (PB86 112299/AS)A12.

UCB/EERC-85/02 "Estimation of Seismic Wave Coherency and Rupture Velocity using the SMART 1 Strong-Motion Array Recordings," by Abrahamson, N.A., March 1985, (PB86 214 343)A07.

UCB/EERC-85/03 "Dynamic Properties of a Thirty Story Condominium Tower Building," by Stephen, R.M., Wilson, E.L. and Stander, N., April 1985, (PB86 118965/AS)A06.

UCB/EERC-85/04 "Development of Substructuring Techniques for On-Line Computer Controlled Seismic Performance Testing," by Dermitzakis, S. and Mahin, S., February 1985, (PB86 132941/AS)A08.

UCB/EERC-85/05 "A Simple Model for Reinforcing Bar Anchorages under Cyclic Excitations," by Filippou, F.C., March 1985, (PB86 112 919/AS)A05.

UCB/EERC-85/06 "Racking Behavior of Wood-framed Gypsum Panels under Dynamic Load," by Oliva, M.G., June 1985.

UCB/EERC-85/07 "Earthquake Analysis and Response of Concrete Arch Dams," by Fok, K.-L. and Chopra, A.K., June 1985, (PB86 139672/AS)A10.

UCB/EERC-85/08 "Effect of Inelastic Behavior on the Analysis and Design of Earthquake Resistant Structures," by Lin, J.P. and Mahin, S.A., June 1985, (PB86 135340/AS)A08.

UCB/EERC-85/09 "Earthquake Simulator Testing of a Base-Isolated Bridge Deck," by Kelly, J.M., Buckle, I.G. and Tsai, H.-C., January 1986, (PB87 124 152/AS)A06.

UCB/EERC-85/10 "Simplified Analysis for Earthquake Resistant Design of Concrete Gravity Dams," by Fenves, G. and Chopra, A.K., June 1986, (PB87 124 160/AS)A08.

UCB/EERC-85/11 "Dynamic Interaction Effects in Arch Dams," by Clough, R.W., Chang, K.-T., Chen, H.-Q. and Ghanaat, Y., October 1985, (PB86 135027/AS)A05.

UCB/EERC-85/12 "Dynamic Response of Long Valley Dam in the Mammoth Lake Earthquake Series of May 25-27, 1980," by Lai, S. and Seed, H.B., November 1985, (PB86 142304/AS)A05.

UCB/EERC-85/13 "A Methodology for Computer-Aided Design of Earthquake-Resistant Steel Structures," by Austin, M.A., Pister, K.S. and Mahin, S.A., December 1985, (PB86 159480/AS)A10 .

UCB/EERC-85/14 "Response of Tension-Leg Platforms to Vertical Seismic Excitations," by Liou, G.-S., Penzien, J. and Yeung, R.W., December 1985, (PB87 124 871/AS)A08.

UCB/EERC-85/15 "Cyclic Loading Tests of Masonry Single Piers: Volume 4 - Additional Tests with Height to Width Ratio of 1," by Sveinsson, B., McNiven, H.D. and Sucuoglu, H., December 1985.

UCB/EERC-85/16 "An Experimental Program for Studying the Dynamic Response of a Steel Frame with a Variety of Infill Partitions," by Yanev, B. and McNiven, H.D., December 1985.

UCB/EERC-86/01 "A Study of Seismically Resistant Eccentrically Braced Steel Frame Systems," by Kasai, K. and Popov, E.P., January 1986, (PB87 124 178/AS)A14.

UCB/EERC-86/02 "Design Problems in Soil Liquefaction," by Seed, H.B., February 1986, (PB87 124 186/AS)A03.

UCB/EERC-86/03 "Implications of Recent Earthquakes and Research on Earthquake-Resistant Design and Construction of Buildings," by Bertero, V.V., March 1986, (PB87 124 194/AS)A05.

UCB/EERC-86/04 "The Use of Load Dependent Vectors for Dynamic and Earthquake Analyses," by Leger, P., Wilson, E.L. and Clough, R.W., March 1986, (PB87 124 202/AS)A12.

UCB/EERC-86/05 "Two Beam-To-Column Web Connections," by Tsai, K.-C. and Popov, E.P., April 1986, (PB87 124 301/AS)A04.

UCB/EERC-86/06 "Determination of Penetration Resistance for Coarse-Grained Soils using the Becker Hammer Drill," by Harder, L.F. and Seed, H.B., May 1986, (PB87 124 210/AS)A07.

UCB/EERC-86/07 "A Mathematical Model for Predicting the Nonlinear Response of Unreinforced Masonry Walls to In-Plane Earthquake Excitations," by Mengi, Y. and McNiven, H.D., May 1986, (PB87 124 780/AS)A06.

UCB/EERC-86/08 "The 19 September 1985 Mexico Earthquake: Building Behavior," by Bertero, V.V., July 1986.

UCB/EERC-86/09 "EACD-3D: A Computer Program for Three-Dimensional Earthquake Analysis of Concrete Dams," by Fok, K.-L., Hall, J.F. and Chopra, A.K., July 1986, (PB87 124 228/AS)A08.

UCB/EERC-86/10 "Earthquake Simulation Tests and Associated Studies of a 0.3-Scale Model of a Six-Story Concentrically Braced Steel Structure," by Uang, C.-M. and Bertero, V.V., December 1986, (PB87 163 564/AS)A17.

UCB/EERC-86/11 "Mechanical Characteristics of Base Isolation Bearings for a Bridge Deck Model Test," by Kelly, J.M., Buckle, I.G. and Koh, C.-G., November 1987.

UCB/EERC-86/12 "Effects of Axial Load on Elastomeric Isolation Bearings," by Koh, C.-G. and Kelly, J.M., November 1987.

UCB/EERC-87/01 "The FPS Earthquake Resisting System: Experimental Report," by Zayas, V.A., Low, S.S. and Mahin, S.A., June 1987.

UCB/EERC-87/02 "Earthquake Simulator Tests and Associated Studies of a 0.3-Scale Model of a Six-Story Eccentrically Braced Steel Structure," by Whittaker, A., Uang, C.-M. and Bertero, V.V., July 1987.

UCB/EERC-87/03 "A Displacement Control and Uplift Restraint Device for Base-Isolated Structures," by Kelly, J.M., Griffith, M.C. and Aiken, I.D., April 1987.

UCB/EERC-87/04 "Earthquake Simulator Testing of a Combined Sliding Bearing and Rubber Bearing Isolation System," by Kelly, J.M. and Chalhoub, M.S., 1987.

UCB/EERC-87/05 "Three-Dimensional Inelastic Analysis of Reinforced Concrete Frame-Wall Structures," by Moazzami, S. and Bertero, V.V., May 1987.

UCB/EERC-87/06 "Experiments on Eccentrically Braced Frames with Composite Floors," by Ricles, J. and Popov, E., June 1987.

UCB/EERC-87/07 "Dynamic Analysis of Seismically Resistant Eccentrically Braced Frames," by Ricles, J. and Popov, E., June 1987.

UCB/EERC-87/08 "Undrained Cyclic Triaxial Testing of Gravels-The Effect of Membrane Compliance," by Evans, M.D. and Seed, H.B., July 1987.

UCB/EERC-87/09 "Hybrid Solution Techniques for Generalized Pseudo-Dynamic Testing," by Thewalt, C. and Mahin, S.A., July 1987.

UCB/EERC-87/10 "Ultimate Behavior of Butt Welded Splices in Heavy Rolled Steel Sections," by Bruneau, M., Mahin, S.A. and Popov, E.P., July 1987.

UCB/EERC-87/11 "Residual Strength of Sand from Dam Failures in the Chilean Earthquake of March 3, 1985," by De Alba, P., Seed, H.B., Retamal, E. and Seed, R.B., September 1987.

UCB/EERC-87/12 "Inelastic Seismic Response of Structures with Mass or Stiffness Eccentricities in Plan," by Bruneau, M. and Mahin, S.A., September 1987.

UCB/EERC-87/13 "CSTRUCT: An Interactive Computer Environment for the Design and Analysis of Earthquake Resistant Steel Structures," by Austin, M.A., Mahin, S.A. and Pister, K.S., September 1987.

UCB/EERC-87/14 "Experimental Study of Reinforced Concrete Columns Subjected to Multi-Axial Loading," by Low, S.S. and Moehle, J.P., September 1987.

UCB/EERC-87/15 "Relationships between Soil Conditions and Earthquake Ground Motions in Mexico City in the Earthquake of Sept. 19, 1985," by Seed, H.B., Romo, M.P., Sun, J., Jaime, A. and Lysmer, J., October 1987.

UCB/EERC-87/16 "Experimental Study of Seismic Response of R. C. Setback Buildings," by Shahrooz, B.M. and Moehle, J.P., October 1987.

UCB/EERC-87/17 "The Effect of Slabs on the Flexural Behavior of Beams," by Pantazopoulou, S.J. and Moehle, J.P., October 1987.

UCB/EERC-87/18 "Design Procedure for R-FBI Bearings," by Mostaghel, N. and Kelly, J.M., November 1987.

UCB/EERC-87/19 "Analytical Models for Predicting the Lateral Response of R C Shear Walls: Evaluation of their Reliability," by Vulcano, A. and Bertero, V.V., November 1987.

UCB/EERC-87/20 "Earthquake Response of Torsionally-Coupled Buildings," by Hejal, R. and Chopra, A.K., December 1987.

UCB/EERC-87/21 "Dynamic Reservoir Interaction with Monticello Dam," by Clough, R.W., Ghanaat, Y. and Qiu, X-F., December 1987.

UCB/EERC-87/22 "Strength Evaluation of Coarse-Grained Soils," by Siddiqi, F.H., Seed, R.B., Chan, C.K., Seed, H.B. and Pyke, R.M., December 1987.

UCB/EERC-88/01 "Seismic Behavior of Concentrically Braced Steel Frames," by Khatib, I., Mahin, S.A. and Pister, K.S., January 1988.

UCB/EERC-88/02 "Experimental Evaluation of Seismic Isolation of Medium-Rise Structures Subject to Uplift," by Griffith, M.C., Kelly, J.M., Coveney, V.A. and Koh, C.G., January 1988.

UCB/EERC-88/03 "Cyclic Behavior of Steel Double Angle Connections," by Astaneh-Asl, A. and Nader, M.N., January 1988.

UCB/EERC-88/04 "Re-evaluation of the Slide in the Lower San Fernando Dam in the Earthquake of Feb. 9, 1971," by Seed, H.B., Seed, R.B., Harder, L.F. and Jong, H.-L., April 1988.

UCB/EERC-88/05 "Experimental Evaluation of Seismic Isolation of a Nine-Story Braced Steel Frame Subject to Uplift," by Griffith, M.C., Kelly, J.M. and Aiken, I.D., May 1988.

UCB/EERC-88/06 "DRAIN-2DX User Guide.," by Allahabadi, R. and Powell, G.H., March 1988.

UCB/EERC-88/07 "Cylindrical Fluid Containers in Base-Isolated Structures," by Chalhoub, M.S. and Kelly, J.M., April 1988.

UCB/EERC-88/08 "Analysis of Near-Source Waves: Separation of Wave Types using Strong Motion Array Recordings," by Darragh, R.B., June 1988.

UCB/EERC-88/09 "Alternatives to Standard Mode Superposition for Analysis of Non-Classically Damped Systems," by Kusainov, A.A. and Clough, R.W., June 1988.

UCB/EERC-88/10 "The Landslide at the Port of Nice on October 16, 1979," by Seed, H.B., Seed, R.B., Schlosser, F., Blondeau, F. and Juran, I., June 1988.

UCB/EERC-88/11 "Liquefaction Potential of Sand Deposits Under Low Levels of Excitation," by Carter, D.P. and Seed, H.B., August 1988.

UCB/EERC-88/12 "Nonlinear Analysis of Reinforced Concrete Frames Under Cyclic Load Reversals," by Filippou, F.C. and Issa, A., September 1988.

UCB/EERC-88/13 "Implications of Recorded Earthquake Ground Motions on Seismic Design of Building Structures," by Uang, C.-M. and Bertero, V.V., November 1988.

UCB/EERC-88/14 "An Experimental Study of the Behavior of Dual Steel Systems," by Whittaker, A.S., Uang, C.-M. and Bertero, V.V., September 1988.

UCB/EERC-88/15 "Dynamic Moduli and Damping Ratios for Cohesive Soils," by Sun, J.I., Golesorkhi, R. and Seed, H.B., August 1988.

UCB/EERC-88/16 "Reinforced Concrete Flat Plates Under Lateral Load: An Experimental Study Including Biaxial Effects," by Pan, A. and Moehle, J., October 1988.

UCB/EERC-88/17 "Earthquake Engineering Research at Berkeley - 1988," by EERC, November 1988.

UCB/EERC-88/18 "Use of Energy as a Design Criterion in Earthquake-Resistant Design," by Uang, C.-M. and Bertero, V.V., November 1988.

UCB/EERC-88/19 "Steel Beam-Column Joints in Seismic Moment Resisting Frames," by Tsai, K.-C. and Popov, E.P., November 1988.

UCB/EERC-88/20 "Base Isolation in Japan, 1988," by Kelly, J.M., December 1988.

UCB/EERC-89/01 "Behavior of Long Links in Eccentrically Braced Frames," by Engelhardt, M.D. and Popov, E.P., January 1989.

UCB/EERC-89/02 "Earthquake Simulator Testing of Steel Plate Added Damping and Stiffness Elements," by Whittaker, A., Bertero, V.V., Alonso, J. and Thompson, C., January 1989.

UCB/EERC-89/03 "Implications of Site Effects in the Mexico City Earthquake of Sept. 19, 1985 for Earthquake-Resistant Design Criteria in the San Francisco Bay Area of California," by Seed, H.B. and Sun, J.I., March 1989.

UCB/EERC-89/04 "Earthquake Analysis and Response of Intake-Outlet Towers," by Goyal, A. and Chopra, A.K., July 1989.

UCB/EERC-89/05 "The 1985 Chile Earthquake: An Evaluation of Structural Requirements for Bearing Wall Buildings," by Wallace, J.W. and Moehle, J.P., July 1989.

UCB/EERC-89/06 "Effects of Spatial Variation of Ground Motions on Large Multiply-Supported Structures," by Hao, H., July 1989.

UCB/EERC-89/07 "EADAP - Enhanced Arch Dam Analysis Program: User's Manual," by Ghanaat, Y. and Clough, R.W., August 1989.